nature portfolio

https://doi.org/10.1038/s41550-021-01306-2

Supplementary information

Dynamical evidence for Phobos and Deimos as remnants of a disrupted common progenitor

In the format provided by the authors and unedited

Supplementary material

Dynamical evidence for a captured planetesimal as a common progenitor of Phobos and Deimos

Amirhossein Bagheri[1*], Amir Khan[1,2], Michael Efroimsky[3], Mikhail Kruglyakov[1], and Domenico Giardini[1]

[1]*Institute of Geophysics, ETH Zürich, Zürich, Switzerland,*

[2]*Physik-Institut, University of Zürich, Zürich, Switzerland*

[3]*US Naval Observatory, Washington DC, USA*

1 Orbital and planetary parameters

Since the discovery of Phobos and Deimos, their orbits and ephemerides have been measured by several missions[1]. The values of orbital and planetary parameters of Mars, Phobos, and Deimos that are used in this study are summarised in Supplementary Table 1.

	Mars	Phobos	Deimos
k_2	0.169 ± 0.006 [2]	$10^{-3} - 10^{-7}$	$10^{-3} - 10^{-7}$
Q_2	95 ± 10 [3]	$1 - 200$	$1 - 200$
Semi-major axis (km)	–	9377 [4]	23463 [4]
Eccentricity	–	0.0151 [4]	0.00033 [4]
Dimensions (km)			
Ellipsoid			
a×b×c	–	$13 \times 11.4 \times 9.14$ [5]	$7.5 \times 6.1 \times 5.2$ [6]
Spheroid			
Mean radius (R)	3389.5 [5]	11.3	6.3
Mass ($\times 10^{16}$kg)	$6.417 \pm 0.0003 \times 10^7$ [2]	1.059 ± 0.03 [7]	0.148 ± 0.003 [8]
Density (kg/m^3)	3935 ± 1.2 [9]	1862 ± 20 [7]	1480 ± 220 [10]
Rotational period (h)	24.62	7.66	30.3
Principal MoI			
A/MR^2	–	0.3615 [6]	0.338 [11]
B/MR^2	–	0.4265 [6]	0.461 [11]
C/MR^2	–	0.5024 [6]	0.508 [11]
I/MR^2 (mean)	0.36379 ± 0.0001 [2]	–	–
Libration amplitude	–	$1.2° \pm 0.15°$ [6]	0.08° [12]
Inclination	–	1.093°	0.93°

Supplementary Table 1: Observed orbital characteristics and measured and modeled parameters of Mars, Phobos, and Deimos. Unless noted, observed characteristics refer to the present-day values.

2 On the separation between Phobos and Deimos

The present-time inclinations of Phobos and Deimos on the Martian equator are miniscule; and, as found in this study (cf. inset in Figure 1C in the main text), these inclinations have remained very small for long. In the course of the equinoctial precession of Mars, these inclinations stay small while oscillating about zero (i.e. about the Martian equator); so the two orbital planes get to coincide from time to time.

A planetocentric distance[13] is

$$\mathrm{R_p} = \frac{a\,(1\,-\,e^2)}{1\,+e\,\cos f}\quad , \tag{1}$$

f being the true anomaly. Consequently, r assumes the values within the following interval

$$a\,(1\,-\,e) \leq \mathrm{R_p} \leq a\,(1\,+\,e)\quad , \tag{2}$$

so a satellite always resides between the two circles.

Integrating back in time, we approach the instant when the outer limiting circle corresponding to Phobos touches the inner limiting circle of Deimos, i.e. when the (growing, back in time) value of Phobos's distance, $\mathrm{R_p^{Phobos}}$, catches up with that of Deimos, $\mathrm{R_p^{Deimos}}$

$$\mathrm{R_p^{Phobos}} \;=\; \mathrm{R_p^{Deimos}} \quad \Longleftrightarrow \quad a_{\mathrm{Phobos}}\,(1\,+\,e_{\mathrm{Phobos}}) = a_{\mathrm{Deimos}}\,(1\,-\,e_{\mathrm{Deimos}})\quad . \tag{3}$$

The disruption of the common progenitor must have had happened earlier than that time (later, in terms of the back-in-time integration).

3 Viscoelastic model

The tidal response of Mars is computed using a spectral element method for a set of different viscoelastic dissipation models[14]. The viscoelastic models (Andrade, extended Burgers, and Sundberg-Cooper[15]) are experimentally constrained and temperature-, frequency-, and grain size-dependent[16] and are experimentally tested.

In the calculations below, we rely on the Andrade model. For this model, real and imaginary parts of the compliance are

$$\Re(J(\omega)) = J_U + \beta\Gamma(1+\alpha)\omega^{-\alpha}\cos(\frac{\alpha\pi}{2}), \tag{4}$$

$$\Im(J(\omega)) = \beta\Gamma(1+\alpha)\omega^{-\alpha}\sin(\frac{\alpha\pi}{2}) + \frac{J_U}{\omega\tau_M}, \tag{5}$$

where β is a measure of the anelastic relaxation strength, α is the frequency exponent, Γ is the Gamma function, J_U is the unrelaxed, i.e., infinite-frequency, compliance, $\tau_M = \eta J_U$ is the Maxwell relaxation time, and η is viscosity. The dependence of the shear modulus relaxation on temperature, pressure and grain size is included by replacing the actual frequency with the pseudo-frequency master variable ω_B[16]

$$\omega_B = \omega\left(\frac{d}{d_0}\right)^{m_a} \exp\left[\frac{E}{R}\left(\frac{1}{T} - \frac{1}{T_0}\right)\right] \exp\left[\frac{V}{R}\left(\frac{P}{T} - \frac{P_0}{T_0}\right)\right], \tag{6}$$

where d is grain size, T is temperature, P is pressure, V and E are activation volume and activation energy, respectively, R is the gas constant, m_a is grain size exponent, and the subscript 0 refers to a reference value. Parameters are those compiled in a previous study[14].

4 Models of Mars, Phobos, and Deimos

Models of Mars's interior structure and attenuation properties are obtained from inversion of the currently available geophysical data (tidal response and mean mass and moment of inertia, see Supplementary Table 1) as outlined in the previous studies[3,14]. The models are constructed using thermodynamic phase equilibria[17–19] that allow for self-consistent computation of mantle adiabats, elastic properties, and the density of Mars's interior for a given composition[20]. We assume that it is well mixed and convecting, and compute its depth-dependent thermoelastic properties using equations of state for liquid iron and liquid iron-sulfur alloys[21].

For the purposes of the orbital evolution calculations, we chose the best-fitting among all inverted models. Best-fitting radial profiles of seismic wave velocities (V_P, V_S), density (ρ), shear-wave attenuation (Q_μ), and temperature that are needed for the computation of k_l and Q_l are shown in Supplementary Figure 1. The model contains a 57 km thick crust, a 340 km thick lithosphere, a mantle adiabat with a potential temperature of 1500 K, and a liquid Fe-S core with a radius of $\sim$1830 km and a sulfur content of $\sim$19 wt%. As the core is entirely fluid, dissipation in the core is zero ($Q_\mu = 0$). For the Andrade viscoelastic model, we used the following (best-fitting) parameters: $\alpha = 0.27$ (frequency-dependence), $d = 0.01$ m (grain size), and $\beta = 10^{-13}$ (anelastic relaxation strength). In comparison, the interiors of Phobos and Deimos are less constrained. The Stickney crater, which extends over almost one face of Phobos, further strengthens the probability of a highly porous interior structure with a thin overlying regolith layer[22]. An impact of this size would have been sufficient to catastrophically disrupt Phobos if it were either a complete rubble-pile or an undamaged rigid object. This observation favours a Phobos with modest fragmentation and some internal strength[23,23–27]. In addition, the ubiquitous grooves and fractures on the surfaces of the satellites are most likely to be present on a tidally disrupted and loosely-connected body[28–30]. Tides on such bodies can reach several meters[28], with an associated tidal dissipation that contributes significantly to the orbital evolution of the system. Accordingly, we consider a relatively broad range of parameters encompassing models from consolidated to pure rubble-pile bodies, in addition to the intermediate cases of a granular outer layer and a solid interior with both layers making up half of the radius of either satellite. Of the latter, we consider two models with monolithic interior cores and granular outer layers (labelled "more consolidated rubble aggregate" and "less consolidated rubble aggregate"), that differ in core and outer layer shear moduli and viscosities[31]. The tidal Love number for these models is computed using the effective shear modulus obtained by the approach of Goldreich and Sari[32]. The quality factors for the rubble pile and rubble aggregate cases can be scaled by Nimmo and Matsuyama[33]. The values for Deimos are scaled from Phobos based on the same approach. For Phobos and Deimos, We assumed a frequency exponent, which describes how dissipation within the satellites scales with frequency, similar to that obtained for Mars. k_2 and Q_2 values are compiled in Supplementary Table 1. Exponent α (cf. equations 4–5) describes how dissipation within Mars scales with frequency.

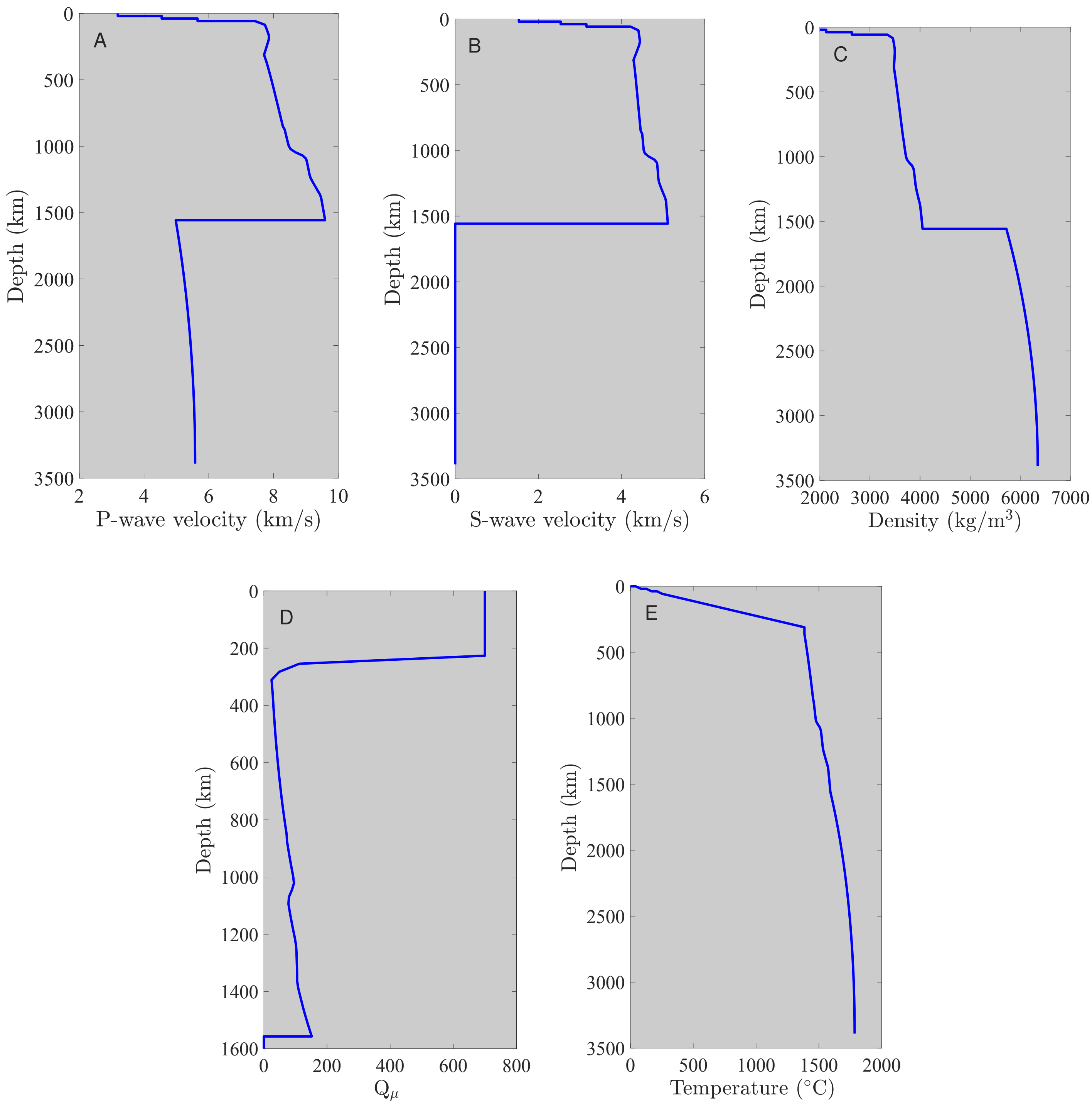

Supplementary Figure 1. Radial profiles of the Martian seismic P- and S-wave velocity (A, B), density (C), shear attenuation (D), and temperature (E). The profiles have been obtained by inversion of the current set of Martian geophysical data.

5 Disruption process

As is known, a sub-catastrophic low-energy disruptive event can result in production of two fragments[34–36]. Such a low-energy event permits each fragment to retain some inner bonds, i.e., to stay slightly stronger than complete rubble as argued previously. After such a low-energy event, each of the two major fragments will retain the bonds and remain slightly stronger than complete rubble — which agrees well with the properties of Phobos presumed from the observation of the Stickney crater, and with the ability of Phobos and Deimos to sustain their irregular shapes. Aside from this likely option, consistent with our scenario is the possibility that the disruptive event produced more fragments, Phobos and Deimos being the only two to survive until now. The other fragments may already have fallen onto Mars[37–39], producing part of what we observe today as the Martian cratering record or have been deplete by solar radiations.

Being of different shapes, the post-disruptive orbits of Phobos and Deimos had different periods, which greatly reduces the probability of a later encounter. Even if such a putative encounter happened, it is more likely to have been grazing, owing to the accumulating divergence of orbits, and it also would be at a very low relative speed, owing to the low-energy nature of the disruption. Such an encounter, had it ever occurred, would have contributed to the irregularity of Phobos's and Deimos's shapes. Modeling the details of the disruption process are beyond the scope of the present study and will need to be considered in the future.

6 Tidal response

Several different modes are employed to describe the orbital evolution of the semi-major axis and eccentricity. This necessitates computing the tidal response of Mars for each mode at each time step of the orbital evolution calculation. The tidal response of the various contributing modes is shown in Supplementary Figure 2 for both Phobos and Deimos. As shown in the figure, in the course of the orbital evolution of each satellite several modes pass through the zero frequency. In the case of Phobos, the zero-crossing of the main semidiurnal mode (thick dashed line) corresponds to the satellite orbit passing through the synchronous radius, as tidal dissipation in both satellite and planet drives it toward Mars. Above the synchronous radius, the satellite's orbit lags behind the tidal bulge on Mars, while below the synchronous radius the tidal bulge is lagging behind the satellite. This is not the case for Deimos. Although a highly dissipative rubble-pile Deimos was initially descending toward the synchronous radius (cf.Supplementary Figure 1 in the main manuscript), it never crossed the synchronism because of the two circumstances mitigating the dissipation in Deimos: its smaller size and lower eccentricity. Hence, the main semidiurnal tidal mode in Deimos never becomes zero, and the curve for the most part stays flat.

In Supplementary Figure 3, we have plotted the frequency-dependent tidal response of Mars, for the main (semidiurnal) tide (i.e. $K_2 = k_2 \sin\epsilon_2$). On the tidal response curve, we see a peak located at long periods; so $\sin\epsilon_l$ vanishes in the zero-frequency limit. The latter point is understandable on general physical grounds. Suppose the satellite is crossing an $lmpq$ spin-orbit resonance, the one where the tidal Fourier mode $\beta_{lmpq0} = \omega_{lmpq}$ crosses zero. Clearly, the quality function $K_l(\omega_{lmpq}) = k_l(\omega_{lmpq}) \sin\epsilon_l(\omega_{lmpq})$ must also pass continuously through zero, to ensure that the corresponding $lmpq$ Fourier component of the tidal torque transcends zero continuously (Supplementary Figure 3A)[40,41]. This fact stays valid also in the presence of longitudinal libration, though the spectrum of tidal modes in that case is parameterised with five, not four integers (cf. Eq. 17). Of a special importance here, and in planetary astronomy in general, is the process of crossing of the 2200 spin-orbit resonance, i.e. of the synchronous orbit. This is a resonance wherein the principal (semidiurnal) tidal mode vanishes, $\omega_{2200} = 2\,(n - \dot{\theta}) = 0$; so the mean motion equals the primary's spin rate. A common fallacy has it that a satellite located above the synchronous radius always recedes from the planet. This belief is

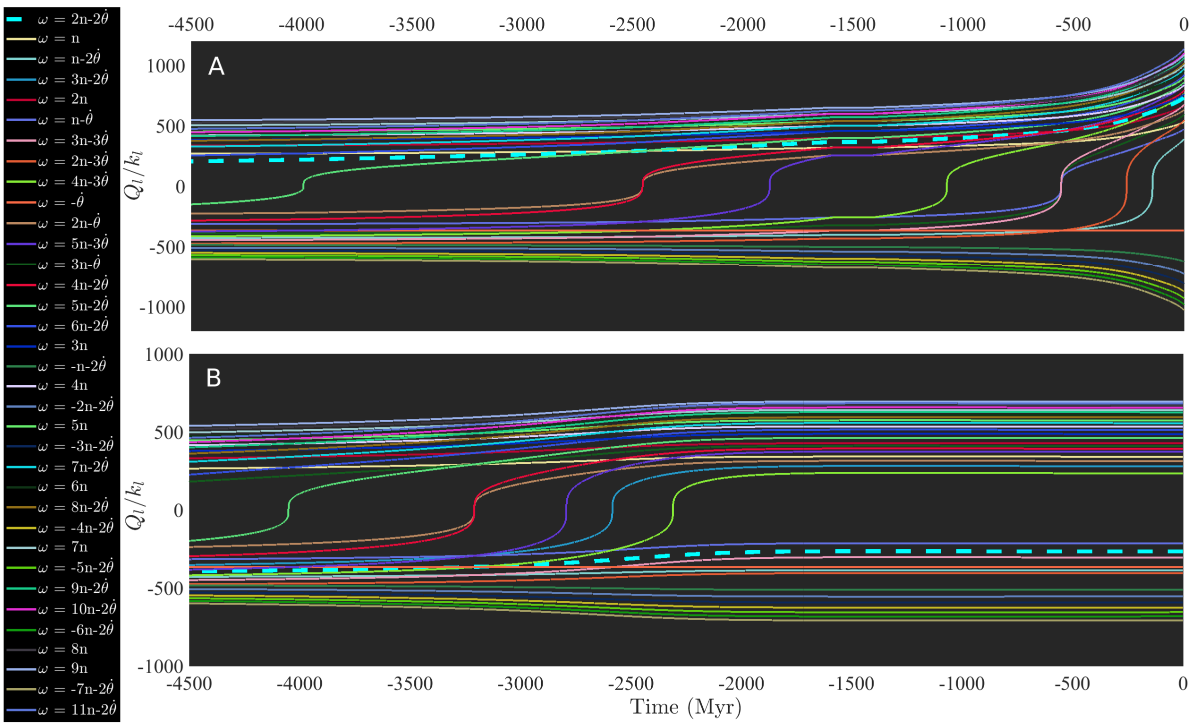

Supplementary Figure 2. Dissipation Q_l/k_l for $l = 2, 3$ for different contributing modes ω for (A) Phobos and (B) Deimos. n and $\dot{\theta}$ are mean motion and true anomaly, respectively. In each of the two panels, the thick dashed line depicts the tidal response associated with the main semi-diurnal tide ($\omega_{2200} = 2n - 2\dot{\theta}$). Note that the main tide for Phobos, unlike that for Deimos, crosses zero frequency as Phobos passes through the synchronous radius. See text for further details.

seemingly supported by equation (35) that governs dissipation in the planet. There, the sign of the first (leading) term depends on whether the mean motion n of the satellite is lower or higher than the spin rate $\dot{\theta}$ of the planet or, equivalently, whether the satellite is residing above or below the synchronous orbit. For a satellite higher than that altitude, $\omega_{2200} = 2\,(n - \dot{\theta})$ becomes negative and so does the value of the quality function $K_2(\omega_{2200})$ that enters the leading (over the powers of e) term in the expression for da/dt. That term contains a "minus" sign, wherefore the overall semidiurnal input becomes positive and works to increase the value of da/dt, thus making the satellite recede from the planet. The outcome, however, may change if we also take into consideration the tidal dissipation in the satellite itself. Specifically, we shall be interested in synchronous case, where the spin rate is equal to the mean motion, $\dot{\theta}\,' = n$.

In this situation, the semidiurnal ($lmpq = 2200$) input into da/dt due to the tides in the satellite becomes zero, while the next-order term due to the friction in the satellite turns out to be of the order e^2 (see the second term in equation (35)). Setting aside all the other terms, we now single out, for illustrative purposes, only the leading (semidiurnal) term due to the friction in the planet and the leading term due to the friction in the synchronised satellite:

$$\frac{da}{dt} \approx -3\,n\,a\,\frac{M'}{M}\left(\frac{R}{a}\right)^5 K_2(\omega_{2200}) - 57\,n\,a\,e^2\,\frac{M}{M'}\left(\frac{R'}{a}\right)^5 K_2'(n)$$
$$= -3\,n\,a\,\frac{M'}{M}\left(\frac{R}{a}\right)^5 \left[K_2(\omega_{2200}) + 19\,e^2\left(\frac{R'}{R}\right)^5\left(\frac{M}{M'}\right)^2 K_2'(n)\right] \quad . \tag{7}$$

The two terms shown in equation (7) coincide with the first two terms in the comprehensive expression (35). We see that the term with e^2 (related to tides in the satellite) always stays negative, regardless of the distance between the two bodies, which implies that the dissipation in a synchronised satellite is always working to decrease the semi-major axis, even if the satellite is above the synchronous radius. This is different from the dissipation in the planet which tends to "push" the satellite away from the synchronous orbit. Consequently, if the eccentricity of the orbit and the dissipation in the satellite (represented by $K_2'(n)$) are high enough, the e^2-order term in the above expression may become leading and define the overall sign of da/dt. In this case, the satellite will migrate inwards and may even cross the synchronous orbit.

Consider the first term in equation (7). Its tidal-mode-dependence is defined by that of $K_2(\omega_{2200})$.

For any physically reasonable rheology, the interplay of the rheological response and self-gravitation renders a kink-shaped quality function. It is symmetric, because k_l is an even function of the Fourier mode, while ϵ_l is odd (see, e.g.[42] for details). Setting the sign aside for the time being, and concentrating solely on the shape, it will be sufficient to study K_2 as a function of the physical frequency $\chi_{2200} = |\omega_{2200}| = 2|n - \dot{\theta}|$, see Supplementary Figure 3B.

In Supplementary Figure 3B, the horizontal axis shows the values of χ_{2200}, while the peak value of the tidal interaction is marked with a yellow dot. Now suppose that the satellite is orbiting above the synchronous altitude and is descending. As we just saw from equation (7), this is possible when the dissipation inside the satellite and the eccentricity are sufficiently high. With the planet's $\dot{\theta}$ being fixed, the mean motion n is growing and approaching $\dot{\theta}$ as the satellite descends. In this plot, this process implies a gradual decrease in the frequency χ_{2200}. The initial value of χ_{2200} is represented in Supplementary Figure 3B with a red dot, and as the satellite approaches the synchronous radius this dot is moving to the left. As it does so, the value of $K_2(\chi_{2200})$ rapidly increases (i.e. the tidal push from the planet increases), and it becomes more and more difficult for the second term in equation (7) to overpower the first term. If the dissipation in the satellite multiplied by the squared eccentricity (the second term in equation (7)) is still high enough to overcome the pushing force from the planet, the satellite continues migrating inwards and the pushing force from the planet decreases, see the left-hand side of the curve (represented by the green dot) [1]

Eventually, the satellite will cross the synchronous radius. After that, the dissipation in both the planet and the satellite will be contributing to the increasing rate of descent and inwards migration. (Recall that K_l is an odd function of the tidal mode.) If, however, the tidal dissipation in the satellite and/or the eccentricity of the orbit is not strong enough to overcome the outward pushing force of the planet, da/dt changes sign and the satellite starts to recede from the planet.

[1] Note that during this process the eccentricity of the orbit is decreasing, see equation (41). Hence the necessity for a caveat that, after the peak gets transcended, the moon continues its migration towards the synchronous radius and reaches it, provided the value of e has not decreased noticeably during this span of time.

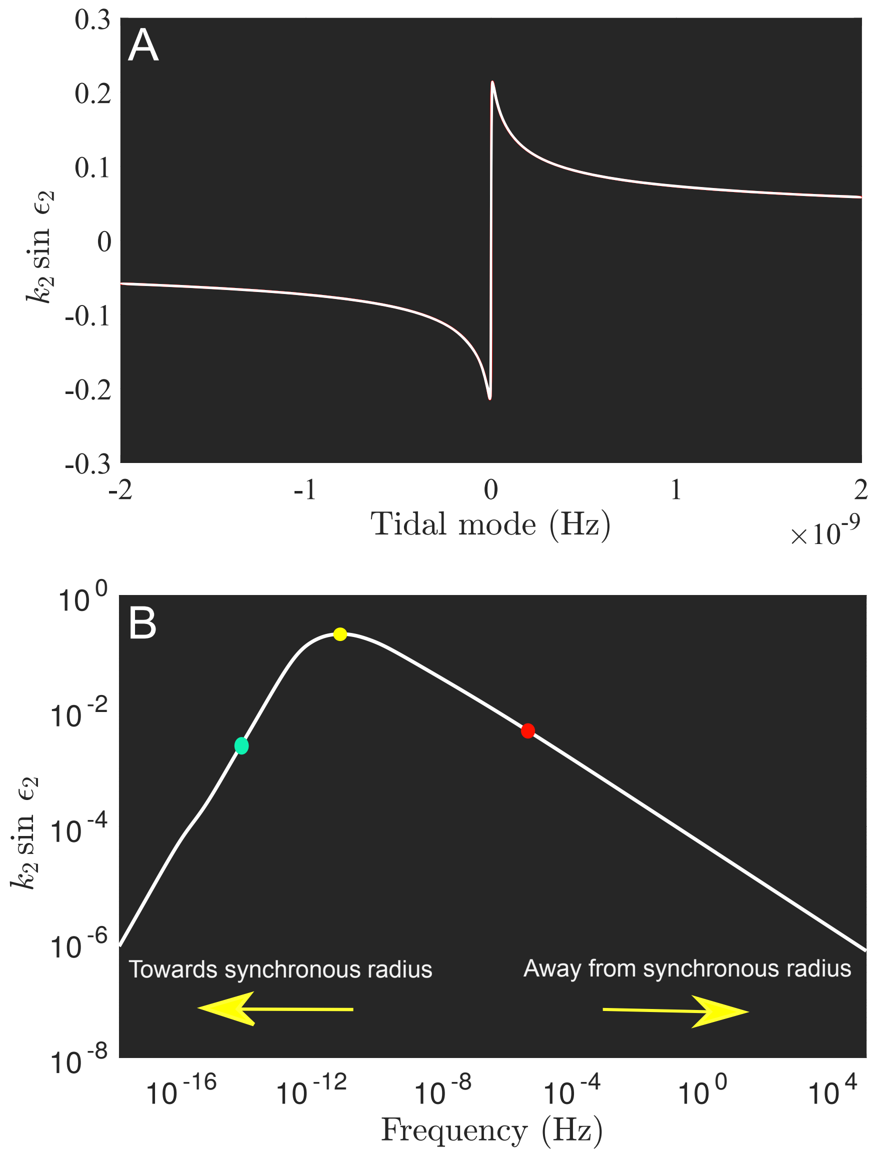

Supplementary Figure 3. Second-degree tidal response ($k_2 \sin \epsilon_2$) as a function of the forcing frequency of a satellite in orbit about a primary. (B) shows a zoom-in around the peak in (A). Arrows and points indicate directions relative to synchronous radius and are discussed in the text.

7 Effect of libration in longitude on the orbital evolution

Both Martian moons are librating in longitude, in the 1:1 spin-orbit resonance. This affects the tidal dissipation in the system and, therefore, the orbital evolution. For Phobos, measurements indicate the present-day libration magnitude of $1.2^{\circ} \pm 0.15^{\circ}$ [6], while for Deimos it has been estimated to be $\sim 0.08^{\circ}$ [12] which is in good agreement with the value obtained from equation (49). Note that due to the past higher eccentricity of the orbits, the amplitudes of the libration of the moons were considerably higher in the past (cf. equation 49). Based on the derivation in Section 13, the orbital evolution of a loosely-connected librating Phobos is compared to the evolution under no libration. A similar comparison is carried out for a loosely-connected Deimos. The comparison is shown in Supplementary Figure 4, and the results indicate that tidal dissipation is considerably enhanced by libration, as was predicted in [43] (Table 2). The libration-caused additional dissipation in the satellites contributed to efficient damping of the initial eccentricity and of the eccentricity jumps caused by the resonances.

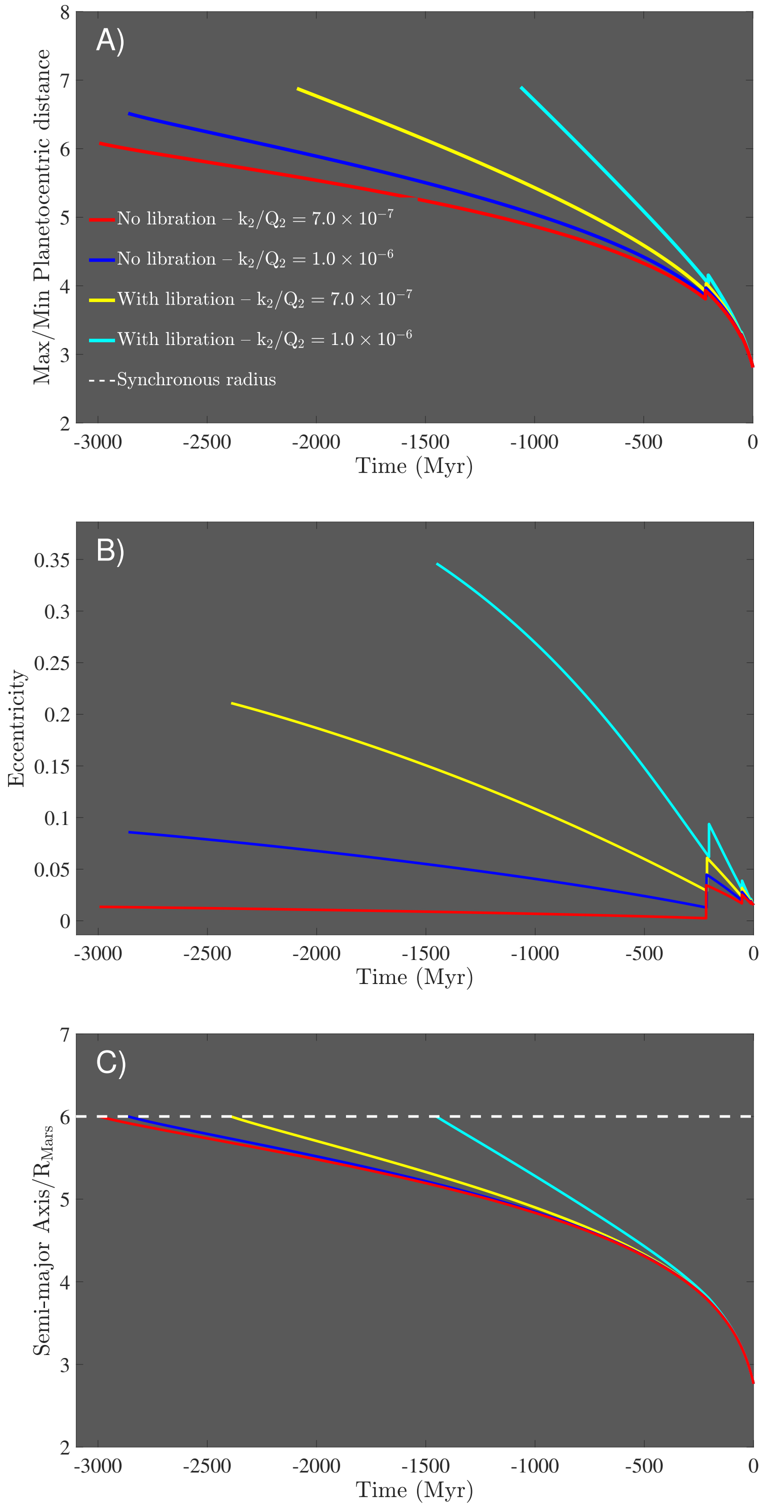

Supplementary Figure 4. Effect of the libration of Phobos on the orbital evolution of (A) the planetocentric distance, (B) eccentricity, and (C) the semi-major axis of rubble aggregate models of Phobos. Panels (A) and (C) are normalised to the mean radius R_M of Mars.

8 Effect of the initial eccentricity on orbital evolution

Since the results in the main text are based on backward integration of the orbits, we examined the effect on the orbital evolution from using different initial eccentricities (e_0) by forward integrating the equations for three different k_2/Q_2 cases considered in the main text (representative k_2/Q_2 values for these cases are given in Supplementary Table 1). As initial eccentricities, we chose 0.015, 0.15, and 0.3 as representative of small, medium, and large values, respectively, resulting in nine different cases. The results are shown in Supplementary Figure 5 and indicate that the least dissipative Phobos ($k_2/Q_2 = 3.3 \times 10^{-7}$, see section 9) would have impacted Mars's surface between 2 and 3.1 Gyr of orbital evolution; between $\sim$1.8 and 3.1 Gyr in the casse of $k_2/Q_2 = 10^{-6}$; and between 1.6 and 3.1 Gyr in the representative case of highly dissipative satellite ($k_2/Q_2 = 10^{-5}$). Hence, concomitant formation of Phobos and Deimos with Mars seems less likely.

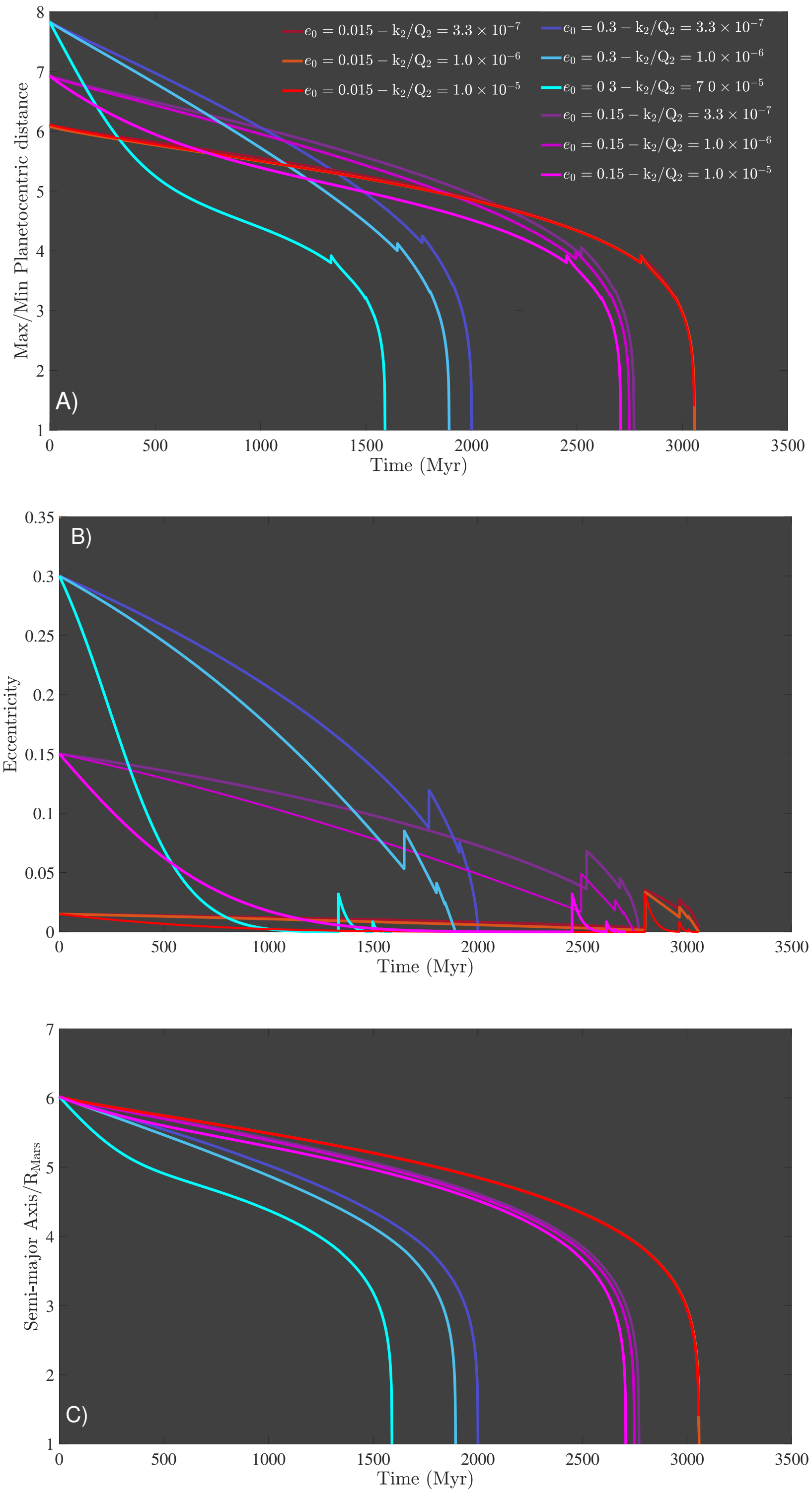

Supplementary Figure 5. Effect of the initial eccentricity (e_0) on the orbital evolution (forward integration) of the planetocentric distance (A), eccentricity (B), and semi-major axis (C) for a range of Phobos models: less consolidated rubble aggregate ($k_2/Q_2 = 10^{-5}$), consolidated rubble aggregates ($k_2/Q_2 = 1.0 \times 10^{-6}$), and the least dissipative ($k_2/Q_2 = 3.3 \times 10^{-7}$). Panels (A) and (C) are normalised to the mean radius R_M of Mars.

9 Dissipation in the satellites

The results in the main text are based on Phobos and Deimos being loosely connected (though not necessarily complete rubble). Here we investigate the orbital evolution in the case of these moons being monoliths, i.e., entirely solid. Representative k_2/Q_2 values for this particular case are given in Supplementary Table 1. Shown in Supplementary Figure 6, the results of the backward integrations of the orbits of solid Phobos and Deimos demonstrate that in order for them to damp the eccentricity jumps associated with the resonances (described in the main text), a certain minimal level of dissipation in the satellites is required. We find that the minimal values of k_2/Q_2 for Phobos and Deimos are approximately equal to 3.7×10^{-7} and 1.2×10^{-4}, respectively. Less intensive dissipation fails to render the present-day orbital configuration. The minimal acceptable value of k_2/Q_2 indicates that Phobos and Deimos cannot be monolithic and must be at least partially fractured.

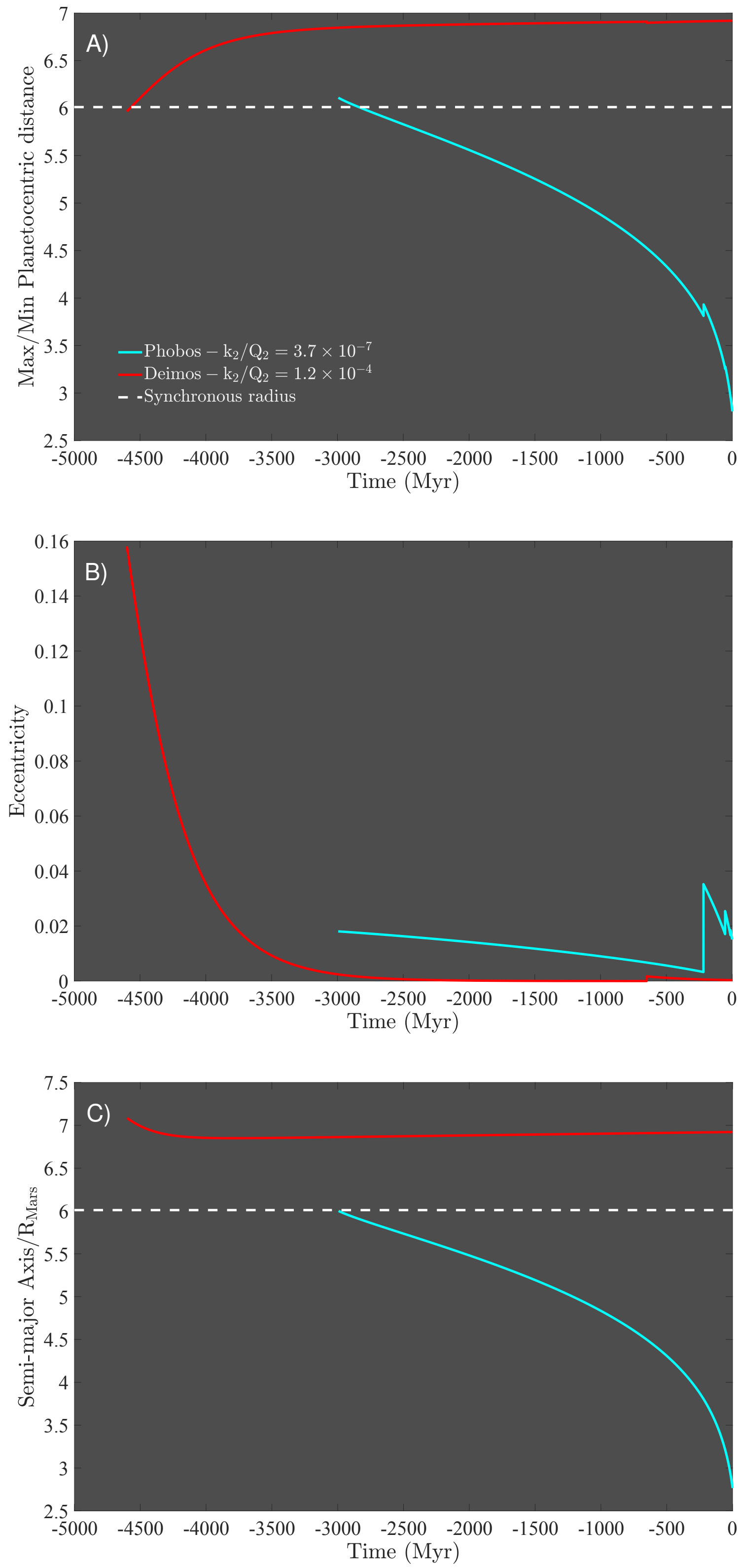

Supplementary Figure 6. Tidal evolution (backwards integration over time) of (A) the planetocentric distance, (B) eccentricity, and (C) semi-major axis for models of Phobos and Deimos with the lowest possible k_2/Q_2 to ensure the required eccentricity damping. Panels (A) and (C) are normalised to the mean radius $\mathrm{R_M}$ of Mars.

10 Effect of the frequency-dependence of tidal dissipation on orbital evolution

The results presented in the main text are based on a particular value of the Andrade exponential α (cf. equations 4–5) that describes how dissipation within Mars scales with frequency. Here, we wish to consider the effect on the orbital evolution from using a different exponent. In our work, we set (cf. Section 3), $\alpha = 0.27$, based on the inversion of the current geophysical data available for Mars (cf. Section 4). To model orbital evolution using a different α, we chose among the stochastically inverted models[14], in order to ensure that a model fitting the current geophysical data is employed. From the set of sampled models, models with $\alpha = 0.22$ and $\alpha = 0.36$ were extracted. Note that a "model" is not simply restricted to α, but involves, in addition to α, an ensemble of other model parameters (see Section 3 for more details). Using this machinery, we backwards-integrate the orbital evolution for the rubble aggregate cases of Phobos considered in the main text. The results are shown in Supplementary Figure 7 and are compared to the case with $\alpha = 0.27$. The main effect of a lower α is to extend the lifetime of Phobos further back in time to $\sim$2.8 Gyr (from 2.7 Gyr for α=0.27) in the case of a more consolidated rubble aggregate, whereas for a less consolidated rubble aggregate the effect is negligible (<100 Myr). This suggests that even if dissipation scales less strongly with frequency, Phobos is still unlikely to have formed *in situ* through co-accretion or re-accretion of debris following a giant impact about 500 Myr after the formation of Mars as suggested in some models[44–47]. While changes in α generally result in relatively minor changes in the lifetime of a rubble aggregate Phobos, there are arguments against too low values of α: first of all, independent inversions[3,14] of the Martian geophysical data, but relying on different viscoelastic models, both find $\alpha \geq 0.3$; and secondly, low values of α (< 0.3) appear to be inconsistent with current InSight observations of a seismic high-Q environment that suggest upper mantle seismic Q values around 200–400[48,49]. In comparison, for $\alpha = 0.22$ the Q estimates obtained from the Andrade rheological model are <1000, whereas for $\alpha = 0.27$, Q >1000, both at seismic periods. The future seismic recordings from InSight will improve estimates of crust and mantle Q and therefore a better understanding of α[14] and through that the orbital evolution of the Martian satellites.

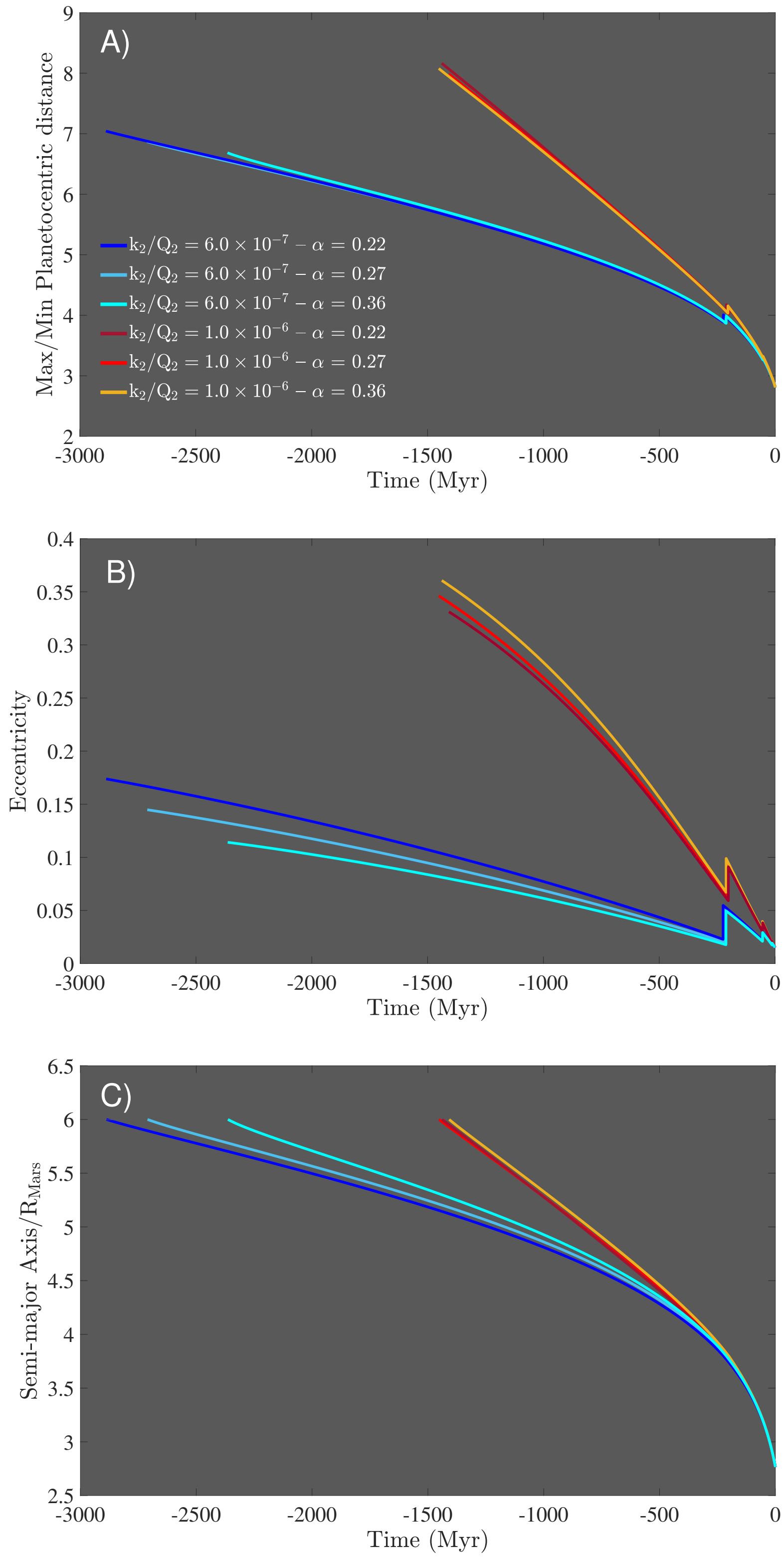

Supplementary Figure 7. Effect of frequency-dependence (α) on the evolution of (A) the planetocentric distance, (B) eccentricity, and (C) semi-major axis for two rubble aggregate models of Phobos. Panels (A) and (C) are normalised to the mean radius R_M of Mars.

11 Effect of Mars's temperature on the orbital evolution

The present-day thermal structure of Mars is the product of ~4.5 Gyr of dynamical evolution that started with the formation of a global magma ocean, subsequent core formation, and ended with a differentiated planet. As a result, it is predicted to undergo secular cooling[50–52], and here we consider the effect of a time-varying thermal structure on the orbital evolution of Phobos and Deimos. The principal effect of an earlier hotter Mars, is to reduce the shear moduli thereby leading to a "softening" (shear modulus reduction) with a resultant overall increase in dissipation[52]. The thermal history model[50], which is shown as insert in Supplementary Figure 8, and involves an increase in mantle temperature of ~120 °C over the past 3 Gyr from the present (backwards in time). These time-dependent temperature variations are divided into 30 time steps and employed as values for the lithospheric temperature in our thermodynamic modeling scheme discussed in Section 4 and detailed in our previous studies[3,14]. The resultant self-consistently computed adiabatic thermal profiles are shown in Supplementary Figure 8 and represent the change in thermal state of Mars over the last 3 Gyr. Based on these, we recompute geophysical properties (e.g., P- and S-wave velocities, density, shear attenuation) of Mars at each time step and employ these for determining the orbital evolution backwards in time.

The changes in orbital evolution incurred by considering the "thermal history model" are shown in Supplementary Figure 9 for Phobos. For comparison, the orbital evolution based on the constant temperature model is also shown. The main effect of considering thermal variations is, as expected, to increase the rate of tidal dissipation and therefore speed up the orbital evolution by ~0.1 Gyr for a highly dissipative satellite and ~0.5 Gyr for the least dissipative case. We can therefore conclude that the constant-temperature model underestimates tidal dissipation in the planet, wherefore it should be considered a lower bound. Any additional contribution that acts to increase tidal dissipation, will move the semi-major axis curve to the right, i.e., closer to the present, but not alter the shape of the curve and therefore the main conclusion.

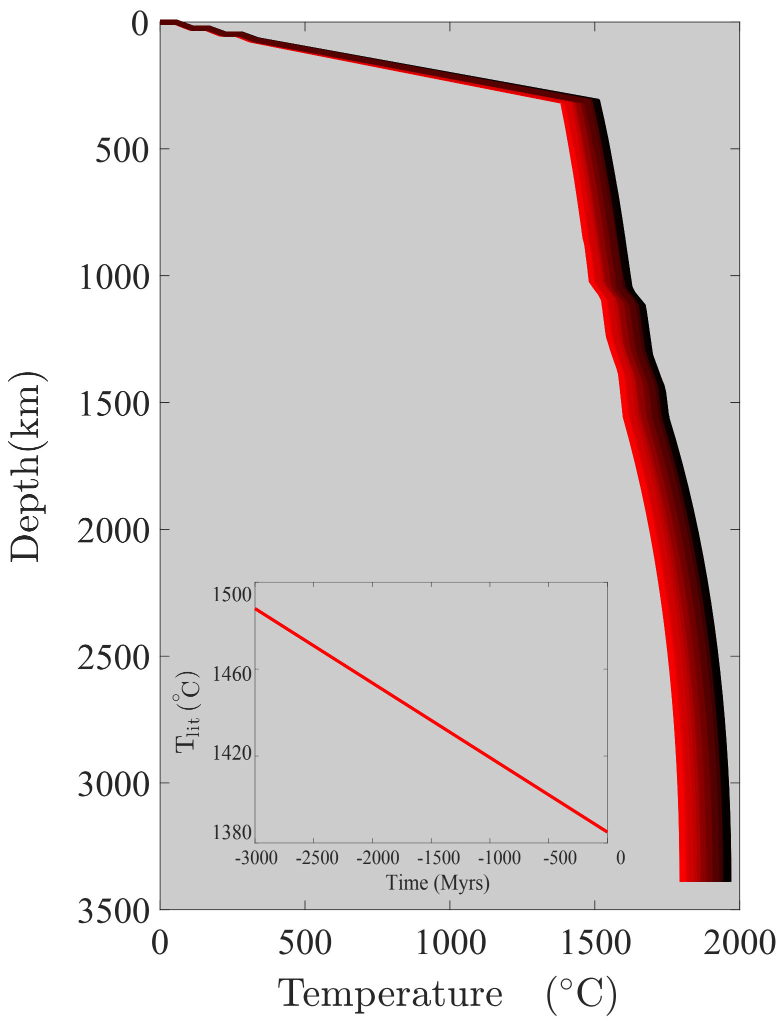

Supplementary Figure 8. Variations in the thermal structure of Mars over time. The insert shows the time evolution of the lithospheric temperature[50]. The thermal profiles have been computed at 30 time steps covering the last 3 Gyr of thermal evolution (after the insert) and are colour-coded so that the present-day thermal structure is represented by the red thermal profile and increasingly darker hues represent the thermal structure backwards in time.

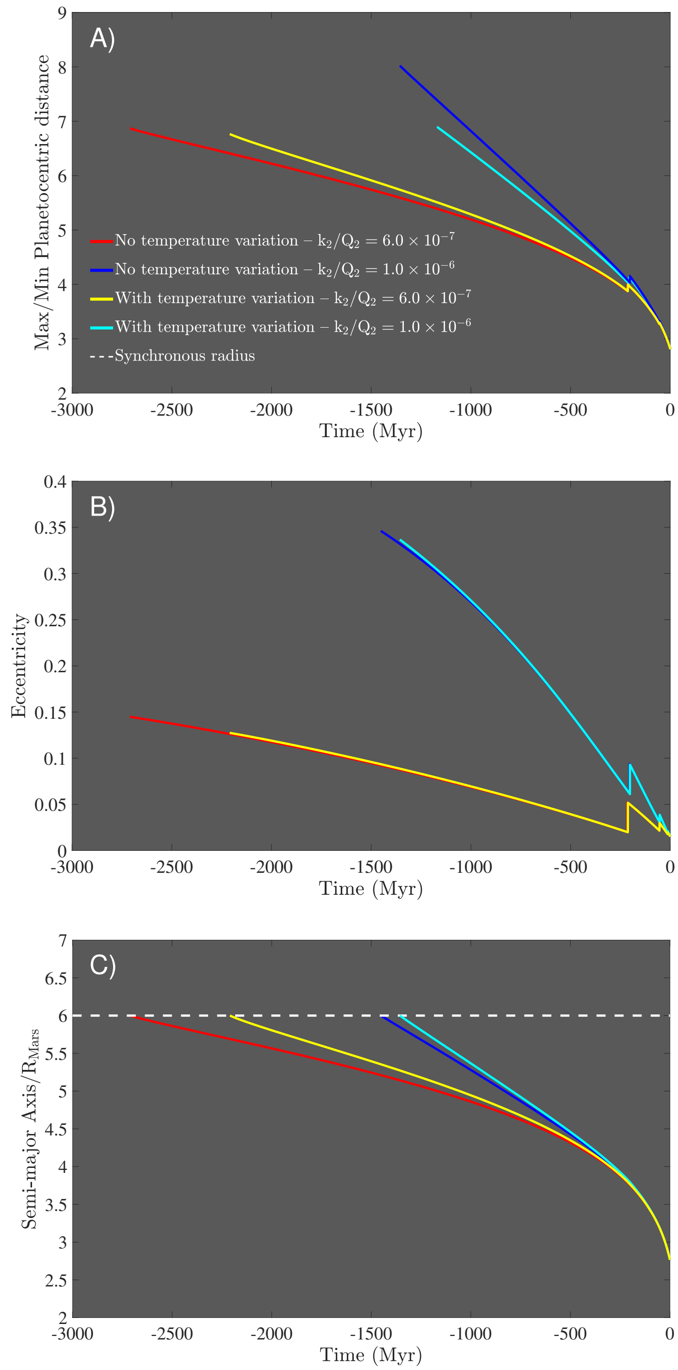

Supplementary Figure 9. Effect of the thermal history on the evolution of (A) planetocentric distance, (B) eccentricity, and (C) the semi-major axis for two rubble aggregate models of Phobos. Panels (A) and (C) are normalised to the mean radius R_M of Mars. "Varying temperature" refers to the use of the thermal history model shown in Supplementary Figure 8, whereas "Fixed temperature" refers to the use of a constant temperature model as a function of time. Relative to the cases considered in the main text, here we integrated backwards until Phobos reached the synchronous limit, as a result of which the eccentricity (B) is capable of exceeding 0.35.

12 The future of Phobos and Deimos

The tidal interaction of Deimos with Mars is, at present, very weak because of the low eccentricity, small size, and large distance from Mars (cf. Supplementary Figure 1 in the main manuscript). Phobos, on the other hand, is migrating inwards and will impact on Mars in a not-so-distant future[27,53,54]. To investigate this in more detail, we have also computed the future evolution of the orbits of Phobos and Deimos, by starting with the current semi-major axis and eccentricity of Phobos. The results shown in Supplementary Figure 10 indicate that in $\sim$39 Myr, in agreement with the aforementioned studies, Phobos will either crash onto Mars or, more likely, be torn apart by tidal stresses as it crosses the Roche radius (in 38 Myrs), and will produce a cloud of particles, to be spread into a ring[27]. These computations have demonstrated that over this stage of Phobos's history, the roles of dissipation in and libration of the satellite are negligible, even for a rubble-pile. This happens because the eccentricity rapidly approaches zero in the course of the final fall. Our results further show that due to the proximity of Phobos to Mars (9375 km), the present contribution of the degree-3 tide is approximately 10% of that of degree 2. The figure also shows that currently Phobos is in-between the fluid and solid Roche limits. The same calculations have been performed using other rheological models (extended Burgers and Sundberg-Cooper), but the difference between the results was found to be negligible.

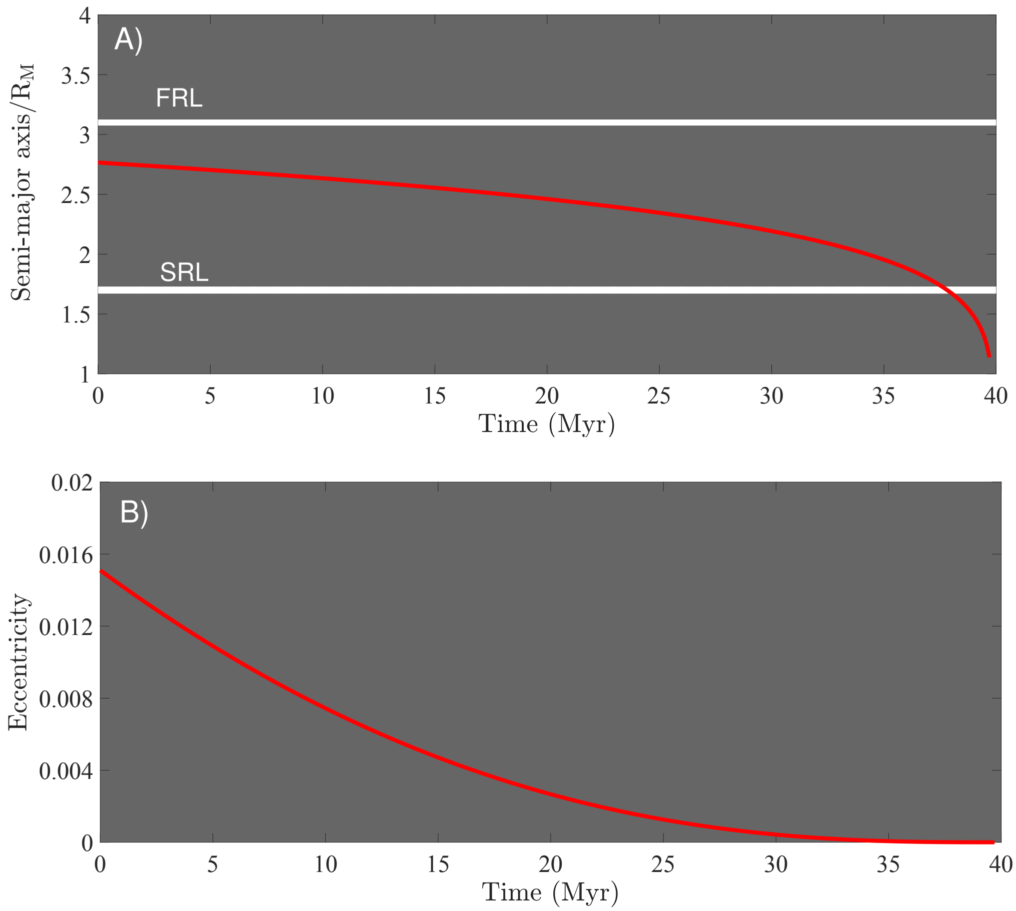

Supplementary Figure 10. Evolution of the semi-major axis (A), normalised to the mean radius R_M of Mars and eccentricity (B) of Phobos into the future. SRL and FRL refer to sold and fluid Roche limits, respectively. Because of the present-day low eccentricity, differences between dissipation in the satellite is negligible regardless of the interior properties of the moon.

13 Orbital evolution theory – general formulation

Here we present a detailed model of orbital evolution of two tidally interacting bodies. For this purpose, we extend the theory of tides to the situation where the secondary (in our case, Phobos or Deimos) follows a highly eccentric orbit and, simultaneously, performs libration in longitude. The formulation builds upon the classical Darwin-Kaula theory extended to the case with libration[55]. The derivation consists of two main steps: 1) to write down the tidally-generated evolution rates of the semi-major axis, eccentricity, and spin rate, with the effect of libration included and 2) to expand the eccentricity functions $G_{lpq}(e)$ to sufficiently high powers of e in order to stabilise the solution for eccentric orbits. We would like to note that the developments in this section simply represent the full derivation of what is given in the Methods section of the main text.

The time derivatives of the semi-major axis, a, and eccentricity, e can be written as[56]

$$\frac{da}{dt} = \frac{2}{na}\frac{\partial \mathcal{R}}{\partial \mathcal{M}} \quad , \tag{8}$$

$$\frac{de}{dt} = \frac{1-e^2}{na^2 e}\frac{\partial \mathcal{R}}{\partial \mathcal{M}} - \frac{(1-e^2)^{1/2}}{na^2 e}\left(\frac{\partial \mathcal{R}}{\partial \omega} + \frac{\partial \mathcal{R}}{\partial \omega'}\right) \quad , \tag{9}$$

$$\frac{d\dot{\theta}}{dt} = -\frac{\gamma}{C}\frac{\partial \mathcal{R}}{\partial \Omega} \tag{10}$$

where $\mathcal{M}$ is the mean anomaly, ω is the argument of the pericentre on the body's equator, n is the mean motion, Ω is longitude of the ascending node on the primary's equator, C is the moment of inertia, and $\mathcal{R}$ is the disturbing function, and $\gamma = MM'/(M+M')$. Within the two-body problem perturbed by tides in both partners, the disturbing function comprises two inputs. One is proportional to the additional tidal potential U of the primary deformed by the pull from the secondary. Another is proportional to the tidal potential U' of the secondary deformed by the primary:

$$\mathcal{R} \;=\; -\,\frac{M+M'}{M\;M'}\,\left[M'U(\mathbf{r},\mathbf{r}^*)\Big|_{\mathbf{r}^*=\mathbf{r}} + MU'(-\mathbf{r}',-\mathbf{r}^\star)\Big|_{\mathbf{r}^\star=\mathbf{r}'}\right] \quad , \tag{11}$$

where M and M' are the masses of the bodies, while the vectors are defined in the co-rotating frames of the partners. The vector $\mathbf{r}$ is pointing from the centre of mass of the primary to that of the secondary as seen in a frame co-rotating with the primary. Similarly, $-\mathbf{r}'$ is pointing from the centre of mass of the secondary to that of the primary as seen in a frame co-rotating with the secondary. These vectors are then linked by some rotation matrices to the inertial vector pointing from the centre of mass of the primary to that of the secondary. It is implied in equation (11) that in the orbital equations the differentiation of $\mathcal{R}$ should be carried out before $\mathbf{r}^*$ (respectively, $\mathbf{r}^\star$) is set equal to $\mathbf{r}$ (respectively, $\mathbf{r}'$). The tidal potential of a near-spherical librating body, which is tidally deformed by the pull from a point perturber, can be expressed through the orbital elements as[55]

$$U(\mathbf{r},\mathbf{r^*}) = -\frac{GM'}{a^*}\sum_{l=2}^{\infty}\left(\frac{R}{a}\right)^{l+1}\left(\frac{R}{a^*}\right)^{l}\sum_{m=0}^{l}\frac{(l-m)!}{(l+m)!}(2-\delta_{0m})\sum_{h=0}^{l}F_{lmh}(i)\sum_{j=-\infty}^{\infty}G_{lhj}(e)\times$$
$$\sum_{p=0}^{l}F_{lmp}(i^*)\sum_{q=-\infty}^{\infty}G_{lpq}(e^*)\sum_{s_1=-\infty}^{\infty}\sum_{s=-\infty}^{\infty}J_{s_1}(m\,\mathcal{A})\,J_s(m\,\mathcal{A})\times$$
$$k_l\cos([v^*_{lmpq}-m\theta^*-s\mathcal{M}]-[v_{lmhj}-m\theta-s_1\mathcal{M}]-\epsilon_l)\ \ , \quad (12)$$

where $\mathcal{A}$ is the perturbed body's longitudinal libration magnitude, R is its mean radius, while k_l and ϵ_l are its dynamical Love numbers and phase lags, respectively. G denotes the gravitational constant, while $F_{lmp}(i)$, $G_{lpq}(e)$, and $J_s(m\mathcal{A})$ are the inclination, eccentricity, and Bessel functions, respectively. The auxiliary quantities v_{lmpq} and v^*_{lmpq} are defined as

$$v_{lmpq} = (l-2p)\omega + (l-2p+q)\mathcal{M} + m\Omega\ \ , \quad (13)$$

$$v^*_{lmpq} = (l-2p)\omega^* + (l-2p+q)\mathcal{M} + m\Omega^*\ \ , \quad (14)$$

where ω is the argument of the pericentre, Ω is the longitude of the ascending node on the body's equator, while n is the anomalistic mean motion approximated with its Keplerian counterpart:

$$n = \dot{\mathcal{M}} \approx \sqrt{G\,(M+M')/a^3}\ \ . \quad (15)$$

The Love numbers and phase lags,

$$k_l = k_l(\beta_{lmpqs})\ \ , \qquad \epsilon_l = \epsilon_l(\beta_{lmpqs})\ \ , \quad (16)$$

are functions of the tidal Fourier modes given by

$$\beta_{lmpqs} = (l-2p)\dot{\omega} + (l-2p+q-s_1)n + m\dot{\Omega} - m\dot{\theta} \approx (l-2p+q-s_1)n - m\dot{\theta}\ \ . \quad (17)$$

This expression differs from the standard expression for the tidal Fourier mode ω_{lmpq} by the summand $-\,s_1 n$ emerging due to libration in longitude. However, in the limit of no libration ($\mathcal{A}=0$) the terms with $s_1=0$ are the only to remain. So all β_{lmpqs_1} with $s_1\neq 0$ vanish, while the expression for β_{lmpq0} matches that for ω_{lmpq}:

$$\beta_{lmpq0}\;=\;\omega_{lmpq}\;=\;(l-2p)\,\dot{\omega}\;+\;(l-2p+q)\,n\;+\;m\,\dot{\Omega}\;-\;m\,\dot{\theta}\;\approx\;(l-2p+q)\,n\;-\;m\,\dot{\theta}\;\;. \tag{18}$$

The physical forcing frequencies in a tidally perturbed body, in the absence of libration, are[57]

$$\chi_{lmpq}\;=\;|\,\omega_{lmpq}\,|\;=\;|\,\beta_{lmpq0}\,|\;\;, \tag{19}$$

while under libration the spectrum of frequencies comprises all $|\,\beta_{lmpqs_1}\,|$. In the orbital equations (8) and (9), we need to differentiate the disturbing function over the mean anomaly. Equation (11) renders us:

$$\frac{\partial\mathcal{R}}{\partial\mathcal{M}}\;=\;\frac{M+M'}{M\;M'}\,\frac{\partial}{\partial\mathcal{M}}\,\left(-\,M'\,U\;-\;M\,U'\right)\;=\;-\,\frac{M+M'}{M}\,\frac{\partial\,U}{\partial\mathcal{M}}\;-\;\frac{M+M'}{M'}\,\frac{\partial\,U'}{\partial\mathcal{M}}\;\;, \tag{20}$$

where the derivative of U is given by

$$\frac{\partial U(\mathbf{r},\mathbf{r}^*)}{\partial\mathcal{M}}=-\frac{GM'}{a^*}\sum_{l=2}^{\infty}\left(\frac{R}{a}\right)^{l+1}\left(\frac{R}{a^*}\right)^{l}\sum_{m=0}^{l}\frac{(l-m)!}{(l+m)!}(2-\delta_{0m})\sum_{h=0}^{l}F_{lmh}(i)\sum_{j=-\infty}^{\infty}G_{lhj}(e)\,\times$$

$$\sum_{p=0}^{l}F_{lmp}(i^*)\sum_{q=-\infty}^{\infty}G_{lpq}(e^*)\sum_{s_1=-\infty}^{\infty}\sum_{s=-\infty}^{\infty}J_{s_1}(m\,\mathcal{A})\,J_s(m\,\mathcal{A})(l-2p+q-s)\,\times$$

$$k_l\cos([v^*_{lmpq}-m\theta^*-s\mathcal{M}]-[v_{lmhj}-m\theta-s_1\mathcal{M}]-\epsilon_l)\;\;, \tag{21}$$

The derivative of U' is similar to (21), *mutatis mutandis*. The prime is used to mark quantities pertaining to the satellite.

Both equations (12) and (21) provide the potential in an external point $\mathbf{r}$ under the assumption that the perturber is residing at $\mathbf{r}^*$. We, however, are interested in a situation when the perturber causes the tidal deformation of its partner and then "feels" the resulting tidal potential. To describe this interaction, in these equations we should set $\mathbf{r}^*$ equal to $\mathbf{r}$ and drop the superscript, which now becomes redundant. On doing this, we notice that averaging over the apsidal precession leaves only the terms with $h = p$, while averaging over an orbital cycle leaves only the terms with $q - s = j - s_1$. This observation enables us to write down the secular parts of both $\partial U/\partial \mathcal{M}$ and $\partial U'/\partial \mathcal{M}$:

$$\left\langle\left\langle\frac{\partial U}{\partial \mathcal{M}}\right\rangle\right\rangle = \sum_{l=2}^{\infty}\left(\frac{R}{a}\right)^{2l+1}\frac{GM'}{a}\sum_{m=0}^{l}\frac{(l-m)!}{(l+m)!}(2-\delta_{0m})\sum_{p=0}^{l}F^2_{lmp}(i)$$
$$\sum_{q=-\infty}^{\infty}\sum_{j=-\infty}^{\infty}G_{lpq}(e)G_{lpj}(e)(l-2p+q)k_l\sin\epsilon_l \ , \qquad (22)$$

$$\left\langle\left\langle\frac{\partial U'}{\partial \mathcal{M}}\right\rangle\right\rangle = \sum_{l=2}^{\infty}\left(\frac{R'}{a}\right)^{2l+1}\frac{GM}{a}\sum_{m=0}^{l}\frac{(l-m)!}{(l+m)!}(2-\delta_{0m})\sum_{p=0}^{l}F^2_{lmp}(i')\sum_{q=-\infty}^{\infty}\sum_{j=-\infty}^{\infty}G_{lpj}(e)G_{lpq}(e)$$
$$\sum_{s=-\infty}^{\infty}(l-2p+q-s)J_{j-q+s}(m\mathcal{A})J_s(m\mathcal{A})k'_l\sin\epsilon'_l \ .(23)$$

Note that in expression (22) we dropped the libration-generated terms (and kept only the terms with $s_1 = s = 0$), while in (23) we preserved such terms (to be precise, those of them which are secular, i.e., satisfy $q - s = j - s_1$). We have done this, assuming that the primary has a relatively small triaxiality and, therefore, a relatively small contribution from longitudinal libration into tidal dynamics. For the secondary, this assumption is often inapplicable and the libration terms must be kept[58]. In equation (22), i is the inclination of the secondary's orbit on the primary's equator, while i' in equation (23) denotes the inclination of the primary's apparent orbit on the secondary's equator. As was explained above, the quality functions of the primary, $k_l\,\sin\epsilon_{lmpq}$, depend on the tidal modes in the primary, equations (16–17). Similarly, the quality functions of the secondary, $k'_l\,\sin\epsilon'_{lmpq}$, depend on the tidal modes in the secondary:

$$k'_l \ = \ k'_l(\beta'_{lmpqs}) \ \ , \quad \ \epsilon'_l \ = \ \epsilon'_l(\beta'_{lmpqs}) \ \ , \qquad (24)$$

where the Fourier modes excited in the secondary are

$$\beta'_{lmpqs} = (l-2p)\dot{\omega}' + (l-2p+q-s_1)n + m\dot{\Omega}' - m\dot{\theta}' \approx \ (l\ -\ 2p\ -\ m\ +\ q\ -\ s)n, \qquad (25)$$

ω' being the argument of the pericentre (as seen from the secondary), Ω', being the longitude of the ascending node on the secondary's equator, and $\dot{\theta}'$ being the secondary's spin rate.

To make use of equation (9), we need to differentiate $\mathcal{R}$ with respect to the argument of the pericentre ω. From expression (12), we obtain

$$\frac{\partial \mathcal{R}}{\partial \omega} + \frac{\partial \mathcal{R}}{\partial \omega'} = \frac{M+M'}{M\,M'}\left(\frac{\partial}{\partial \omega}\left(-M'U\right) + \frac{\partial}{\partial \omega'}\left(-M\,U'\right)\right) \tag{26}$$

In neglect of the libration of the primary, the derivative of the potential with respect to ω is

$$\left\langle\left\langle\frac{\partial U}{\partial \omega}\right\rangle\right\rangle = \sum_{l=2}^{\infty}\left(\frac{R}{a}\right)^{2l+1}\frac{G\,M'}{a}\sum_{m=0}^{l}\frac{(l-m)!}{(l+m)!}\,(2-\delta_{0m})\sum_{p=0}^{l}F^2_{lmp}(i)(l-2p)\;k_l\,\sin\epsilon_l \sum_{q=-\infty}^{\infty}\sum_{j=-\infty}^{\infty}G_{lpq}(e)G_{lpj}(e), \tag{27}$$

which agrees with the non-librating case[56]. For the librating secondary, the result is:

$$\left\langle\left\langle\frac{\partial U'}{\partial \omega'}\right\rangle\right\rangle = \sum_{l=2}^{\infty}\left(\frac{R'}{a}\right)^{2l+1}\frac{G\,M}{a}\sum_{m=0}^{l}\frac{(l-m)!}{(l+m)!}\,(2-\delta_{0m})\sum_{p=0}^{l}F^2_{lmp}(i')\sum_{j=-\infty}^{\infty}\sum_{q=-\infty}^{\infty}G_{lpq}(e)G_{lpj}(e) \sum_{s=-\infty}^{\infty}(l-2p)\,J_{j-q+s}(m\,\mathcal{A})\,J_s(m\,\mathcal{A})\;k'_l\,\sin\epsilon_l \tag{28}$$

The insertion of equations (22), (23), (27), and (28) in formulae (8) and (9) renders us the following expressions for the secular parts of the rates:

$$\frac{da}{dt} = -2an\sum_{l=2}^{\infty}\sum_{m=0}^{l}\frac{(l-m)!}{(l+m)!}(2-\delta_{0m})\sum_{p=0}^{l}\sum_{q=-\infty}^{\infty}\sum_{s=-\infty}^{\infty}\sum_{j=-\infty}^{\infty}G_{lpq}(e)G_{lpj}(e)(l-2p+q-s) \left[\left(\frac{R}{a}\right)^{2l+1}\frac{M'}{M}F^2_{lmp}(i)K_l(\beta)+\left(\frac{R'}{a}\right)^{2l+1}\frac{M}{M'}J_{j-q+s}(m\mathcal{A})J_s(m\mathcal{A})F^2_{lmp}(i')K_l(\beta')\right] \tag{29}$$

and

$$\begin{aligned}\frac{de}{dt} = &-\frac{1-e^2}{e}\frac{n}{MM'}\sum_{l=2}^{\infty}\sum_{m=0}^{l}\frac{(l-m)!}{(l+m)!}(2-\delta_{0m})\sum_{p=0}^{l}\sum_{q=-\infty}^{\infty}\sum_{s=-\infty}^{\infty}\sum_{j=-\infty}^{\infty}G_{lpq}(e)G_{lpj}(e)(l-2p+q-s)\\ &\left[\left(\frac{R}{a}\right)^{2l+1}\frac{M'}{M}F^2_{lmp}(i)K_l(\beta)+\left(\frac{R'}{a}\right)^{2l+1}\frac{M}{M'}J_{j-q+s}(m\mathcal{A})J_s(m\mathcal{A})F^2_{lmp}(i')K'_l(\beta')\right]+\\ &-\frac{\sqrt{1-e^2}}{e}\frac{n}{MM'}\sum_{l=2}^{\infty}\sum_{m=0}^{l}\frac{(l-m)!}{(l+m)!}(2-\delta_{0m})\sum_{p=0}^{l}\sum_{q=-\infty}^{\infty}\sum_{s=-\infty}^{\infty}\sum_{j=-\infty}^{\infty}G_{lpq}(e)G_{lpj}(e)(l-2p)\\ &\left[\left(\frac{R}{a}\right)^{2l+1}\frac{M'}{M}F^2_{lmp}(i)K_l(\beta)+\left(\frac{R'}{a}\right)^{2l+1}\frac{M}{M'}J_{j-q+s}(m\mathcal{A})J_s(m\mathcal{A})F^2_{lmp}(i')K'_l(\beta')\right],\end{aligned} \tag{30}$$

where $K_l(\beta) = k_l \sin\epsilon_l$ and $K_l'(\beta') = k_l' \sin\epsilon_l'$ are the tidal response functions of the primary and the secondary, respectively. A similar expression for the inclination rate will be presented at the end of this section. Given the above series' slow convergence over the powers of e, we have to include high-order terms, to ensure precision of our results and stability of integration for fairly high eccentricities. The eccentricities we deal with in this study remain below 0.35 but the formulation presented here is stable at least for $e < 0.5$. For this purpose, we have computed the terms to degree 18 in the eccentricity and the libration magnitude, assuming that the magnitude of libration is of the same order as eccentricity, which is true for synchronised bodies[55]. The terms in the expansion of the eccentricity functions $G_{lpq}(e)$ to degree 18 are compiled in Table S2.

The expanded equations for da/dt and de/dt are presented below. Each rate comprises three contributions: the main (unrelated to libration) contribution due to the tides in the planet, the main contribution from the tides in the satellite, and the contribution due to the longitudinal libration of the satellite:

$$\left(\frac{da}{dt}\right) = \left(\frac{da}{dt}\right)^{main}_{planet} + \left(\frac{da}{dt}\right)^{main}_{satellite} + \left(\frac{da}{dt}\right)^{libration}_{satellite} \quad , \tag{31}$$

$$\left(\frac{de}{dt}\right) = \left(\frac{de}{dt}\right)^{main}_{planet} + \left(\frac{de}{dt}\right)^{main}_{satellite} + \left(\frac{de}{dt}\right)^{libration}_{satellite} \quad . \tag{32}$$

$$\left(\frac{di}{dt}\right) = \left(\frac{di}{dt}\right)_{planet} \tag{33}$$

Expanding equations (29) and (30), as shown in Table 13, and employing the expressions for each of the terms, we obtain

$$\left(\frac{da}{dt}\right)^{main}_{planet} = n\left(\frac{R^5}{a^4}\right)\left(\frac{M'}{M}\right) \times \mathcal{F}(K_l,\, \dot{\theta},\, n,\, e) \quad , \tag{34}$$

l	p	q	l	p	q	G
2	0	-2	2	2	2	0
2	0	-1	2	2	1	$1+\frac{1}{2}e+\frac{1}{16}e^3-\frac{5}{384}e^5-\frac{143}{8432}e^7-\frac{9097}{1474560}e^9-\frac{878959}{176947200}e^{11}-\frac{121671181}{29727129600}e^{13}-\frac{4582504819}{1331775406080}e^{15}-\frac{5642260227857}{1917756584755200}e^{17}$
2	0	0	2	2	0	$-\frac{5}{2}e^2+\frac{13}{16}e^4-\frac{35}{288}e^6-\frac{5}{576}e^8-\frac{49}{3600}e^{10}-\frac{3725}{331776}e^{12}-\frac{7767869}{812851200}e614-\frac{5345003}{650280960}e^{16}-\frac{753254387}{105345515520}e^{18}$
2	0	1	2	2	-1	$\frac{7}{2}e-\frac{123}{16}e^3+\frac{489}{128}e^5-\frac{1763}{2048}e^7+\frac{13527}{163840}e^9-\frac{180369}{6553600}e^{11}-\frac{5986093}{367001600}e^{13}-\frac{24606987}{1677721600}e^{15}-\frac{33790034193}{2630667468800}e^{17}$
2	0	2	2	2	-2	$\frac{17}{2}e^2-\frac{115}{6}e^4+\frac{601}{48}e^6-\frac{1423}{360}e^8+\frac{48619}{69120}e^{10}-\frac{275587}{2419200}e^{12}-\frac{157057}{11612160}e^{14}-\frac{17992547}{914457600}e^{16}-\frac{4986336247}{292626432000}e^{18}$
2	1	-2	2	1	2	$\frac{9}{4}e^2+\frac{7}{4}e^4+\frac{141}{64}e^6+\frac{197}{80}e^8+\frac{62401}{23040}e^{10}+\frac{262841}{89600}e^{12}+\frac{9010761}{2867200}e^{14}+\frac{8142135359}{2438553600}e^{16}+\frac{32739616891}{9289728000}e^{18}$
2	1	-1	2	1	1	$\frac{3}{2}e+\frac{27}{16}e^3+\frac{261}{128}e^5+\frac{14309}{6144}e^7+\frac{423907}{163840}e^9+\frac{55489483}{19660800}e^{11}+\frac{30116927341}{9909043200}e^{13}+\frac{2398598468863}{739875225600}e^{15}+\frac{731422665109147}{213084064972800}e^{17}$
			2	1	0	$\frac{3}{2}e^2+\frac{15}{8}e^4+\frac{35}{16}e^6+\frac{315}{128}e^8+\frac{693}{256}e^{10}+\frac{3003}{1024}e^{12}+\frac{6435}{2048}e^{14}+\frac{109395}{32768}e^{16}+\frac{230945}{65536}e^{18}$
			2	0	3	$\frac{845}{48}e^3-\frac{32525}{768}e^5+\frac{208225}{6144}e^7-\frac{6122725}{442368}e^9+\frac{169407625}{49545216}e^{11}-\frac{138861515}{226492416}e^{13}+\frac{16018198925}{342456532992}e^{15}-\frac{572721715525}{19177565847552}e^{17}$
			2	0	4	$\frac{533}{16}e^4-\frac{13827}{160}e^6+\frac{104127}{1280}e^8-\frac{146017}{3584}e^{10}+\frac{1832259}{143360}e^{12}-\frac{4045953}{1433600}e^{14}+\frac{6006701}{14336000}e^{16}-\frac{180571023}{2207744000}e^{18}$
			2	0	-3	$\frac{1}{48}e^3+\frac{11}{768}e^5+\frac{313}{30720}e^7+\frac{3355}{442368}e^9+\frac{1459489}{247726080}e^{11}+\frac{187662659}{39636172800}e^{13}+\frac{33454202329}{8561413324800}e^{15}+\frac{7896099250367}{2397195730944000}e^{17}$
2	1	3	2	1	-3	$\frac{53}{16}e^3+\frac{393}{256}e^5+\frac{24753}{10240}e^7+\frac{211557}{81920}e^9+\frac{3702771}{1310720}e^{11}+\frac{4463853417}{1468006400}e^{13}+\frac{38085221651}{11744051200}e^{15}+\frac{11289940750071}{3288334336000}e^{17}$
2	1	4	2	1	-4	$\frac{77}{16}e^4+\frac{129}{160}e^6+\frac{899}{320}e^8+\frac{107279}{40320}e^{10}+\frac{421681}{143360}e^{12}+\frac{4507393}{1433600}e^{14}+\frac{5818175177}{1741824000}e^{16}+\frac{4093627549}{1161216000}e^{18}$
2	1	6	2	1	-6	$\frac{3167}{320}e^6-\frac{2187}{560}e^8+\frac{195147}{35840}e^{10}+\frac{78881}{35840}e^{12}+\frac{9427827}{2867200}e^{14}+\frac{261967071}{78848000}e^{16}+\frac{318020577}{90112000}e^{18}$
			2	0	-6	$\frac{4}{45}e^6+\frac{2}{45}e^8+\frac{11}{252}e^{10}+\frac{2419}{68040}e^{12}+\frac{40777}{1360800}e^{14}+\frac{3814807}{149688000}e^{16}+\frac{67569937}{3079296000}e^{18}$
			2	0	6	$\frac{73369}{720}e^6-\frac{775727}{2520}e^8+\frac{7527241}{20160}e^{10}-\frac{138794029}{544320}e^{12}+\frac{9897062071}{87091200}e^{14}-\frac{43199752201}{1197504000}e^{16}+\frac{737494329571}{86220288000}e^{18}$
			2	0	7	$\frac{12144273}{71680}e^7-\frac{252361629}{458752}e^9+\frac{13581249561}{18350080}e^{11}-\frac{59958476649}{104857600}e^{13}+\frac{37773814995027}{129184563200}e^{15}-\frac{158692610820879}{1476395008000}e^{17}$
			2	0	-7	$\frac{15625}{129024}e^7+\frac{171875}{4128768}e^9+\frac{16015625}{297271296}e^{11}+\frac{43328125}{1019215872}e^{13}+\frac{46167453125}{1255673954304}e^{15}+\frac{24778859375}{782757789696}e^{17}$
			2	0	8	$\frac{634085}{2304}e^8-\frac{277861775}{290304}e^{10}+\frac{3282005975}{2322432}e^{12}-\frac{186605367425}{153280512}e^{14}+\frac{3669781375}{5225472}e^{16}-\frac{501594707815}{1707982848}e^{18}$
			2	0	-8	$\frac{729}{4480}e^8+\frac{243}{8960}e^{10}+\frac{24057}{358400}e^{12}+\frac{75087}{1576960}e^{14}+\frac{84807}{1971200}e^{16}+\frac{76433463}{2050048000}e^{18}$
2	1	8	2	1	-8	$\frac{178331}{8960}e^8-\frac{9009241}{483840}e^{10}+\frac{17569129}{1075200}e^{12}-\frac{17659127}{7884800}e^{14}+\frac{37460681513}{7664025600}e^{16}+\frac{151625977559}{47443968000}e^{18}$
2	1	7	2	1	-7	$\frac{432091}{30720}e^7-\frac{3073843}{327680}e^9+\frac{215487317}{23592960}e^{11}+\frac{7927962371}{8493465600}e^{13}+\frac{169854242467}{45298483200}e^{15}+\frac{400339112403797}{119587995648000}e^{17}$
			2	0	-4	$\frac{1}{24}e^4+\frac{7}{240}e^6+\frac{131}{5760}e^8+\frac{4303}{241920}e^{10}+\frac{27617}{1935360}e^{12}+\frac{2041741}{174182400}e^{14}+\frac{7336259}{746496000}e^{16}+\frac{13490862223}{1609445376000}e^{18}$

Supplementary Table 2: Expansion of the eccentricity function G where $\mathcal{F}$ is a function of the eccentricity and mean motion of the orbit, as well as of the spin rate and the tidal response $K_l(\beta)$ of the body:

$$\mathcal{F}(K_l, n, \dot{\theta}, e) = -3K_l(2n-2\dot{\theta}) + e^2\left(-\frac{9\,K_l(n)}{4} - \frac{3}{8}\,K_l(n-2\dot{\theta}) + 15\,K_l(2n-2\dot{\theta}) - \frac{441}{8}\,K_l(3n-2\dot{\theta})\right)+$$
$$e^4\left(-\frac{81\,K_l(n)}{16} - \frac{81}{8}\,K_l(2n) + \frac{3}{32}\,K_l(n-2\dot{\theta}) - \frac{189}{8}\,K_l(2n-2\dot{\theta}) + \frac{7749}{32}\,K_l(3n-2\dot{\theta}) - \frac{867}{2}\,K_l(4n-2\dot{\theta})\right)+$$
$$e^6\left(-\frac{2295\,K_l(n)}{256} - \frac{63}{4}\,K_l(2n) - \frac{8427}{256}\,K_l(3n) + \frac{K_l(-n-2\dot{\theta})}{1536} - \frac{13}{512}\,K_l(n-2\dot{\theta}) + \frac{155}{12}\,K_l(2n-2\dot{\theta}) -\right.$$
$$\left.\frac{197775}{512}\,K_l(3n-2\dot{\theta}) + 1955\,K_l(4n-2\dot{\theta}) - \frac{3570125\,K_l(5n-2\dot{\theta})}{1536}\right)+$$
$$e^8\left(-\frac{28403\,K_l(n)}{2048} - \frac{1661}{64}\,K_l(2n) - \frac{62487\,K_l(3n)}{2048} - \frac{5929}{64}\,K_l(4n) + \frac{11\,K_l(-n-2\dot{\theta})}{12288} - \frac{113\,K_l(n-2\dot{\theta})}{12288} -\right.$$
$$\frac{2881}{768}\,K_l(2n-2\dot{\theta}) + \frac{1193715\,K_l(3n-2\dot{\theta})}{4096} - \frac{83551}{24}\,K_l(4n-2\dot{\theta}) + \frac{137418125\,K_l(5n-2\dot{\theta})}{12288} -$$
$$\left.\frac{2556801}{256}\,K_l(6n-2\dot{\theta}) + \frac{1}{192}\,K_l(-2(n+\dot{\theta}))\right)+$$
$$e^{10}\left(-\frac{3240741\,K_l(n)}{163840} - \frac{12027}{320}\,K_l(2n) - \frac{18059643\,K_l(3n)}{327680} - \frac{9933}{320}\,K_l(4n) - \frac{15717645\,K_l(5n)}{65536} +\right.$$
$$+\frac{59049\,K_l(-3n-2\dot{\theta})}{3276800} + \frac{619\,K_l(-n-2\dot{\theta})}{655360} - \frac{2639\,K_l(n-2\dot{\theta})}{327680} + \frac{3481\,K_l(2n-2\dot{\theta})}{6400} - \frac{41889501\,K_l(3n-2\dot{\theta})}{327680} +$$
$$\frac{131319}{40}\,K_l(4n-2\dot{\theta}) -$$
$$\left.\frac{2936126875\,K_l(5n-2\dot{\theta})}{131072} + \frac{66328119\,K_l(6n-2\dot{\theta})}{1280} - \frac{364996466863\,K_l(7n-2\dot{\theta})}{9830400} + \frac{7}{960}\,K_l(-2(n+\dot{\theta}))\right)+$$
$$e^{12}\left(-\frac{87480539\,K_l(n)}{3276800} - \frac{525521\,K_l(2n)}{10240} - \frac{96458913\,K_l(3n)}{1310720} - \frac{708871\,K_l(4n)}{6400} + \frac{14736585\,K_l(5n)}{262144} -\right.$$
$$\frac{30089667\,K_l(6n)}{51200} + \frac{59049\,K_l(-3n-2\dot{\theta})}{2621440} + \frac{64537\,K_l(-n-2\dot{\theta})}{70778880} - \frac{129709\,K_l(n-2\dot{\theta})}{19660800} -$$
$$\frac{12791\,K_l(2n-2\dot{\theta})}{92160} + \frac{237091671\,K_l(3n-2\dot{\theta})}{6553600} - \frac{2459537\,K_l(4n-2\dot{\theta})}{1280} + \frac{356500341875\,K_l(5n-2\dot{\theta})}{14155776} -$$
$$\frac{5938832817\,K_l(6n-2\dot{\theta})}{51200} + \frac{981779068235\,K_l(7n-2\dot{\theta})}{4718592} -$$
$$\left.\frac{5383010161\,K_l(8n-2\dot{\theta})}{43200} + \frac{949\,K_l(-2(n+\dot{\theta}))}{115200} + \frac{32}{675}\,K_l(-2(2n+\dot{\theta}))\right)+$$

$$e^{14}\Bigg(-\frac{76230921863K_l(n)}{2202009600} - \frac{13519469K_l(2n)}{201600} - \frac{10219795947K_l(3n)}{104857600} - \frac{1736021K_l(4n)}{14400}$$
$$+\frac{20778687K_l(6n)}{44800} - \frac{1306918425967K_l(7n)}{943718400} + \frac{1220703125K_l(-5n-2\dot{\theta})}{11098128384} + \frac{38558997K_l(-3n-2\dot{\theta})}{1468006400}+$$
$$\frac{33683687K_l(-n-2\dot{\theta})}{39636172800} - \frac{73185503K_l(n-2\dot{\theta})}{13212057600} - \frac{288163K_l(2n-2\dot{\theta})}{5644800} - \frac{1586248587K_l(3n-2\dot{\theta})}{209715200}+$$
$$\frac{232033433K_l(4n-2\dot{\theta})}{302400} - \frac{29029068521875K_l(5n-2\dot{\theta})}{1585446912} + \frac{13527027819K_l(6n-2\dot{\theta})}{89600}-$$
$$\frac{2921128205246293K_l(7n-2\dot{\theta})}{5662310400} + \frac{56914314263K_l(8n-2\dot{\theta})}{75600} - \frac{3982050900860283K_l(9n-2\dot{\theta})}{10276044800}+$$
$$\frac{10193K_l(-2(n+\dot{\theta}))}{1209600} + \frac{32}{675}K_l(-2(2n+\dot{\theta})) - \frac{67620980465K_l(5n)}{264241152}\Bigg)+$$
$$e^{16}\Bigg(-\frac{143189681823K_l(n)}{3288334336} - \frac{729537581K_l(2n)}{8601600} - \frac{1455222699297K_l(3n)}{11744051200} - \frac{27865091K_l(4n)}{172032}-$$
$$\frac{212874343975K_l(5n)}{1409286144} - \frac{592612065K_l(6n)}{802816} + \frac{9297259269991K_l(7n)}{5033164800} - \frac{31801945561K_l(8n)}{10035200}+$$
$$\frac{13427734375K_l(-5n-2\dot{\theta})}{177570054144} + -\frac{1497798429597K_l(6n-2\dot{\theta})}{11468800}$$
$$\frac{18482337K_l(-3n-2\dot{\theta})}{671088640} + \frac{165074183K_l(-n-2\dot{\theta})}{211392921600} - \frac{21004537637K_l(n-2\dot{\theta})}{4439251353600} - \frac{1190849K_l(2n-2\dot{\theta})}{24084480}+$$
$$\frac{863843049K_l(3n-2\dot{\theta})}{939524096} - \frac{77502109K_l(4n-2\dot{\theta})}{345600} + \frac{79231092391625K_l(5n-2\dot{\theta})}{8455716864}$$
$$+\frac{2760195487312025K_l(7n-2\dot{\theta})}{3623878656} - \frac{578658802849K_l(8n-2\dot{\theta})}{282240} + \frac{82748209967119359K_l(9n-2\dot{\theta})}{32883343360}-$$
$$\frac{2010318936125K_l(10n-2\dot{\theta})}{1769472} + \frac{127453K_l(-2(n+\dot{\theta}))}{15482880} + \frac{92K_l(-2(2n+\dot{\theta}))}{1575} + \frac{4782969K_l(-2(3n+\dot{\theta}))}{20070400}\Bigg)+$$

$$
\begin{aligned}
&e^{18}\Bigg(-\frac{3798168072196597K_l(n)}{71028021657600} - \frac{56670971611K_l(2n)}{541900800} - \frac{28832512267869K_l(3n)}{187904819200} - \frac{2578148063K_l(4n)}{12902400} - \\
&\frac{13593131130225K_l(5n)}{52613349376} - \frac{124700799K_l(6n)}{20070400} - \frac{6999935835286093K_l(7n)}{2899102924800} + \frac{1606626956771K_l(8n)}{270950400} - \\
&\frac{3729229127718641K_l(9n)}{5261334937600} + \frac{232630513987207K_l(-7n-2\dot{\theta})}{469654673817600} + \frac{1619873046875K_l(-5n-2\dot{\theta})}{14611478740992} + \\
&\frac{72655602021K_l(-3n-2\dot{\theta})}{2630667468800} + \frac{195618433037K_l(-n-2\dot{\theta})}{273965226393600} - \frac{5242619992367K_l(n-2\dot{\theta})}{1278504389836800} \\
&-\frac{535500317K_l(2n-2\dot{\theta})}{12541132800} - \frac{220413818169K_l(3n-2\dot{\theta})}{751619276800} \\
&+\frac{1505096129K_l(4n-2\dot{\theta})}{30481920} - \frac{5599532275549375K_l(5n-2\dot{\theta})}{1565515579392} + \frac{931614290433K_l(6n-2\dot{\theta})}{11468800} - \\
&\frac{99407098665529983 23K_l(7n-2\dot{\theta})}{13045963161600} + \frac{77318558814617K_l(8n-2\dot{\theta})}{22861440} - \frac{112305921952666663 89K_l(9n-2\dot{\theta})}{1503238553600} \\
&+\frac{880939918004375K_l(10n-2\dot{\theta})}{111476736} - \frac{731370370431554889900 59K_l(11n-2\dot{\theta})}{23013079017062400} + \frac{781813K_l(-2(n+\dot{\theta}))}{99532800} + \\
&\frac{7808K_l(-2(2n+\dot{\theta}))}{127575} + \frac{1594323K_l(-2(3n+\dot{\theta}))}{20070400}\Bigg)
\end{aligned}
\tag{35}
$$

The "main" (i.e. unrelated to libration) contribution from the tides in the satellite reads as

$$
\left(\frac{da}{dt}\right)^{main}_{satellite} = n\left(\frac{{R'}^5}{a^4}\right)\left(\frac{M}{M'}\right) \times \mathcal{F}(K_l',\,\dot{\theta}',\,n,\,e). \tag{36}
$$

The above equations are general, with neither of the bodies assumed synchronous. In the specific situation of a synchronised moon, we have $\dot{\theta}' = n$, wherefore the semidiurnal term in equation (35) vanishes: $K_l(2n-2\dot{\theta}') = 0$. In the contribution from the planet, the semidiurnal term vanishes when the satellite is at the synchronous orbit, i.e. when $n = \dot{\theta}$. Longitudinal libration of a synchronised satellite renders the following contribution:

$$
\left(\frac{da}{dt}\right)^{libration}_{satellite} = n\left(\frac{{R'}^5}{a^4}\right)\left(\frac{M}{M'}\right) \times \mathcal{G}(K_l',\,n,\,e,\,\mathcal{A}), \tag{37}
$$

where the function $\mathcal{G}$ is given by

$$\left(-3\mathcal{A}^2+3\mathcal{A}^4-\frac{5\mathcal{A}^6}{4}+\frac{7\mathcal{A}^8}{24}-\frac{7\mathcal{A}^{10}}{160}+\frac{11\mathcal{A}^{12}}{2400}-\frac{143\mathcal{A}^{14}}{403200}+\frac{143\mathcal{A}^{16}}{6773760}-\frac{2431\mathcal{A}^{18}}{2438553600}\right)K_l(n)+$$
$$\left(-\frac{3\mathcal{A}^4}{2}+\mathcal{A}^6-\frac{7\mathcal{A}^8}{24}+\frac{\mathcal{A}^{10}}{20}-\frac{11\mathcal{A}^{12}}{1920}+\frac{143\mathcal{A}^{14}}{302400}-\frac{143\mathcal{A}^{16}}{4838400}+\frac{221\mathcal{A}^{18}}{152409600}\right)K_l(2n)+$$
$$\left(-\frac{\mathcal{A}^6}{4}+\frac{\mathcal{A}^8}{8}-\frac{9\mathcal{A}^{10}}{320}+\frac{11\mathcal{A}^{12}}{2880}-\frac{143\mathcal{A}^{14}}{403200}+\frac{13\mathcal{A}^{16}}{537600}-\frac{221\mathcal{A}^{18}}{174182400}\right)K_l(3n)+$$
$$\left(-\frac{\mathcal{A}^8}{48}+\frac{\mathcal{A}^{10}}{120}-\frac{11\mathcal{A}^{12}}{7200}+\frac{13\mathcal{A}^{14}}{75600}-\frac{13\mathcal{A}^{16}}{967680}+\frac{17\mathcal{A}^{18}}{21772800}\right)K_l(4n)+$$
$$\left(-\frac{\mathcal{A}^{10}}{960}+\frac{\mathcal{A}^{12}}{2880}-\frac{13\mathcal{A}^{14}}{241920}+\frac{\mathcal{A}^{16}}{193536}-\frac{17\mathcal{A}^{18}}{48771072}\right)K_l(5n)+$$
$$\left(-\frac{\mathcal{A}^{12}}{28800}+\frac{\mathcal{A}^{14}}{100800}-\frac{\mathcal{A}^{16}}{752640}+\frac{17\mathcal{A}^{18}}{152409600}\right)K_l(6n)+$$
$$\left(-\frac{\mathcal{A}^{14}}{1209600}+\frac{\mathcal{A}^{16}}{4838400}-\frac{17\mathcal{A}^{18}}{696729600}\right)K_l(7n)+$$
$$\left(-\frac{\mathcal{A}^{16}}{67737600}+\frac{\mathcal{A}^{18}}{304819200}\right)K_l(8n)-\frac{\mathcal{A}^{18}K_l(9n)}{4877107200}+$$

$$
e\Bigg(\left(30\mathcal{A}-42\mathcal{A}^3+\frac{45\mathcal{A}^5}{2}-\frac{77\mathcal{A}^7}{12}+\frac{91\mathcal{A}^9}{80}-\frac{11\mathcal{A}^{11}}{80}+\frac{2431\mathcal{A}^{13}}{201600}-\frac{2717\mathcal{A}^{15}}{3386880}+\frac{2431\mathcal{A}^{17}}{58060800}\right)K_l(n)
$$

$$
+\left(21\mathcal{A}^3-18\mathcal{A}^5+\frac{77\mathcal{A}^7}{12}-\frac{13\mathcal{A}^9}{10}+\frac{11\mathcal{A}^{11}}{64}-\frac{2431\mathcal{A}^{13}}{151200}+\frac{2717\mathcal{A}^{15}}{2419200}-\frac{221\mathcal{A}^{17}}{3628800}\right)K_l(2n)
$$

$$
+\left(\frac{9\mathcal{A}^5}{2}-\frac{11\mathcal{A}^7}{4}+\frac{117\mathcal{A}^9}{160}-\frac{11\mathcal{A}^{11}}{96}+\frac{2431\mathcal{A}^{13}}{201600}-\frac{247\mathcal{A}^{15}}{268800}+\frac{221\mathcal{A}^{17}}{4147200}\right)K_l(3n)
$$

$$
+\left(\frac{11\mathcal{A}^7}{24}-\frac{13\mathcal{A}^9}{60}+\frac{11\mathcal{A}^{11}}{240}-\frac{221\mathcal{A}^{13}}{37800}+\frac{247\mathcal{A}^{15}}{483840}-\frac{17\mathcal{A}^{17}}{518400}\right)K_l(4n)
$$

$$
+\left(\frac{13\mathcal{A}^9}{480}-\frac{\mathcal{A}^{11}}{96}+\frac{221\mathcal{A}^{13}}{120960}-\frac{19\mathcal{A}^{15}}{96768}+\frac{17\mathcal{A}^{17}}{1161216}\right)K_l(5n)
$$

$$
+\left(\frac{\mathcal{A}^{11}}{960}-\frac{17\mathcal{A}^{13}}{50400}+\frac{19\mathcal{A}^{15}}{376320}-\frac{17\mathcal{A}^{17}}{3628800}\right)K_l(6n)
$$

$$
+\left(\frac{17\mathcal{A}^{13}}{604800}-\frac{19\mathcal{A}^{15}}{2419200}+\frac{17\mathcal{A}^{17}}{16588800}\right)K_l(7n)+\left(\frac{19\mathcal{A}^{15}}{33868800}-\frac{\mathcal{A}^{17}}{7257600}\right)K_l(8n)+\frac{\mathcal{A}^{17}K_l(9n)}{116121600}\Bigg)+e^2\times
$$

$$
\Bigg(\left(\frac{825\mathcal{A}^2}{4}-\frac{2753\mathcal{A}^4}{16}+\frac{6313\mathcal{A}^6}{96}-\frac{9303\mathcal{A}^8}{640}+\frac{20153\mathcal{A}^{10}}{9600}-\frac{68959\mathcal{A}^{12}}{322560}+\frac{2192333\mathcal{A}^{14}}{135475200}-\frac{9231079\mathcal{A}^{16}}{9754214400}\right)K_l(n)
$$

$$
+\left(-\frac{249}{2}\mathcal{A}^2+\frac{305\mathcal{A}^4}{2}-\frac{421\mathcal{A}^6}{6}+\frac{139\mathcal{A}^8}{8}-\frac{5207\mathcal{A}^{10}}{1920}+\frac{176803\mathcal{A}^{12}}{604800}-\frac{55913\mathcal{A}^{14}}{2419200}+\frac{426439\mathcal{A}^{16}}{304819200}\right)K_l(2n)
$$

$$
+\left(-\frac{709}{16}\mathcal{A}^4+\frac{1063\mathcal{A}^6}{32}-\frac{2685\mathcal{A}^8}{256}+\frac{21953\mathcal{A}^{10}}{11520}-\frac{52613\mathcal{A}^{12}}{230400}+\frac{14001\mathcal{A}^{14}}{716800}-\frac{125099\mathcal{A}^{16}}{99532800}\right)K_l(3n)
$$

$$
+\left(-\frac{301}{48}\mathcal{A}^6+\frac{817\mathcal{A}^8}{240}-\frac{2941\mathcal{A}^{10}}{3600}+\frac{101\mathcal{A}^{12}}{864}-\frac{54847\mathcal{A}^{14}}{4838400}+\frac{4987\mathcal{A}^{16}}{6220800}\right)K_l(4n)
$$

$$
+\left(-\frac{1817\mathcal{A}^8}{3840}+\frac{2323\mathcal{A}^{10}}{11520}-\frac{37753\mathcal{A}^{12}}{967680}+\frac{17803\mathcal{A}^{14}}{3870720}-\frac{72977\mathcal{A}^{16}}{195084288}\right)K_l(5n)
$$

$$
+\left(-\frac{637\mathcal{A}^{10}}{28800}+\frac{313\mathcal{A}^{12}}{40320}-\frac{789\mathcal{A}^{14}}{627200}+\frac{38419\mathcal{A}^{16}}{304819200}\right)K_l(6n)
$$

$$
+\left(-\frac{3397\mathcal{A}^{12}}{4838400}+\frac{811\mathcal{A}^{14}}{3870720}-\frac{81401\mathcal{A}^{16}}{2786918400}\right)K_l(7n)
$$

$$
+\left(-\frac{1091\mathcal{A}^{14}}{67737600}+\frac{2549\mathcal{A}^{16}}{609638400}\right)K_l(8n)
$$

$$
-\frac{5449\mathcal{A}^{16}K_l(9n)}{19508428800}\Bigg)+e^3\times\Bigg(
$$

$$\left(-\frac{1647\mathcal{A}}{4}+\frac{5561\mathcal{A}^3}{8}-\frac{38129\mathcal{A}^5}{96}+\frac{11165\mathcal{A}^7}{96}-\frac{40039\mathcal{A}^9}{1920}+\frac{2042161\mathcal{A}^{11}}{806400}-\frac{4303871\mathcal{A}^{13}}{19353600}+\frac{6010433\mathcal{A}^{15}}{406425600}\right)\times$$
$$K_l(n)+\left(357\mathcal{A}-\frac{2993\mathcal{A}^3}{4}+\frac{23023\mathcal{A}^5}{48}-\frac{36377\mathcal{A}^7}{240}+\frac{11029\mathcal{A}^9}{384}-\frac{4400891\mathcal{A}^{11}}{1209600}+\frac{639353\mathcal{A}^{13}}{1935360}-\frac{655343\mathcal{A}^{15}}{29030400}\right)\times$$
$$K_l(2n)+\left(\frac{2137\mathcal{A}^3}{8}-\frac{8463\mathcal{A}^5}{32}+\frac{32879\mathcal{A}^7}{320}-\frac{50911\mathcal{A}^9}{2304}+\frac{2464253\mathcal{A}^{11}}{806400}-\frac{1911013\mathcal{A}^{13}}{6451200}+\frac{11453\mathcal{A}^{15}}{537600}\right)K_l(3n)$$
$$+\left(\frac{5551\mathcal{A}^5}{96}-\frac{3619\mathcal{A}^7}{96}+\frac{7553\mathcal{A}^9}{720}-\frac{515197\mathcal{A}^{11}}{302400}+\frac{595907\mathcal{A}^{13}}{3225600}-\frac{419393\mathcal{A}^{15}}{29030400}\right)K_l(4n)$$
$$+\left(\frac{1881\mathcal{A}^7}{320}-\frac{6605\mathcal{A}^9}{2304}+\frac{300767\mathcal{A}^{11}}{483840}-\frac{104549\mathcal{A}^{13}}{1290240}+\frac{2095\mathcal{A}^{15}}{290304}\right)K_l(5n)$$
$$+\left(\frac{1991\mathcal{A}^9}{5760}-\frac{54389\mathcal{A}^{11}}{403200}+\frac{77323\mathcal{A}^{13}}{3225600}-\frac{19639\mathcal{A}^{15}}{7526400}\right)K_l(6n)$$
$$+\left(\frac{31991\mathcal{A}^{11}}{2419200}-\frac{83323\mathcal{A}^{13}}{19353600}+\frac{75289\mathcal{A}^{15}}{116121600}\right)K_l(7n)+\left(\frac{6871\mathcal{A}^{13}}{19353600}-\frac{40321\mathcal{A}^{15}}{406425600}\right)K_l(8n)+\frac{13\mathcal{A}^{15}K_l(9n)}{1843200})\Bigg)+$$
$$e^4\Bigg(\left(-\frac{47555}{32}\mathcal{A}^2+\frac{190709\mathcal{A}^4}{128}-\frac{400233\mathcal{A}^6}{640}+\frac{1121033\mathcal{A}^8}{7680}-\frac{23458073\mathcal{A}^{10}}{1075200}+\frac{35199901\mathcal{A}^{12}}{15482880}-\frac{852863297\mathcal{A}^{14}}{4877107200}\right)K_l(n)$$
$$+\left(\frac{8687\mathcal{A}^2}{4}-\frac{34773\mathcal{A}^4}{16}+\frac{4644\mathcal{A}^6}{5}-\frac{425111\mathcal{A}^8}{1920}+\frac{1512829\mathcal{A}^{10}}{44800}-\frac{1387199\mathcal{A}^{12}}{387072}+\frac{85408297\mathcal{A}^{14}}{304819200}\right)K_l(2n)$$
$$+\left(-\frac{32127}{32}\mathcal{A}^2+\frac{185441\mathcal{A}^4}{128}-\frac{934671\mathcal{A}^6}{1280}+\frac{8842181\mathcal{A}^8}{46080}-\frac{100865411\mathcal{A}^{10}}{3225600}+\frac{9994067\mathcal{A}^{12}}{2867200}-\frac{98657507\mathcal{A}^{14}}{348364800}\right)\times$$
$$K_l(3n)+\left(-\frac{23833}{64}\mathcal{A}^4+\frac{12277\mathcal{A}^6}{40}-\frac{196591\mathcal{A}^8}{1920}+\frac{1944769\mathcal{A}^{10}}{100800}-\frac{9191771\mathcal{A}^{12}}{3870720}+\frac{9035869\mathcal{A}^{14}}{43545600}\right)K_l(4n)$$
$$+\left(-\frac{68941\mathcal{A}^6}{1280}+\frac{31835\mathcal{A}^8}{1024}-\frac{998839\mathcal{A}^{10}}{129024}+\frac{17575681\mathcal{A}^{12}}{15482880}-\frac{10930351\mathcal{A}^{14}}{97542144}\right)K_l(5n)$$
$$+\left(-\frac{23699\mathcal{A}^8}{5760}+\frac{737969\mathcal{A}^{10}}{403200}-\frac{5213\mathcal{A}^{12}}{14336}+\frac{13298189\mathcal{A}^{14}}{304819200}\right)K_l(6n)+$$
$$\left(-\frac{208333\mathcal{A}^{10}}{1075200}+\frac{5434133\mathcal{A}^{12}}{77414400}-\frac{16170799\mathcal{A}^{14}}{1393459200}\right)K_l(7n)+$$
$$\left(-\frac{239213\mathcal{A}^{12}}{38707200}+\frac{1152077\mathcal{A}^{14}}{609638400}\right)K_l(8n)$$
$$-\frac{1387327\mathcal{A}^{14}K_l(9n)}{9754214400}\Bigg)+e^5\times\Bigg($$

$$
\left(\frac{22769\mathcal{A}}{16}-\frac{1296283\mathcal{A}^3}{384}+\frac{4380193\mathcal{A}^5}{1920}-\frac{42520013\mathcal{A}^7}{57600}+\frac{113941067\mathcal{A}^9}{806400}-\frac{463361041\mathcal{A}^{11}}{25804800}+\frac{1135527679\mathcal{A}^{13}}{696729600}\right)K_l(n)+
$$

$$
\left(-\frac{13539\mathcal{A}}{4}+\frac{2484625\mathcal{A}^3}{384}-\frac{1952053\mathcal{A}^5}{480}+\frac{58912711\mathcal{A}^7}{46080}-\frac{292763719\mathcal{A}^9}{1209600}+\frac{2374678163\mathcal{A}^{11}}{77414400}-\frac{53957761\mathcal{A}^{13}}{19353600}\right)K_l(2n)
$$

$$
+\left(\frac{71825\mathcal{A}}{32}-\frac{697647\mathcal{A}^3}{128}+\frac{9779869\mathcal{A}^5}{2560}-\frac{14726891\mathcal{A}^7}{11520}+\frac{813614173\mathcal{A}^9}{3225600}-\frac{850321511\mathcal{A}^{11}}{25804800}+\frac{854790599\mathcal{A}^{13}}{278691840}\right)K_l(3n)
$$

$$
+\left(\frac{81433\mathcal{A}^3}{48}-\frac{3590417\mathcal{A}^5}{1920}+\frac{89371417\mathcal{A}^7}{115200}-\frac{210499391\mathcal{A}^9}{1209600}+\frac{958855703\mathcal{A}^{11}}{38707200}-\frac{854451569\mathcal{A}^{13}}{348364800}\right)K_l(4n)
$$

$$
+\left(\frac{191637\mathcal{A}^5}{512}-\frac{303739\mathcal{A}^7}{1152}+\frac{149339629\mathcal{A}^9}{1935360}-\frac{200654617\mathcal{A}^{11}}{15482880}+\frac{400813631\mathcal{A}^{13}}{278691840}\right)K_l(5n)
$$

$$
+\left(\frac{8889011\mathcal{A}^7}{230400}-\frac{8043643\mathcal{A}^9}{403200}+\frac{116210893\mathcal{A}^{11}}{25804800}-\frac{105142393\mathcal{A}^{13}}{174182400}\right)K_l(6n)
$$

$$
+\left(\frac{11083823\mathcal{A}^9}{4838400}-\frac{10353229\mathcal{A}^{11}}{11059200}+\frac{159751717\mathcal{A}^{13}}{928972800}\right)K_l(7n)
$$

$$
+\left(\frac{2277181\mathcal{A}^{11}}{25804800}-\frac{20783387\mathcal{A}^{13}}{696729600}\right)K_l(8n)
$$

$$
\left.+\frac{1327271\mathcal{A}^{13}K_l(9n)}{557383680}\right)+
$$

$$
e^6\times\left(\left(\frac{6360697\mathcal{A}^2}{1536}-\frac{83914747\mathcal{A}^4}{15360}+\frac{205972691\mathcal{A}^6}{76800}-\frac{238333495\mathcal{A}^8}{344064}+\frac{34401989173\mathcal{A}^{10}}{309657600}-\frac{67943553227\mathcal{A}^{12}}{5573836800}\right)K_l(n)\right.
$$

$$
+\left(-\frac{4527427}{384}\mathcal{A}^2+\frac{11995117\mathcal{A}^4}{960}-\frac{85032277\mathcal{A}^6}{15360}+\frac{218343289\mathcal{A}^8}{161280}-\frac{1086174427\mathcal{A}^{10}}{5160960}+\frac{7897450723\mathcal{A}^{12}}{348364800}\right)K_l(2n)
$$

$$
+\left(\frac{6894791\mathcal{A}^2}{512}-\frac{149105731\mathcal{A}^4}{10240}+\frac{67081587\mathcal{A}^6}{10240}-\frac{2785868387\mathcal{A}^8}{1720320}+\frac{2911274687\mathcal{A}^{10}}{11468800}-\frac{25580115979\mathcal{A}^{12}}{928972800}\right)K_l(3n)
$$

$$
+\left(-\frac{1024813}{192}\mathcal{A}^2+\frac{818159\mathcal{A}^4}{96}-\frac{22057967\mathcal{A}^6}{4800}+\frac{1273775\mathcal{A}^8}{1008}-\frac{4112465311\mathcal{A}^{10}}{19353600}+\frac{421956389\mathcal{A}^{12}}{17418240}\right)K_l(4n)
$$

$$
+\left(-\frac{20343329\mathcal{A}^4}{10240}+\frac{54424859\mathcal{A}^6}{30720}-\frac{644732521\mathcal{A}^8}{1032192}+\frac{7580219749\mathcal{A}^{10}}{61931520}-\frac{8635714091\mathcal{A}^{12}}{557383680}\right)K_l(5n)
$$

$$
\left.+\left(-\frac{7421471\mathcal{A}^6}{25600}+\frac{1913875\mathcal{A}^8}{10752}-\frac{133004803\mathcal{A}^{10}}{2867200}+\frac{816994861\mathcal{A}^{12}}{116121600}\right)K_l(6n)\right)
$$

$$
+\left(-\frac{115244509\mathcal{A}^8}{5160960}+\frac{1077524291\mathcal{A}^{10}}{103219200}-\frac{960692647\mathcal{A}^{12}}{445906944}\right)K_l(7n)
$$

$$
\left.+\left(-\frac{5122889\mathcal{A}^{10}}{4838400}+\frac{1242901\mathcal{A}^{12}}{3110400}\right)K_l(8n)-\frac{18025373\mathcal{A}^{12}K_l(9n)}{530841600}\right)+e^7\times\Bigg(
$$

$$\left(-\frac{1663559\mathcal{A}}{768}+\frac{121709581\mathcal{A}^3}{15360}-\frac{312427823\mathcal{A}^5}{46080}+\frac{19673089399\mathcal{A}^7}{7741440}-\frac{291425548999\mathcal{A}^9}{541900800}+\frac{2867948486117\mathcal{A}^{11}}{39016857600}\right)K_l(n)$$
$$+\left(\frac{4244105\mathcal{A}}{384}-\frac{195851269\mathcal{A}^3}{7680}+\frac{811588697\mathcal{A}^5}{46080}-\frac{12636131167\mathcal{A}^7}{2150400}+\frac{1402888481\mathcal{A}^9}{1209600}-\frac{986035976887\mathcal{A}^{11}}{6502809600}\right)K_l(2n)+$$
$$\left(-\frac{9859807\mathcal{A}}{512}+\frac{24914363\mathcal{A}^3}{640}-\frac{4694903647\mathcal{A}^5}{184320}+\frac{11825097051\mathcal{A}^7}{1433600}-\frac{23555895221\mathcal{A}^9}{14745600}+\frac{1149280143791\mathcal{A}^{11}}{5573836800}\right)K_l(3n)$$
$$+\left(\frac{4053463\mathcal{A}}{384}-\frac{3400213\mathcal{A}^3}{120}+\frac{1948423099\mathcal{A}^5}{92160}-\frac{317943461\mathcal{A}^7}{43008}+\frac{11099163623\mathcal{A}^9}{7372800}-\frac{280439920391\mathcal{A}^{11}}{1393459200}\right)K_l(4n)$$
$$+\left(\frac{121754083\mathcal{A}^3}{15360}-\frac{1736132939\mathcal{A}^5}{184320}+\frac{31935948797\mathcal{A}^7}{7741440}-\frac{19885290673\mathcal{A}^9}{20643840}+\frac{1102592661521\mathcal{A}^{11}}{7803371520}\right)K_l(5n)$$
$$+\left(\frac{8062469\mathcal{A}^5}{4608}-\frac{1689833129\mathcal{A}^7}{1290240}+\frac{4530651799\mathcal{A}^9}{11289600}-\frac{1362209431217\mathcal{A}^{11}}{19508428800}\right)K_l(6n)$$
$$+\left(\frac{7010016683\mathcal{A}^7}{38707200}-\frac{15241243613\mathcal{A}^9}{154828800}+\frac{14310329239\mathcal{A}^{11}}{619315200}\right)K_l(7n)$$
$$\left.+\left(\frac{23423982107\mathcal{A}^9}{2167603200}-\frac{89822032001\mathcal{A}^{11}}{19508428800}\right)K_l(8n)+\frac{2039795207\mathcal{A}^{11}}{4877107200}K_l(9n)\right)+$$

$$e^8\times\left(\left(-\frac{36667771\mathcal{A}^2}{6144}+\frac{137576377\mathcal{A}^4}{12288}-\frac{58268412071\mathcal{A}^6}{8601600}+\frac{3483804392591\mathcal{A}^8}{1734082560}-\frac{3962944769797\mathcal{A}^{10}}{11147673600}\right)K_l(n)\right.$$
$$+\left(\frac{7932001\mathcal{A}^2}{256}-\frac{3629434021\mathcal{A}^4}{92160}+\frac{62558288021\mathcal{A}^6}{3225600}-\frac{393958246799\mathcal{A}^8}{77414400}+\frac{1159836156341\mathcal{A}^{10}}{1393459200}\right)K_l(2n)$$
$$+\left(-\frac{1378786789\mathcal{A}^2}{20480}+\frac{5365102241\mathcal{A}^4}{73728}-\frac{847780261361\mathcal{A}^6}{25804800}+\frac{3370548827407\mathcal{A}^8}{412876800}-\frac{5974574495\mathcal{A}^{10}}{4644864}\right)K_l(3n)$$
$$+\left(\frac{124022959\mathcal{A}^2}{1920}-\frac{425217367\mathcal{A}^4}{5760}+\frac{13920972659\mathcal{A}^6}{403200}-\frac{34003821749\mathcal{A}^8}{3870720}+\frac{122575184351\mathcal{A}^{10}}{87091200}\right)K_l(4n)$$
$$+\left(-\frac{1391241377\mathcal{A}^2}{61440}+\frac{4788563821\mathcal{A}^4}{122880}-\frac{114133290857\mathcal{A}^6}{5160960}+\frac{1565177035693\mathcal{A}^8}{247726080}-\frac{609862623793\mathcal{A}^{10}}{557383680}\right)K_l(5n)$$
$$+\left(-\frac{154509701\mathcal{A}^4}{18432}+\frac{3653368319\mathcal{A}^6}{460800}-\frac{105576999331\mathcal{A}^8}{36126720}+\frac{275386936571\mathcal{A}^{10}}{464486400}\right)K_l(6n)$$
$$+\left(-\frac{31536438929\mathcal{A}^6}{25804800}+\frac{975977916433\mathcal{A}^8}{1238630400}-\frac{4758029916799\mathcal{A}^{10}}{22295347200}\right)K_l(7n)$$
$$\left.+\left(-\frac{25549718947\mathcal{A}^8}{270950400}+\frac{4573097093\mathcal{A}^{10}}{99532800}\right)K_l(8n)-\frac{99964117517\mathcal{A}^{10}K_l(9n)}{22295347200}\right)+$$

$$e^9\Bigg(\left(\frac{72574433\mathcal{A}}{40960}-\frac{33250133\mathcal{A}^3}{3072}+\frac{321566834083\mathcal{A}^5}{25804800}-\frac{48892934193757\mathcal{A}^7}{8670412800}+\frac{424304933869777\mathcal{A}^9}{312134860800}\right)K_l(n)$$
$$+\left(-\frac{139238303\mathcal{A}}{7680}+\frac{2812070945\mathcal{A}^3}{49152}-\frac{1815292535809\mathcal{A}^5}{38707200}+\frac{21601089607747\mathcal{A}^7}{1238630400}-\frac{144839901437071\mathcal{A}^9}{39016857600}\right)K_l(2n)$$
$$+\left(\frac{326578731\mathcal{A}}{5120}-\frac{3318429817\mathcal{A}^3}{23040}+\frac{1712182537183\mathcal{A}^5}{17203200}-\frac{13787028701293\mathcal{A}^7}{412876800}+\frac{295876625683021\mathcal{A}^9}{44590694400}\right)K_l(3n)$$
$$+\left(-\frac{45278785\mathcal{A}}{512}+\frac{8612926109\mathcal{A}^3}{46080}-\frac{4880466678209\mathcal{A}^5}{38707200}+\frac{17258868186769\mathcal{A}^7}{412876800}-\frac{22984018946099\mathcal{A}^9}{2786918400}\right)K_l(4n)$$
$$+\left(\frac{851962171\mathcal{A}}{20480}-\frac{44593891643\mathcal{A}^3}{368640}+\frac{293291537465\mathcal{A}^5}{3096576}-\frac{8497199910629\mathcal{A}^7}{247726080}+\frac{89611617850873\mathcal{A}^9}{12485394432}\right)K_l(5n)$$
$$+\left(\frac{713014643\mathcal{A}^3}{23040}-\frac{41944969211\mathcal{A}^5}{1075200}+\frac{51535195929577\mathcal{A}^7}{2890137600}-\frac{167924593843033\mathcal{A}^9}{39016857600}\right)K_l(6n)$$
$$+\left(\frac{1052720951633\mathcal{A}^5}{154828800}-\frac{6613213406581\mathcal{A}^7}{1238630400}+\frac{151464161578421\mathcal{A}^9}{89181388800}\right)K_l(7n)$$
$$+\left(\frac{76155429263\mathcal{A}^7}{108380160}-\frac{31037807709701\mathcal{A}^9}{78033715200}\right)K_l(8n)$$
$$+\frac{26184666395077\mathcal{A}^9K_l(9n)}{624269721600}\Bigg)$$

$$e^{10}\Bigg(\left(\frac{4188185133\mathcal{A}^2}{819200}-\frac{668034376553\mathcal{A}^4}{45875200}+\frac{298635437603\mathcal{A}^6}{26214400}-\frac{5008680379354717\mathcal{A}^8}{1248539443200}\right)K_l(n)$$
$$+\left(-\frac{69622578569\mathcal{A}^2}{1474560}+\frac{288361412803\mathcal{A}^4}{3686400}-\frac{3733878109439\mathcal{A}^6}{82575360}+\frac{14728473880769\mathcal{A}^8}{1114767360}\right)K_l(2n)$$
$$+\left(\frac{105043267843\mathcal{A}^2}{589824}-\frac{90447675495017\mathcal{A}^4}{412876800}+\frac{176246672641693\mathcal{A}^6}{1651507200}-\frac{2489696844203003\mathcal{A}^8}{89181388800}\right)K_l(3n)$$
$$+\left(-\frac{72784945777\mathcal{A}^2}{230400}+\frac{560166907039\mathcal{A}^4}{1612800}-\frac{49295772110719\mathcal{A}^6}{309657600}+\frac{13961643516553\mathcal{A}^8}{348364800}\right)K_l(4n)$$
$$+\left(\frac{776330530877\mathcal{A}^2}{2949120}-\frac{1732963120055\mathcal{A}^4}{5505024}+\frac{30099792470603\mathcal{A}^6}{198180864}-\frac{705923122737949\mathcal{A}^8}{17836277760}\right)K_l(5n)$$
$$+\left(-\frac{613186054801\mathcal{A}^2}{7372800}+\frac{436748965809\mathcal{A}^4}{2867200}-\frac{37201323168383\mathcal{A}^6}{412876800}+\frac{1036259700960391\mathcal{A}^8}{39016857600}\right)K_l(6n)$$
$$+\left(-\frac{4206593801911\mathcal{A}^4}{137625600}+\frac{7158257783303\mathcal{A}^6}{235929600}-\frac{4137506209801739\mathcal{A}^8}{356725555200}\right)K_l(7n)$$
$$+\left(-\frac{229049541811\mathcal{A}^6}{51609600}+\frac{58107407588357\mathcal{A}^8}{19508428800}\right)K_l(8n)-\frac{645135681793\mathcal{A}^8K_l(9n)}{1887436800}+$$

$$e^{11}\Bigg(\left(-\frac{4390861889\mathcal{A}}{4915200}+\frac{1961183621879\mathcal{A}^3}{206438400}-\frac{38437694104309\mathcal{A}^5}{2477260800}+\frac{5499256218016573\mathcal{A}^7}{624269721600}\right)K_l(n)$$
$$+\left(\frac{12960937279\mathcal{A}}{737280}-\frac{25335942630283\mathcal{A}^3}{309657600}+\frac{1196416018969\mathcal{A}^5}{14155776}-\frac{1266083597711297\mathcal{A}^7}{34681651200}\right)K_l(2n)$$
$$+\left(-\frac{20979287141\mathcal{A}}{184320}+\frac{22404670502027\mathcal{A}^3}{68812800}-\frac{141336992746169\mathcal{A}^5}{550502400}+\frac{38716231419983\mathcal{A}^7}{412876800}\right)K_l(3n)$$
$$+\left(\frac{561041955133\mathcal{A}}{1843200}-\frac{6585350448109\mathcal{A}^3}{9676800}+\frac{2333996611139251\mathcal{A}^5}{4954521600}-\frac{1416438955564847\mathcal{A}^7}{8918138880}\right)K_l(4n)$$
$$+\left(-\frac{518643543809\mathcal{A}}{1474560}+\frac{2994059366393\mathcal{A}^3}{3870720}-\frac{17684742866503\mathcal{A}^5}{33030144}+\frac{3766355622175117\mathcal{A}^7}{20808990720}\right)K_l(5n)$$
$$+\left(\frac{16753583267\mathcal{A}}{115200}-\frac{1461464779987\mathcal{A}^3}{3225600}+\frac{76285236828841\mathcal{A}^5}{206438400}-\frac{2867374053933953\mathcal{A}^7}{20808990720}\right)K_l(6n)$$
$$+\left(\frac{33195983160521\mathcal{A}^3}{309657600}-\frac{234766934917157\mathcal{A}^5}{1651507200}+\frac{1501695875492263\mathcal{A}^7}{22295347200}\right)K_l(7n)$$
$$+\left(\frac{966755431567\mathcal{A}^5}{41287680}-\frac{249061450017451\mathcal{A}^7}{13005619200}\right)K_l(8n)+\frac{1505225192085113\mathcal{A}^7K_l(9n)}{624269721600}\Bigg)$$

$$e^{12}\Bigg(\left(-\frac{112405393703\mathcal{A}^2}{39321600}+\frac{256194365128103\mathcal{A}^4}{19818086400}-\frac{2434459781946581\mathcal{A}^6}{178362777600}\right)K_l(n)$$
$$+\left(\frac{14313033811823\mathcal{A}^2}{309657600}-\frac{12498570084137\mathcal{A}^4}{117964800}+\frac{1677509997505583\mathcal{A}^6}{22295347200}\right)K_l(2n)$$
$$+\left(-\frac{239571154081783\mathcal{A}^2}{825753600}+\frac{2904792531811861\mathcal{A}^4}{6606028800}-\frac{120767420385113\mathcal{A}^6}{495452160}\right)K_l(3n)$$
$$+\left(\frac{16651792420267\mathcal{A}^2}{19353600}-\frac{3664938831889\mathcal{A}^4}{3538944}+\frac{3986190927755\mathcal{A}^6}{7962624}\right)K_l(4n)$$
$$+\left(-\frac{91659779628347\mathcal{A}^2}{70778880}+\frac{1912786165948037\mathcal{A}^4}{1321205760}-\frac{5996938416572659\mathcal{A}^6}{8918138880}\right)K_l(5n)$$
$$+\left(\frac{32945086429187\mathcal{A}^2}{34406400}-\frac{28119643773793\mathcal{A}^4}{23592960}+\frac{1463376996779051\mathcal{A}^6}{2477260800}\right)K_l(6n)$$
$$+\left(-\frac{684201699957701\mathcal{A}^2}{2477260800}+\frac{10590857503323379\mathcal{A}^4}{19818086400}-\frac{23381239709702027\mathcal{A}^6}{71345111040}\right)K_l(7n)$$
$$+\left(-\frac{62410695774613\mathcal{A}^4}{619315200}+\frac{166206910739587\mathcal{A}^6}{1592524800}\right)K_l(8n)-\frac{577143489956477\mathcal{A}^6K_l(9n)}{39636172800}\Bigg)$$

$$
\begin{aligned}
&e^{13}\Bigg(\left(\frac{4480458061\mathcal{A}}{14745600}-\frac{113509427927533\mathcal{A}^3}{19818086400}+\frac{4932648254178133\mathcal{A}^5}{356725555200}\right)K_l(n)\\
&+\left(-\frac{692621429069\mathcal{A}}{61931520}+\frac{1586490110623811\mathcal{A}^3}{19818086400}-\frac{811950375727963\mathcal{A}^5}{7431782400}\right)K_l(2n)\\
&+\left(\frac{104673184486151\mathcal{A}}{825753600}-\frac{3256104685646191\mathcal{A}^3}{6606028800}+\frac{4461263791004999\mathcal{A}^5}{9512681472}\right)K_l(3n)\\
&+\left(-\frac{91340140787233\mathcal{A}}{154828800}+\frac{156492482258165\mathcal{A}^3}{99090432}-\frac{14394426401891911\mathcal{A}^5}{11890851840}\right)K_l(4n)\\
&+\left(\frac{314766782631703\mathcal{A}}{247726080}-\frac{2809659549121933\mathcal{A}^3}{990904320}+\frac{281042178651130801\mathcal{A}^5}{142690222080}\right)K_l(5n)\\
&+\left(-\frac{1355991878713\mathcal{A}}{1075200}+\frac{39617412502949\mathcal{A}^3}{13762560}-\frac{336875717415931\mathcal{A}^5}{165150720}\right)K_l(6n)\\
&+\left(\frac{72172041424697\mathcal{A}}{154828800}-\frac{15307727148091081\mathcal{A}^3}{9909043200}+\frac{233096036944318531\mathcal{A}^5}{178362777600}\right)K_l(7n)\\
&+\left(\frac{105529641662017\mathcal{A}^3}{309657600}-\frac{376559490960019\mathcal{A}^5}{796262400}\right)K_l(8n)+\frac{26397815834028073\mathcal{A}^5K_l(9n)}{356725555200}\Bigg)+\\
&e^{14}\Bigg(\left(\frac{206796563366483\mathcal{A}^2}{184968806400}-\frac{82215574092860581\mathcal{A}^4}{9988315545600}\right)K_l(n)+\\
&\left(-\frac{618579830111987\mathcal{A}^2}{19818086400}+\frac{64337807855429791\mathcal{A}^4}{624269721600}\right)K_l(2n)\\
&+\left(\frac{8402777041707077\mathcal{A}^2}{26424115200}-\frac{447073478617395173\mathcal{A}^4}{713451110400}\right)K_l(3n)\\
&+\left(-\frac{7430296569379097\mathcal{A}^2}{4954521600}+\frac{17606260552429\mathcal{A}^4}{8257536}\right)K_l(4n)\\
&+\left(\frac{6461512425366487\mathcal{A}^2}{1761607680}-\frac{4349564850250920329\mathcal{A}^4}{998831554560}\right)K_l(5n)\\
&+\left(-\frac{222276140779005643\mathcal{A}^2}{46242201600}+\frac{3412415816069604403\mathcal{A}^4}{624269721600}\right)K_l(6n)\\
&+\left(\frac{253818565838765371\mathcal{A}^2}{79272345600}-\frac{1685837673188956681\mathcal{A}^4}{407686348800}\right)K_l(7n)+\\
&\left(-\frac{7380514090083647\mathcal{A}^2}{8670412800}+\frac{540458699263271861\mathcal{A}^4}{312134860800}\right)K_l(8n)\\
&-\frac{1232692494304457819\mathcal{A}^4K_l(9n)}{3995326218240}\Bigg)+
\end{aligned}
$$

$$
e^{15}\Bigg(\left(-\frac{3469384763227\mathcal{A}}{46242201600}+\frac{1187663466854671\mathcal{A}^3}{475634073600}\right) K_l(n) + \left(\frac{19888331524783\mathcal{A}}{3963617280}-\frac{127712690841809\mathcal{A}^3}{2264924160}\right) K_l(2n)
+ \left(-\frac{2547496947290741\mathcal{A}}{26424115200}+\frac{31541032831484593\mathcal{A}^3}{59454259200}\right) K_l(3n)
+ \left(\frac{4883476194008213\mathcal{A}}{6606028800}-\frac{18839933887964653\mathcal{A}^3}{7431782400}\right) K_l(4n)
+ \left(-\frac{469284844441745\mathcal{A}}{176160768}+\frac{648190780936041043\mathcal{A}^3}{95126814720}\right) K_l(5n)
+ \left(\frac{6936784270529417\mathcal{A}}{1445068800}-\frac{799144237774121117\mathcal{A}^3}{7431782400}\right) K_l(6n)+
\left(-\frac{109591789469563\mathcal{A}}{26214400}+\frac{783868077139349141\mathcal{A}^3}{79272345600}\right) K_l(7n)
+ \left(\frac{17967831915895\mathcal{A}}{12845056}-\frac{18230346413898349\mathcal{A}^3}{3715891200}\right) K_l(8n)+
\frac{30182462841350683\mathcal{A}^3 K_l(9n)}{29727129600}\Bigg) - e^{16}\Bigg(\frac{131482629287941\mathcal{A}^2 K_l(n)}{407686348800}+\frac{7661258420564069\mathcal{A}^2 K_l(2n)}{499415777280}
-\frac{22226193309071407\mathcal{A}^2 K_l(3n)}{89181388800}+\frac{5778045333852317\mathcal{A}^2 K_l(4n)}{3185049600}
-\frac{1363999477757941669\mathcal{A}^2 K_l(5n)}{199766310912}+\frac{3551079915645715\,2389\mathcal{A}^2 K_l(6n)}{2497078886400}
-\frac{943408482922478897\,69\mathcal{A}^2 K_l(7n)}{5707608883200}+\frac{12526197981986130907\mathcal{A}^2 K_l(8n)}{1248539443200}-\frac{19789563585947876009\mathcal{A}^2 K_l(9n)}{7990652436480}\Bigg)
+\frac{2182742993065681\mathcal{A}e^{17} K_l(n)}{159813048729600}-\frac{398344686909419\mathcal{A}e^{17} K_l(2n)}{237817036800}+\frac{6081437884285115\mathcal{A}e^{17} K_l(3n)}{114152177664}
-\frac{463925804816385011\mathcal{A}e^{17} K_l(4n)}{713451110400}+\frac{4224989067263492609\mathcal{A}e^{17} K_l(5n)}{1141521776640}-\frac{1691336870677414609\mathcal{A}e^{17} K_l(6n)}{156067430400}+
\frac{2394690952542562729\mathcal{A}e^{17} K_l(7n)}{142690222080}-\frac{508396579603772017\mathcal{A}e^{17} K_l(8n)}{39016857600}+\frac{2843691151639550671\mathcal{A}e^{17} K_l(9n)}{713451110400}
\tag{38}
$$

To compute the eccentricity evolution, we have to write down all the terms entering equation (32). The term generated by the tides in the planet is:

$$
\left(\frac{de}{dt}\right)^{main}_{planet} = -n\frac{M'}{M}\left(\frac{R}{a}\right)^5 \times \mathcal{L}(K_l,\, n,\, \dot{\theta},\, e) \;\; , \tag{39}
$$

where the function $\mathcal{L}$ is calculated from equation (30) and has the form of

$$
\begin{aligned}
&\mathcal{L} = e\big(-\frac{9K_l(n)}{8} + \frac{3}{16}K_l(n-2\dot{\theta}) + \frac{3}{4}K_l(2n-2\dot{\theta}) - \frac{147}{16}K_l(3n-2\dot{\theta})\big)+ \\
&e^3\big(-\frac{45K_l(n)}{32} - \frac{81}{16}K_l(2n) - \frac{3}{64}K_l(n-2\dot{\theta}) - \frac{63}{16}K_l(2n-2\dot{\theta}) + \frac{3759}{64}K_l(3n-2\dot{\theta}) - \frac{867}{8}K_l(4n-2\dot{\theta})\big)+ \\
&e^5\big(-\frac{999K_l(n)}{512} - \frac{45}{16}K_l(2n) - \frac{8427}{512}K_l(3n) + \frac{K_l(-n-2\dot{\theta})}{1024} - \frac{35K_l(n-2\dot{\theta})}{1024} + \frac{27}{4}K_l(2n-2\dot{\theta}) - \frac{150933K_l(3n-2\dot{\theta})}{1024} \\
&+ \frac{10421}{16}K_l(4n-2\dot{\theta}) - \frac{714025K_l(5n-2\dot{\theta})}{1024})) + e^7\times \\
&(-\frac{10043K_l(n)}{4096} - \frac{653}{128}K_l(2n) + \frac{4929K_l(3n)}{4096} - \frac{5929}{128}K_l(4n) + \frac{17K_l(-n-2\dot{\theta})}{24576} - \frac{175K_l(n-2\dot{\theta})}{24576} - \frac{3299}{768}K_l(2n-2\dot{\theta}) \\
&+ \frac{1525953K_l(3n-2\dot{\theta})}{8192} - \frac{310463}{192}K_l(4n-2\dot{\theta}) + \frac{105299675K_l(5n-2\dot{\theta})}{24576} - \frac{852267}{256}K_l(6n-2\dot{\theta}) + \frac{1}{192}K_l(-2(n+\dot{\theta}))\big) \\
&+ e^9\big(-\frac{968501K_l(n)}{327680} - \frac{1861}{320}K_l(2n) - \frac{8061723K_l(3n)}{655360} + \frac{154}{5}K_l(4n) - \frac{15717645K_l(5n)}{131072} + \frac{19683K_l(-3n-2\dot{\theta})}{1310720} \\
&+ \frac{577K_l(-n-2\dot{\theta})}{1310720} - \frac{5201K_l(n-2\dot{\theta})}{655360} + \frac{1289K_l(2n-2\dot{\theta})}{1024} - \frac{85340127K_l(3n-2\dot{\theta})}{655360} + \frac{1395551}{640}K_l(4n-2\dot{\theta}) - \\
&\frac{2949543325K_l(5n-2\dot{\theta})}{262144} + \frac{109744167K_l(6n-2\dot{\theta})}{5120} - \frac{52142352409K_l(7n-2\dot{\theta})}{3932160} + \frac{13K_l(-2(n+\dot{\theta}))}{3840}\big)+ \\
&e^{11}\big(-\frac{22665719K_l(n)}{6553600} - \frac{140657K_l(2n)}{20480} - \frac{24220341K_l(3n)}{2621440} - \frac{510211K_l(4n)}{12800} + \frac{77607165K_l(5n)}{524288} - \frac{30089667K_l(6n)}{102400} + \\
&\frac{177147K_l(-3n-2\dot{\theta})}{26214400} + \frac{12769K_l(-n-2\dot{\theta})}{47185920} - \frac{237091K_l(n-2\dot{\theta})}{39321600} - \frac{25999K_l(2n-2\dot{\theta})}{102400} + \frac{725981637K_l(3n-2\dot{\theta})}{13107200} \\
&- \frac{430553}{240}K_l(4n-2\dot{\theta}) + \frac{158224764775K_l(5n-2\dot{\theta})}{9437184} - \frac{6191465853K_l(6n-2\dot{\theta})}{102400} + \frac{21286018449073K_l(7n-2\dot{\theta})}{235929600} \\
&- \frac{5383010161K_l(8n-2\dot{\theta})}{115200} + \frac{563K_l(-2(n+\dot{\theta}))}{230400} + \frac{8}{225}K_l(-2(2n+\dot{\theta}))\big)+ \\
&e^{13}\big(-\frac{3488799931K_l(n)}{880803840} - \frac{50772389K_l(2n)}{6451200} - \frac{2503082907K_l(3n)}{209715200} - \frac{112849K_l(4n)}{23040} - \frac{82475458145K_l(5n)}{528482304} + \\
&\frac{75371433K_l(6n)}{143360} - \frac{1306918425967K_l(7n)}{1887436800} + \frac{244140625K_l(-5n-2\dot{\theta})}{3170893824} + \frac{17970579K_l(-3n-2\dot{\theta})}{2936012800} + \\
&\frac{12959141K_l(-n-2\dot{\theta})}{79272345600} \\
&- \frac{130286017K_l(n-2\dot{\theta})}{26424115200} + \frac{9569K_l(2n-2\dot{\theta})}{921600} - \frac{6616127097K_l(3n-2\dot{\theta})}{419430400} + \frac{4725763337K_l(4n-2\dot{\theta})}{4838400} \\
&- \frac{50749964351125K_l(5n-2\dot{\theta})}{3170893824} + \frac{71414520309K_l(6n-2\dot{\theta})}{716800} - \frac{3103858544107391K_l(7n-2\dot{\theta})}{11324620800} + \\
&\frac{1629711040201K_l(8n-2\dot{\theta})}{4838400} - \frac{442450100095587K_l(9n-2\dot{\theta})}{2936012800} + \frac{3943K_l(-2(n+\dot{\theta}))}{2419200} + \frac{4}{675}K_l(-2(2n+\dot{\theta}))\big)+
\end{aligned}
$$

$$
\begin{aligned}
& e^{15}\Big(-\frac{2201362888069K_l(n)}{493250150400}-\frac{458120711K_l(2n)}{51609600}-\frac{310605553233K_l(3n)}{23488102400}-\frac{534407009K_l(4n)}{25804800}+ \\
& \frac{443312655515K_l(5n)}{8455716864}-\frac{24124153401K_l(6n)}{40140800}+\frac{9760494525089K_l(7n)}{6039797760}-\frac{31801945561K_l(8n)}{20070400}- \\
& \frac{4638671875K_l(-5n-2\dot{\theta})}{355140108288} \\
& +\frac{193818501K_l(-3n-2\dot{\theta})}{46976204800}+\frac{40473781K_l(-n-2\dot{\theta})}{422785843200}-\frac{7343600351K_l(n-2\dot{\theta})}{1775700541440}-\frac{250247K_l(2n-2\dot{\theta})}{15052800}+ \\
& \frac{148062766923K_l(3n-2\dot{\theta})}{46976204800}-\frac{7265523173K_l(4n-2\dot{\theta})}{19353600}+\frac{25510094869225K_l(5n-2\dot{\theta})}{2415919104}-\frac{124297728921K_l(6n-2\dot{\theta})}{1146880} \\
& +\frac{89963543887907011K_l(7n-2\dot{\theta})}{181193932800}-\frac{49681058130967K_l(8n-2\dot{\theta})}{45158400}+\frac{378432207128810421K_l(9n-2\dot{\theta})}{328833433600}- \\
& \frac{402063787225K_l(10n-2\dot{\theta})}{884736}+\frac{2951K_l(-2(n+\dot{\theta}))}{2764800}+\frac{4}{315}K_l(-2(2n+\dot{\theta}))+\frac{1594323K_l(-2(3n+\dot{\theta}))}{10035200}\Big)+ \\
& e^{17}\Big(-\frac{705270944819797K_l(n)}{142056043315200}-\frac{1338763001K_l(2n)}{135475200}-\frac{5548949079117K_l(3n)}{375809638400}-\frac{244133119K_l(4n)}{12902400}- \\
& \frac{16937466865475K_l(5n)}{315680096256}+\frac{7345300413K_l(6n)}{20070400}-\frac{12355157174800909K_l(7n)}{5798205849600}+\frac{1232639743459K_l(8n)}{270950400} \\
& -\frac{37292291277118641K_l(9n)}{10522669875200}+\frac{33232930569601K_l(-7n-2\dot{\theta})}{104367705292800}+\frac{861572265625K_l(-5n-2\dot{\theta})}{29222957481984}+ \\
& \frac{15029958483K_l(-3n-2\dot{\theta})}{5261334937600}+\frac{9536091053K_l(-n-2\dot{\theta})}{182643484262400}-\frac{9052063323217K_l(n-2\dot{\theta})}{2557008779673600}-\frac{818693K_l(2n-2\dot{\theta})}{68812800} \\
& -\frac{151996417911K_l(3n-2\dot{\theta})}{300647710720}+\frac{10430507833K_l(4n-2\dot{\theta})}{97542144}-\frac{37167304047148325K_l(5n-2\dot{\theta})}{7305739370496}+ \\
& \frac{3840730800633K_l(6n-2\dot{\theta})}{45875200}-\frac{1581498309894699 0889K_l(7n-2\dot{\theta})}{26091926323200}+\frac{5306383534261451K_l(8n-2\dot{\theta})}{2438553600} \\
& -\frac{12113553017690673723K_l(9n-2\dot{\theta})}{3006477107200}+\frac{1637474036163575K_l(10n-2\dot{\theta})}{445906944}- \\
& \frac{664882154937771726369K_l(11n-2\dot{\theta})}{5114017559347200}+\frac{1904023K_l(-2(n+\dot{\theta}))}{2786918400}+\frac{61K_l(-2(2n+\dot{\theta}))}{8505}-\frac{6908733K_l(-2(3n+\dot{\theta}))}{80281600}\Big).
\end{aligned}
\tag{40}
$$

The contribution from the tides in the satellite to the evolution of the eccentricity is computed as

$$
\left(\frac{de}{dt}\right)^{main}_{satellite}=-n\frac{M}{M'}\left(\frac{R'}{a}\right)^5\times\mathcal{L}(K_l',\,n,\,\dot{\theta}',\,e)\ \ . \tag{41}
$$

Note that, similarly to da/dt, the expression is written down for the general case where neither of the bodies is *a priori* assumed synchronous. In the case of the Martian moons, which are synchronised, the term associated with the semidiurnal tide in equation (35) vanishes.

The input generated by the satellite's longitudinal libration about the 1:1 spin-orbit resonance is:

$$\left(\frac{de}{dt}\right)^{libration}_{satellite} = n\frac{M}{M'}\left(\frac{R'}{a}\right)^5 \times \mathcal{H}(K_l',\, n,\, \dot{\theta}',\, e) \;\; , \tag{42}$$

where the function $\mathcal{H}$ is given by

$$\frac{1}{e}\Bigg(\Big(-\frac{3\mathcal{A}^2}{2}+\frac{3\mathcal{A}^4}{2}-\frac{5\mathcal{A}^6}{8}+\frac{7\mathcal{A}^8}{48}-\frac{7\mathcal{A}^{10}}{320}+\frac{11\mathcal{A}^{12}}{4800}-\frac{143\mathcal{A}^{14}}{806400}+\frac{143\mathcal{A}^{16}}{13547520}-\frac{2431\mathcal{A}^{18}}{4877107200}\Big)K_l(n)$$
$$+\Big(-\frac{3\mathcal{A}^4}{4}+\frac{\mathcal{A}^6}{2}-\frac{7\mathcal{A}^8}{48}+\frac{\mathcal{A}^{10}}{40}-\frac{11\mathcal{A}^{12}}{3840}+\frac{143\mathcal{A}^{14}}{604800}-\frac{143\mathcal{A}^{16}}{9676800}+\frac{221\mathcal{A}^{18}}{304819200}\Big)K_l(2n)$$
$$+\Big(-\frac{\mathcal{A}^6}{8}+\frac{\mathcal{A}^8}{16}-\frac{9\mathcal{A}^{10}}{640}+\frac{11\mathcal{A}^{12}}{5760}-\frac{143\mathcal{A}^{14}}{806400}+\frac{13\mathcal{A}^{16}}{1075200}-\frac{221\mathcal{A}^{18}}{348364800}\Big)K_l(3n)$$
$$+\Big(-\frac{\mathcal{A}^8}{96}+\frac{\mathcal{A}^{10}}{240}-\frac{11\mathcal{A}^{12}}{14400}+\frac{13\mathcal{A}^{14}}{151200}-\frac{13\mathcal{A}^{16}}{1935360}+\frac{17\mathcal{A}^{18}}{43545600}\Big)K_l(4n)$$
$$+\Big(-\frac{\mathcal{A}^{10}}{1920}+\frac{\mathcal{A}^{12}}{5760}-\frac{13\mathcal{A}^{14}}{483840}+\frac{\mathcal{A}^{16}}{387072}-\frac{17\mathcal{A}^{18}}{97542144}\Big)K_l(5n)$$
$$+\Big(-\frac{\mathcal{A}^{12}}{57600}+\frac{\mathcal{A}^{14}}{201600}-\frac{\mathcal{A}^{16}}{1505280}+\frac{17\mathcal{A}^{18}}{304819200}\Big)K_l(6n)$$
$$+\Big(-\frac{\mathcal{A}^{14}}{2419200}+\frac{\mathcal{A}^{16}}{9676800}-\frac{17\mathcal{A}^{18}}{1393459200}\Big)K_l(7n)$$
$$+\Big(-\frac{\mathcal{A}^{16}}{135475200}+\frac{\mathcal{A}^{18}}{609638400}\Big)K_l(8n)-\frac{\mathcal{A}^{18}K_l(9n)}{9754214400}\Bigg)+$$

$$\Bigg(6\mathcal{A}-12\mathcal{A}^3+\frac{15\mathcal{A}^5}{2}-\frac{7\mathcal{A}^7}{3}+\frac{7\mathcal{A}^9}{16}-\frac{11\mathcal{A}^{11}}{200}+\frac{143\mathcal{A}^{13}}{28800}-\frac{143\mathcal{A}^{15}}{423360}+\frac{2431\mathcal{A}^{17}}{135475200}\Bigg)K_l(n)$$
$$+\Big(6\mathcal{A}^3-6\mathcal{A}^5+\frac{7\mathcal{A}^7}{3}-\frac{\mathcal{A}^9}{2}+\frac{11\mathcal{A}^{11}}{160}-\frac{143\mathcal{A}^{13}}{21600}+\frac{143\mathcal{A}^{15}}{302400}-\frac{221\mathcal{A}^{17}}{8467200}\Big)K_l(2n)$$
$$+\Big(\frac{3\mathcal{A}^5}{2}-\mathcal{A}^7+\frac{9\mathcal{A}^9}{32}-\frac{11\mathcal{A}^{11}}{240}+\frac{143\mathcal{A}^{13}}{28800}-\frac{13\mathcal{A}^{15}}{33600}+\frac{221\mathcal{A}^{17}}{9676800}\Big)K_l(3n)$$
$$+\Big(\frac{\mathcal{A}^7}{6}-\frac{\mathcal{A}^9}{12}+\frac{11\mathcal{A}^{11}}{600}-\frac{13\mathcal{A}^{13}}{5400}+\frac{13\mathcal{A}^{15}}{60480}-\frac{17\mathcal{A}^{17}}{1209600}\Big)K_l(4n)$$
$$+\Big(\frac{\mathcal{A}^9}{96}-\frac{\mathcal{A}^{11}}{240}+\frac{13\mathcal{A}^{13}}{17280}-\frac{\mathcal{A}^{15}}{12096}+\frac{17\mathcal{A}^{17}}{2709504}\Big)K_l(5n)$$
$$+\Big(\frac{\mathcal{A}^{11}}{2400}-\frac{\mathcal{A}^{13}}{7200}+\frac{\mathcal{A}^{15}}{47040}-\frac{17\mathcal{A}^{17}}{8467200}\Big)K_l(6n)$$
$$+\Big(\frac{\mathcal{A}^{13}}{86400}-\frac{\mathcal{A}^{15}}{302400}+\frac{17\mathcal{A}^{17}}{38707200}\Big)K_l(7n)+\Big(\frac{\mathcal{A}^{15}}{4233600}-\frac{\mathcal{A}^{17}}{16934400}\Big)K_l(8n)+\frac{\mathcal{A}^{17}K_l(9n)}{270950400}\Bigg)+$$

$$e\Bigg(\Big(\frac{345\mathcal{A}^2}{8}-\frac{1401\mathcal{A}^4}{32}+\frac{3661\mathcal{A}^6}{192}-\frac{17717\mathcal{A}^8}{3840}+\frac{911\mathcal{A}^{10}}{1280}-\frac{49159\mathcal{A}^{12}}{645120}+\frac{60203\mathcal{A}^{14}}{10035200}-\frac{784927\mathcal{A}^{16}}{2167603200}\Big)K_l(n)$$
$$+\Big(-\frac{63\mathcal{A}^2}{2}+42\mathcal{A}^4e-\frac{1015\mathcal{A}^6}{48}+\frac{169\mathcal{A}^8}{30}-\frac{149\mathcal{A}^{10}}{160}+\frac{3971\mathcal{A}^{12}}{37800}-\frac{83369\mathcal{A}^{14}}{9676800}+\frac{13\mathcal{A}^{16}}{24192}\Big)K_l(2n)$$
$$+\Big(-\frac{429\mathcal{A}^4}{32}+\frac{675\mathcal{A}^6}{64}-\frac{8977\mathcal{A}^8}{2560}+\frac{5123\mathcal{A}^{10}}{7680}-\frac{89353\mathcal{A}^{12}}{1075200}+\frac{94757\mathcal{A}^{14}}{12902400}-\frac{15041\mathcal{A}^{16}}{30965760}\Big)K_l(3n)$$
$$+\Big(-\frac{101\mathcal{A}^6}{48}+\frac{283\mathcal{A}^8}{240}-\frac{281\mathcal{A}^{10}}{960}+\frac{1307\mathcal{A}^{12}}{30240}-\frac{5213\mathcal{A}^{14}}{1209600}+\frac{1511\mathcal{A}^{16}}{4838400}\Big)K_l(4n)$$
$$+\Big(-\frac{87\mathcal{A}^8}{512}+\frac{569\mathcal{A}^{10}}{7680}-\frac{28417\mathcal{A}^{12}}{1935360}+\frac{13711\mathcal{A}^{14}}{7741440}-\frac{911\mathcal{A}^{16}}{6193152}\Big)K_l(5n)$$
$$+\Big(-\frac{\mathcal{A}^{10}}{120}+\frac{\mathcal{A}^{12}}{336}-\frac{11089\mathcal{A}^{14}}{22579200}+\frac{53\mathcal{A}^{16}}{1058400}\Big)K_l(6n)$$
$$+\Big(-\frac{379\mathcal{A}^{12}}{1382400}+\frac{3211\mathcal{A}^{14}}{38707200}-\frac{1453\mathcal{A}^{16}}{123863040}\Big)K_l(7n)$$
$$+\Big(-\frac{73\mathcal{A}^{14}}{11289600}+\frac{23\mathcal{A}^{16}}{13547520}\Big)K_l(8n)-\frac{71\mathcal{A}^{16}K_l(9n)}{619315200}\Bigg)+$$

$$e^2\Bigg(\Big(-\frac{327\mathcal{A}}{4}+\frac{1233\mathcal{A}^3}{8}-\frac{9565\mathcal{A}^5}{96}+\frac{5159\mathcal{A}^7}{160}-\frac{12007\mathcal{A}^9}{1920}+\frac{651761\mathcal{A}^{11}}{806400}-\frac{68783\mathcal{A}^{13}}{921600}+\frac{1261403\mathcal{A}^{15}}{243855360}\Big)K_l(n)$$
$$+\Big(\frac{357\mathcal{A}}{4}-\frac{789\mathcal{A}^3}{4}+\frac{401\mathcal{A}^5}{3}-\frac{3587\mathcal{A}^7}{80}+\frac{34483\mathcal{A}^9}{3840}-\frac{1444399\mathcal{A}^{11}}{1209600}+\frac{2431\mathcal{A}^{13}}{21504}-\frac{99619\mathcal{A}^{15}}{12441600}\Big)K_l(2n)$$
$$+\Big(\frac{641\mathcal{A}^3}{8}-\frac{2611\mathcal{A}^5}{32}+\frac{10467\mathcal{A}^7}{320}-\frac{83851\mathcal{A}^9}{11520}+\frac{839597\mathcal{A}^{11}}{806400}-\frac{224003\mathcal{A}^{13}}{2150400}+\frac{111917\mathcal{A}^{15}}{14515200}\Big)K_l(3n)$$
$$+\Big(\frac{925\mathcal{A}^5}{48}-\frac{6143\mathcal{A}^7}{480}+\frac{10469\mathcal{A}^9}{2880}-\frac{182537\mathcal{A}^{11}}{302400}+\frac{53989\mathcal{A}^{13}}{806400}-\frac{18643\mathcal{A}^{15}}{3483648}\Big)K_l(4n)$$
$$+\Big(\frac{403\mathcal{A}^7}{192}-\frac{11953\mathcal{A}^9}{11520}+\frac{110479\mathcal{A}^{11}}{483840}-\frac{39017\mathcal{A}^{13}}{1290240}+\frac{149\mathcal{A}^{15}}{54432}\Big)K_l(5n)$$
$$+\Big(\frac{1493\mathcal{A}^9}{11520}-\frac{20609\mathcal{A}^{11}}{403200}+\frac{4939\mathcal{A}^{13}}{537600}-\frac{41137\mathcal{A}^{15}}{40642560}\Big)K_l(6n)$$
$$+\Big(\frac{1777\mathcal{A}^{11}}{345600}-\frac{3631\mathcal{A}^{13}}{2150400}+\frac{89399\mathcal{A}^{15}}{348364800}\Big)K_l(7n)$$
$$+\Big(\frac{229\mathcal{A}^{13}}{1612800}-\frac{48731\mathcal{A}^{15}}{1219276800}\Big)K_l(8n)+\frac{67\mathcal{A}^{15}K_l(9n)}{23224320}\Bigg)+$$

$$
\begin{aligned}
e^3\Bigg(&(-\frac{21255}{64}\mathcal{A}^2+\frac{271475\mathcal{A}^4}{768}-\frac{123499\mathcal{A}^6}{768}+\frac{621161\mathcal{A}^8}{15360}-\frac{5939929\mathcal{A}^{10}}{921600}+\frac{21960257\mathcal{A}^{12}}{30965760}-\frac{6879301\mathcal{A}^{14}}{120422400})K_l(n)\\
&+(\frac{4719\mathcal{A}^2}{8}-\frac{116567\mathcal{A}^4}{192}+\frac{128911\mathcal{A}^6}{480}-\frac{255827\mathcal{A}^8}{3840}+\frac{25593509\mathcal{A}^{10}}{2419200}-\frac{45154813\mathcal{A}^{12}}{38707200}+\frac{38392679\mathcal{A}^{14}}{406425600})K_l(2n)\\
&+(-\frac{19275}{64}\mathcal{A}^2+\frac{115821\mathcal{A}^4}{256}-\frac{597223\mathcal{A}^6}{2560}+\frac{641693\mathcal{A}^8}{10240}-\frac{67444943\mathcal{A}^{10}}{6451200}+\frac{61623623\mathcal{A}^{12}}{51609600}-\frac{7693621\mathcal{A}^{14}}{77414400})K_l(3n)\\
&+(-\frac{23833}{192}\mathcal{A}^4+\frac{20147\mathcal{A}^6}{192}-\frac{136771\mathcal{A}^8}{3840}+\frac{4123699\mathcal{A}^{10}}{604800}-\frac{275077\mathcal{A}^{12}}{322560}+\frac{4398301\mathcal{A}^{14}}{58060800})K_l(4n)\\
&+(-\frac{9849}{512}\mathcal{A}^6+\frac{115783\mathcal{A}^8}{10240}-\frac{11048333\mathcal{A}^{10}}{3870720}+\frac{485967\mathcal{A}^{12}}{1146880}-\frac{13765531\mathcal{A}^{14}}{325140480})K_l(5n)\\
&+(-\frac{395}{256}\mathcal{A}^8+\frac{80189\mathcal{A}^{10}}{115200}-\frac{360887\mathcal{A}^{12}}{2580480}+\frac{459229\mathcal{A}^{14}}{27095040})K_l(6n)\\
&+(-\frac{208343\mathcal{A}^{10}}{2764800}+\frac{4275161\mathcal{A}^{12}}{154828800}-\frac{4280917\mathcal{A}^{14}}{928972800})K_l(7n)\\
&+(-\frac{1367\mathcal{A}^{12}}{552960}+\frac{206791\mathcal{A}^{14}}{270950400})K_l(8n)-\frac{126127\mathcal{A}^{14}K_l(9n)}{2167603200}\Bigg)+
\end{aligned}
$$

$$
\begin{aligned}
e^4\Bigg(&(\frac{24193\mathcal{A}}{64}-\frac{20095\mathcal{A}^3}{24}+\frac{2232473\mathcal{A}^5}{3840}-\frac{5702117\mathcal{A}^7}{28800}+\frac{258053953\mathcal{A}^9}{6451200}-\frac{14783483\mathcal{A}^{11}}{2764800}+\frac{707721157\mathcal{A}^{13}}{1393459200})K_l(n)\\
&+(-\frac{15681\mathcal{A}}{16}+\frac{364907\mathcal{A}^3}{192}-\frac{290039\mathcal{A}^5}{240}+\frac{8927209\mathcal{A}^7}{23040}-\frac{364144573\mathcal{A}^9}{4838400}+\frac{401973\mathcal{A}^{11}}{40960}-\frac{53307059\mathcal{A}^{13}}{58060800})K_l(2n)\\
&+(\frac{43095\mathcal{A}}{64}-\frac{55743\mathcal{A}^3}{32}+\frac{400743\mathcal{A}^5}{320}-\frac{545157\mathcal{A}^7}{1280}+\frac{61156327\mathcal{A}^9}{716800}-\frac{36538619\mathcal{A}^{11}}{3225600}+\frac{498263623\mathcal{A}^{13}}{464486400})K_l(3n)\\
&+(\frac{27145\mathcal{A}^3}{48}-\frac{414357\mathcal{A}^5}{640}+\frac{3950587\mathcal{A}^7}{14400}-\frac{18886547\mathcal{A}^9}{302400}+\frac{87118681\mathcal{A}^{11}}{9676800}-\frac{314307277\mathcal{A}^{13}}{348364800})K_l(4n)\\
&+(\frac{513319\mathcal{A}^5}{3840}-\frac{1113803\mathcal{A}^7}{11520}+\frac{22286941\mathcal{A}^9}{774144}-\frac{677069\mathcal{A}^{11}}{138240}+\frac{30624113\mathcal{A}^{13}}{55738368})K_l(5n)\\
&+(\frac{555563\mathcal{A}^7}{38400}-\frac{1367699\mathcal{A}^9}{179200}+\frac{22551787\mathcal{A}^{11}}{12902400}-\frac{13756051\mathcal{A}^{13}}{58060800})K_l(6n)\\
&+(\frac{2463053\mathcal{A}^9}{2764800}-\frac{2386541\mathcal{A}^{11}}{6451200}+\frac{10650713\mathcal{A}^{13}}{154828800})K_l(7n)\\
&+(\frac{341573\mathcal{A}^{11}}{9676800}-\frac{8424559\mathcal{A}^{13}}{696729600})K_l(8n)+\frac{18853\mathcal{A}^{13}K_l(9n)}{19353600}\Bigg)+
\end{aligned}
$$

$$
\begin{aligned}
&e^5\Bigg(\Big(\frac{3704953\mathcal{A}^2}{3072}-\frac{15221377\mathcal{A}^4}{10240}+\frac{112613299\mathcal{A}^6}{153600}-\frac{1118827917\mathcal{A}^8}{5734400}+\frac{20121975317\mathcal{A}^{10}}{619315200}-\frac{13766831089\mathcal{A}^{12}}{3715891200}\Big)K_l(n)\\
&+\Big(-\frac{2892187}{768}\mathcal{A}^2+\frac{1263513\mathcal{A}^4}{320}-\frac{53719409\mathcal{A}^6}{30720}+\frac{695722717\mathcal{A}^8}{1612800}-\frac{10541705029\mathcal{A}^{10}}{154828800}+\frac{868015153\mathcal{A}^{12}}{116121600}\Big)K_l(2n)\\
&+\Big(\frac{4548103\mathcal{A}^2}{1024}-\frac{101354707\mathcal{A}^4}{20480}+\frac{138786857\mathcal{A}^6}{61440}-\frac{29109939893\mathcal{A}^8}{51609600}+\frac{18430053463\mathcal{A}^{10}}{206438400}-\frac{18186003391\mathcal{A}^{12}}{1857945600}\Big)K_l(3n)\\
&+\Big(-\frac{683209}{384}\mathcal{A}^2+\frac{11504597\mathcal{A}^4}{3840}-\frac{10622857\mathcal{A}^6}{6400}+\frac{20787503\mathcal{A}^8}{44800}-\frac{3055769779\mathcal{A}^{10}}{38707200}+\frac{2110699721\mathcal{A}^{12}}{232243200}\Big)K_l(4n)\\
&+\Big(-\frac{8718503\mathcal{A}^4}{12288}+\frac{8058607\mathcal{A}^6}{12288}-\frac{813411079\mathcal{A}^8}{3440640}+\frac{5826124357\mathcal{A}^{10}}{123863040}-\frac{2237882701\mathcal{A}^{12}}{371589120}\Big)K_l(5n)\\
&+\Big(-\frac{16698217\mathcal{A}^6}{153600}+\frac{110558537\mathcal{A}^8}{1612800}-\frac{939128363\mathcal{A}^{10}}{51609600}+\frac{324869249\mathcal{A}^{12}}{116121600}\Big)K_l(6n)\\
&+\Big(-\frac{64024591\mathcal{A}^8}{7372800}+\frac{2567559977\mathcal{A}^{10}}{619315200}-\frac{6458660261\mathcal{A}^{12}}{7431782400}\Big)K_l(7n)\\
&+\Big(-\frac{1170947\mathcal{A}^{10}}{2764800}+\frac{15106919\mathcal{A}^{12}}{92897280}\Big)K_l(8n)\\
&-\frac{14748077\mathcal{A}^{12}K_l(9n)}{1061683200}\Bigg)+
\end{aligned}
$$

$$
\begin{aligned}
&e^6\Bigg(\Big(-\frac{872943\mathcal{A}}{1024}+\frac{4813543\mathcal{A}^3}{1920}-\frac{921770971\mathcal{A}^5}{460800}+\frac{7178895463\mathcal{A}^7}{9676800}-\frac{230130795289\mathcal{A}^9}{1445068800}+\frac{108799751533\mathcal{A}^{11}}{4877107200}\Big)K_l(n)\\
&+\Big(\frac{6210857\mathcal{A}}{1536}-\frac{13555561\mathcal{A}^3}{1536}+\frac{1097036731\mathcal{A}^5}{184320}-\frac{362561267\mathcal{A}^7}{184320}+\frac{40085609077\mathcal{A}^9}{103219200}-\frac{997573407349\mathcal{A}^{11}}{19508428800}\Big)K_l(2n)\\
&+\Big(-\frac{6835241\mathcal{A}}{1024}+\frac{141981907\mathcal{A}^3}{10240}-\frac{23491027\mathcal{A}^5}{2560}+\frac{771402715\mathcal{A}^7}{258048}-\frac{17153333687\mathcal{A}^9}{29491200}+\frac{46732982197\mathcal{A}^{11}}{619315200}\Big)K_l(3n)\\
&+\Big(\frac{1351153\mathcal{A}}{384}-\frac{9745837\mathcal{A}^3}{960}+\frac{225435367\mathcal{A}^5}{28800}-\frac{8993789107\mathcal{A}^7}{3225600}+\frac{6354465407\mathcal{A}^9}{11059200}-\frac{11996360791\mathcal{A}^{11}}{154828800}\Big)K_l(4n)\\
&+\Big(\frac{17393429\mathcal{A}^3}{6144}-\frac{324807233\mathcal{A}^5}{92160}+\frac{175446745\mathcal{A}^7}{110592}-\frac{467138354711\mathcal{A}^9}{123863040}+\frac{145741780141\mathcal{A}^{11}}{2601123840}\Big)K_l(5n)\\
&+\Big(\frac{67187379\mathcal{A}^5}{102400}-\frac{3277329481\mathcal{A}^7}{6451200}+\frac{115045714631\mathcal{A}^9}{722534400}-\frac{2441359969\mathcal{A}^{11}}{86704128}\Big)K_l(6n)\\
&+\Big(\frac{68153083\mathcal{A}^7}{967680}-\frac{2704350493\mathcal{A}^9}{68812800}+\frac{14973217337\mathcal{A}^{11}}{1592524800}\Big)K_l(7n)\\
&+\Big(\frac{260266787\mathcal{A}^9}{60211200}-\frac{7340699509\mathcal{A}^{11}}{3901685760}\Big)K_l(8n)+\frac{1483487713\mathcal{A}^{11}K_l(9n)}{8670412800}\Bigg)+
\end{aligned}
$$

$$e^7\Bigg((-\frac{149727647\mathcal{A}^2}{61440}+\frac{155864751\mathcal{A}^4}{40960}-\frac{4426663009\mathcal{A}^6}{2064384}+\frac{10797972126287\mathcal{A}^8}{17340825600}-\frac{17243822330131\mathcal{A}^{10}}{156067430400})K_l(n)$$
$$+(\frac{93952097\mathcal{A}^2}{7680}-\frac{896925851\mathcal{A}^4}{61440}+\frac{44924873743\mathcal{A}^6}{6451200}-\frac{39763735267\mathcal{A}^8}{22118400}+\frac{5700875160973\mathcal{A}^{10}}{19508428800})K_l(2n)$$
$$+(-\frac{1048933601\mathcal{A}^2}{40960}+\frac{2268428349\mathcal{A}^4}{81920}-\frac{214946221871\mathcal{A}^6}{17203200}+\frac{512367188359\mathcal{A}^8}{165150720}-\frac{129742491151\mathcal{A}^{10}}{265420800})K_l(3n)$$
$$+(\frac{6081475\mathcal{A}^2}{256}-\frac{432634279\mathcal{A}^4}{15360}+\frac{2165962973\mathcal{A}^6}{161280}-\frac{16726054291\mathcal{A}^8}{4838400}+\frac{55551320611\mathcal{A}^{10}}{99532800})K_l(4n)$$
$$+(-\frac{66249643\mathcal{A}^2}{8192}+\frac{3629650189\mathcal{A}^4}{245760}-\frac{17874184561\mathcal{A}^6}{2064384}+\frac{178698259919\mathcal{A}^8}{70778880}-\frac{432464713873\mathcal{A}^{10}}{975421440})K_l(5n)$$
$$+(-\frac{193137247\mathcal{A}^4}{61440}+\frac{1333226933\mathcal{A}^6}{430080}-\frac{424071056197\mathcal{A}^8}{361267200}+\frac{63117639931\mathcal{A}^{10}}{260112384})K_l(6n)$$
$$+(-\frac{3504047651\mathcal{A}^6}{7372800}+\frac{783679385501\mathcal{A}^8}{2477260800}-\frac{558242239781\mathcal{A}^{10}}{6370099200})K_l(7n)$$
$$+(-\frac{1277485193\mathcal{A}^8}{33868800}+\frac{919564435\mathcal{A}^{10}}{48771072})K_l(8n)-\frac{63613501087\mathcal{A}^{10}K_l(9n)}{34681651200}\Bigg)+$$

$$e^8\Bigg((\frac{65652473\mathcal{A}}{61440}-\frac{563582879\mathcal{A}^3}{122880}+\frac{92955405499\mathcal{A}^5}{20643840}-\frac{5483932464937\mathcal{A}^7}{2890137600}+\frac{1285208299777\mathcal{A}^9}{2890137600})K_l(n)$$
$$+(-\frac{269639453\mathcal{A}}{30720}+\frac{739024483\mathcal{A}^3}{30720}-\frac{204074346391\mathcal{A}^5}{11059200}+\frac{273003532891\mathcal{A}^7}{41287680}-\frac{2389160130767\mathcal{A}^9}{1734082560})K_l(2n)$$
$$+(\frac{275400323\mathcal{A}}{10240}-\frac{43435464343\mathcal{A}^3}{737280}+\frac{460345468843\mathcal{A}^5}{11468800}-\frac{5511201000007\mathcal{A}^7}{412876800}+\frac{58779091690057\mathcal{A}^9}{22295347200})K_l(3n)$$
$$+(-\frac{43362121\mathcal{A}}{1280}+\frac{3416637469\mathcal{A}^3}{46080}-\frac{78771223009\mathcal{A}^5}{1548288}+\frac{5273431096139\mathcal{A}^7}{309657600}-\frac{52329578737\mathcal{A}^9}{15482880})K_l(4n)$$
$$+(\frac{121708789\mathcal{A}}{8192}-\frac{34357420961\mathcal{A}^3}{737280}+\frac{2345355924239\mathcal{A}^5}{61931520}-\frac{3473845411853\mathcal{A}^7}{247726080}+\frac{2581617644773\mathcal{A}^9}{867041280})K_l(5n)$$
$$+(\frac{4278085159\mathcal{A}^3}{368640}-\frac{26483840827\mathcal{A}^5}{1720320}+\frac{10491735514513\mathcal{A}^7}{1445068800}-\frac{139668210217891\mathcal{A}^9}{78033715200})K_l(6n)$$
$$+(\frac{116968933337\mathcal{A}^5}{44236800}-\frac{890500845139\mathcal{A}^7}{412876800}+\frac{6978589997179\mathcal{A}^9}{9909043200})K_l(7n)$$
$$+(\frac{25385138803\mathcal{A}^7}{90316800}-\frac{52652632731\mathcal{A}^9}{321126400})K_l(8n)+\frac{10711909210169\mathcal{A}^9K_l(9n)}{624269721600}\Bigg)+$$

$$
\begin{aligned}
e^9\Bigg(&(\frac{44039579957\mathcal{A}^2}{14745600}-\frac{15824165056211\mathcal{A}^4}{2477260800}+\frac{14328069012029\mathcal{A}^6}{3303014400}-\frac{26332156657147\mathcal{A}^8}{18496880640})K_l(n)\\
&+(-\frac{70067602561\mathcal{A}^2}{2949120}+\frac{5369825407643\mathcal{A}^4}{154828800}-\frac{5158776395993\mathcal{A}^6}{275251200}+\frac{6514444951201\mathcal{A}^8}{1238630400})K_l(2n)\\
&+(\frac{158625899173\mathcal{A}^2}{1966080}-\frac{11227169865391\mathcal{A}^4}{117964800}+\frac{29933237272409\mathcal{A}^6}{660602880}-\frac{77153221103897\mathcal{A}^8}{6606028800})K_l(3n)\\
&+(-\frac{121953672479\mathcal{A}^2}{921600}+\frac{354916665553\mathcal{A}^4}{2419200}-\frac{5975801542697\mathcal{A}^6}{88473600}+\frac{15834223266853\mathcal{A}^8}{928972800})K_l(4n)\\
&+(\frac{611761614557\mathcal{A}^2}{5898240}-\frac{338595836519\mathcal{A}^4}{2621440}+\frac{126344102042327\mathcal{A}^6}{1981808640}-\frac{200404252881719\mathcal{A}^8}{11890851840})K_l(5n)\\
&+(-\frac{153296598947\mathcal{A}^2}{4915200}+\frac{3137330952221\mathcal{A}^4}{51609600}-\frac{30768980959823\mathcal{A}^6}{825753600}+\frac{97464415569691\mathcal{A}^8}{8670412800})K_l(6n)\\
&+(-\frac{1402198607219\mathcal{A}^4}{117964800}+\frac{40766822971729\mathcal{A}^6}{3303014400}-\frac{1156044273778537\mathcal{A}^8}{237817036800})K_l(7n)\\
&+(-\frac{20359967739\mathcal{A}^6}{11468800}+\frac{2005898347471\mathcal{A}^8}{1625702400})K_l(8n)-\frac{11084606975429\mathcal{A}^8K_l(9n)}{79272345600}\Bigg)+
\end{aligned}
$$

$$
\begin{aligned}
e^{10}\Bigg(&(-\frac{5936440751\mathcal{A}}{7372800}+\frac{281978655779\mathcal{A}^3}{51609600}-\frac{23197484399917\mathcal{A}^5}{3303014400}+\frac{2190705315745913\mathcal{A}^7}{624269721600})K_l(n)\\
&+(\frac{33884150431\mathcal{A}}{2949120}-\frac{13195184307097\mathcal{A}^3}{309657600}+\frac{3083498074211\mathcal{A}^5}{78643200}-\frac{329558861040259\mathcal{A}^7}{20808990720})K_l(2n)\\
&+(-\frac{369336211\mathcal{A}}{6144}+\frac{10748243908261\mathcal{A}^3}{68812800}-\frac{55407789534559\mathcal{A}^5}{471859200}+\frac{1239018762271579\mathcal{A}^7}{29727129600})K_l(3n)\\
&+(\frac{255337520419\mathcal{A}}{1843200}-\frac{5908578342719\mathcal{A}^3}{19353600}+\frac{520188991137763\mathcal{A}^5}{2477260800}-\frac{3143898589948211\mathcal{A}^7}{44590694400})K_l(4n)\\
&+(-\frac{423037867387\mathcal{A}}{2949120}+\frac{5082108800729\mathcal{A}^3}{15482880}-\frac{153243709285603\mathcal{A}^5}{660602880}+\frac{3305021363349331\mathcal{A}^7}{41617981440})K_l(5n)\\
&+(\frac{16753575491\mathcal{A}}{307200}-\frac{3155846928817\mathcal{A}^3}{17203200}+\frac{36726833683589\mathcal{A}^5}{235929600}-\frac{6190102661048177\mathcal{A}^7}{104044953600})K_l(6n)\\
&+(\frac{3688441064953\mathcal{A}^3}{88473600}-\frac{577733424743393\mathcal{A}^5}{9909043200}+\frac{1019127205812299\mathcal{A}^7}{35672555520})K_l(7n)\\
&+(\frac{2900265243481\mathcal{A}^5}{309657600}-\frac{6483559163023\mathcal{A}^7}{812851200})K_l(8n)\\
&+\frac{27367721939759\mathcal{A}^7K_l(9n)}{27745320960}\Bigg)+
\end{aligned}
$$

$$
\begin{aligned}
&e^{11}\Bigg(-\frac{433172126543\mathcal{A}^2}{183500800}+\frac{292869682869259\mathcal{A}^4}{39636172800}-\frac{755533686525503\mathcal{A}^6}{118908518400})K_l(n)\\
&+(\frac{2660036179859\mathcal{A}^2}{88473600}-\frac{40257079179961\mathcal{A}^4}{707788800}+\frac{539499339154079\mathcal{A}^6}{14863564800})K_l(2n)\\
&+(-\frac{263905748342627\mathcal{A}^2}{1651507200}+\frac{974127678603403\mathcal{A}^4}{4404019200}-\frac{3464935877861461\mathcal{A}^6}{29727129600})K_l(3n)\\
&+(\frac{2030759822381\mathcal{A}^2}{4838400}-\frac{608627628721811\mathcal{A}^4}{1238630400}+\frac{173811058773157\mathcal{A}^6}{743178240})K_l(4n)\\
&+(-\frac{570491186057201\mathcal{A}^2}{990904320}+\frac{1034737867040471\mathcal{A}^4}{1585446912}-\frac{454273880894017\mathcal{A}^6}{1486356480})K_l(5n)\\
&+(\frac{81637985496899\mathcal{A}^2}{206438400}-\frac{848417792268337\mathcal{A}^4}{1651507200}+\frac{554332437901141\mathcal{A}^6}{2123366400})K_l(6n)\\
&+(-\frac{76022436811607\mathcal{A}^2}{707788800}+\frac{1755155869080827\mathcal{A}^4}{7927234560}-\frac{33519955430307049\mathcal{A}^6}{237817036800})K_l(7n)\\
&+(-\frac{24964285882541\mathcal{A}^4}{619315200}+\frac{81273844410421\mathcal{A}^6}{1857945600})K_l(8n)-\frac{202375045386037\mathcal{A}^6K_l(9n)}{33973862400}\Bigg)+\\
&e^{12}\Bigg((\frac{388547729327\mathcal{A}}{990904320}-\frac{12586819797803\mathcal{A}^3}{2831155200}+\frac{225374398759721\mathcal{A}^5}{28538044416})K_l(n)\\
&+(-\frac{2430854986367\mathcal{A}}{247726080}+\frac{258343452813277\mathcal{A}^3}{4954521600}-\frac{10743635536519061\mathcal{A}^5}{178362777600})K_l(2n)\\
&+(\frac{20036945966999\mathcal{A}}{235929600}-\frac{232251792132631\mathcal{A}^3}{825753600}+\frac{58405280353216723\mathcal{A}^5}{237817036800})K_l(3n)\\
&+(-\frac{25175706455981\mathcal{A}}{77414400}+\frac{2015484051149861\mathcal{A}^3}{2477260800}-\frac{107413449480948707\mathcal{A}^5}{178362777600})K_l(4n)\\
&+(\frac{299886137513597\mathcal{A}}{495452160}-\frac{2668022569167251\mathcal{A}^3}{1981808640}+\frac{133343876882760763\mathcal{A}^5}{142690222080})K_l(5n)\\
&+(-\frac{13845777226823\mathcal{A}}{25804800}+\frac{1407300088225909\mathcal{A}^3}{1101004800}-\frac{680562796851687\mathcal{A}^5}{734003200})K_l(6n)\\
&+(\frac{8019113491633\mathcal{A}}{44236800}-\frac{12850249538216431\mathcal{A}^3}{19818086400}+\frac{67956070081136099\mathcal{A}^5}{118908518400})K_l(7n)\\
&+(\frac{4221184611389\mathcal{A}^3}{30965760}-\frac{164903228272031\mathcal{A}^5}{825753600})K_l(8n)+\frac{2399800894049011\mathcal{A}^5K_l(9n)}{79272345600}\Bigg)+
\end{aligned}
$$

$$e^{13}\Bigg((\frac{1409122906677049\mathcal{A}^2}{1109812838400} - \frac{24433255937099561\mathcal{A}^4}{3995326218240}) K_l(n)$$
$$+ (- \frac{38504062021513\mathcal{A}^2}{1468006400} + \frac{84194246367743411\mathcal{A}^4}{1248539443200}) K_l(2n)$$
$$+ (\frac{11370780177215621\mathcal{A}^2}{52848230400} - \frac{175295396102510419\mathcal{A}^4}{475634073600}) K_l(3n) + (- \frac{8564805643401541\mathcal{A}^2}{9909043200}$$
$$+ \frac{51222963017142551\mathcal{A}^4}{44590694400}) K_l(4n) + (\frac{5927961656342663 9\mathcal{A}^2}{31708938240} - \frac{4356874183498906357\mathcal{A}^4}{1997663109120}) K_l(5n)$$
$$+ (- \frac{68523571904642713\mathcal{A}^2}{30828134400} + \frac{1071080624306333789\mathcal{A}^4}{416179814400}) K_l(6n) + (\frac{216876196102131707\mathcal{A}^2}{158544691200} -$$
$$\frac{2107300595320261267\mathcal{A}^4}{1141521776640}) K_l(7n) + (- \frac{11808824968785709\mathcal{A}^2}{34681651200} + \frac{14396140786293431\mathcal{A}^4}{19508428800}) K_l(8n)$$
$$- \frac{560314875104889503\mathcal{A}^4 K_l(9n)}{4439251353600}\Bigg) +$$

$$e^{14}\Bigg((- \frac{146462446424423\mathcal{A}}{1109812838400} + \frac{256973104838417 71\mathcal{A}^3}{9988315545600}) K_l(n) + (\frac{91971870042607\mathcal{A}}{15854469120} -$$
$$\frac{22967132722598487 1\mathcal{A}^3}{4994157772800}) K_l(2n) + (- \frac{4323676913942387\mathcal{A}}{52848230400} + \frac{345241012673170697\mathcal{A}^3}{951268147200}) K_l(3n)$$
$$+ (\frac{657581961441479\mathcal{A}}{1321205760} - \frac{27030185835638917\mathcal{A}^3}{17836277760}) K_l(4n)$$
$$+ (- \frac{2645716616611591\mathcal{A}}{1761607680} + \frac{2925800269902574361\mathcal{A}^3}{799065243648}) K_l(5n) + (\frac{604782405112007\mathcal{A}}{256901120} -$$
$$\frac{882074774612809879\mathcal{A}^3}{166471925760}) K_l(6n)$$
$$+ (- \frac{6054295311544603\mathcal{A}}{3303014400} + \frac{6468895390788443227\mathcal{A}^3}{1426902220800}) K_l(7n)$$
$$+ (\frac{3593565775679\mathcal{A}}{6422528} - \frac{165101957434340557\mathcal{A}^3}{78033715200}) K_l(8n) + \frac{34572633913775987\mathcal{A}^3 K_l(9n)}{83235962880}\Bigg) +$$

$$e^{15}\Bigg(- \frac{259980449939039\mathcal{A}^2 K_l(n)}{532710162432} + \frac{9144448769839927\mathcal{A}^2 K_l(2n)}{554906419200} - \frac{14095713084776741\mathcal{A}^2 K_l(3n)}{67947724800}$$
$$+ \frac{221992170898005827\mathcal{A}^2 K_l(4n)}{178362777600} - \frac{287624123641309919\mathcal{A}^2 K_l(5n)}{71345111040} + \frac{275608308121757381\mathcal{A}^2 K_l(6n)}{36993761280} -$$
$$\frac{12809199119827883699\mathcal{A}^2 K_l(7n)}{1630745395200} + \frac{274436840334357187\mathcal{A}^2 K_l(8n)}{62426972160} - \frac{1285036760811529423\mathcal{A}^2 K_l(9n)}{1268357529600}\Bigg) +$$

$$e^{16}\left(\frac{1033059867325999\mathcal{A}K_l(n)}{31962609745920}-\frac{2371151354170769\mathcal{A}K_l(2n)}{951268147200}+\frac{11984741009891131\mathcal{A}K_l(3n)}{211392921600}\right.$$
$$-\frac{190640670438324823\mathcal{A}K_l(4n)}{356725555200}+\frac{5669553338007335851\mathcal{A}K_l(5n)}{2283043553280}-\frac{285899985423950791\mathcal{A}K_l(6n)}{46242201600}+$$
$$\left.\frac{11973169590973537147\mathcal{A}K_l(7n)}{1426902220800}-\frac{1823347244087926049\mathcal{A}K_l(8n)}{312134860800}+\frac{258517349914243253\mathcal{A}K_l(9n)}{158544691200}\right)$$

(43)

The effect of libration in longitude on the orbital evolution of Phobos and Deimos will be discussed further in Section 7. The variations of inclinations have been found to be small, so the equations presented here are valid (cf. Figure 1 in the main text). The smallness of the inclinations is justified, because in the course of uniform equinoctial precession of an oblate host planet the inclination of a near-equatorial satellite follows the evolving equator, up to slight oscillations about it[58,59]. This behaviour stays also under nonuniform precession[60] and under the pull of the Sun[61]. For this reason, here and hereafter the terms of order $O(i^2)$ are dropped. Hence, among the degree-2 terms, only those with $lmp\,=\,201$ and $lmp\,=\,220$ are important, the corresponding inclination functions being

$$F_{201}\;=\;-\;\frac{1}{2}\;+\;O(i^2)\;\;,\qquad F_{220}\;=\;3\;+\;O(i^2)\;\;. \tag{44}$$

Owing to the proximity of the satellites to Mars, the degree-3 effects have also been taken into account in addition to the degree-2 tides. Of the degree-3 terms, the leading ones are those with $\{lmpq\}\;=\;\{3300\}$ and $\{3110\}$:

$$\left(\frac{da}{dt}\right)_{l=3}=-\;\frac{3}{4}\;a\;n\;\left(\frac{R}{a}\right)^7\;\frac{M'}{M}\;\left[5\;(1\;-\;12\,e^2)\;K_3(3n-3\dot{\theta})\;+\;(1\;+\;4\,e^2)\;K_3(n-\dot{\theta})\right]\;+\;O(e^4)\;+\;O(i^2)\;\;. \tag{45}$$

To derive formula (46), we employed the expressions

$$G_{300}(e) \;=\; 1 \;-\; 6\,e^2 \;+\; O(e^4) \;\;,$$
$$F_{330}(i) \;=\; 15 \;+\; O(i^2) \;\;,$$
$$G_{310}(e) \;=\; 1 \;+\; 2\,e^2 \;+\; O(e^4) \;\;, \tag{46}$$
$$F_{311}(i) \;=\; -\;\frac{3}{2} \;+\; O(i^2) \;\;.$$

Similarly to the principal term with $K_2(2n\,-\,2\dot{\theta})$ in equations (27) and (40), the degree-3 contribution (equation 46) vanishes when the satellite is on the synchronous orbit. Also, similarly to the principal term of sum (35), contribution (46) works to drive the moon away from the synchronous orbit.

To include the degree-3 tides in the expression for the eccentricity rate, we take into account the groups of terms with $lmpq\,=\,330q$ and $lmpq\,=\,311q$. A direct calculation demonstrates that in both these groups the important terms are those with $q\;=\;-1,\,0,\,1$:

$$\left(\frac{de}{dt}\right)_{l=3} = \frac{M'}{M}\,\left(\frac{R}{a}\right)^7 n \times \Bigg\{$$
$$\frac{5}{8}\,e\left(1\;-\;2\,e^2\right)K_3(2n-3\dot{\theta})+\frac{15}{16}e\left(1-\frac{49}{4}e^2\right)K_3(3n-3\dot{\theta})-\frac{125}{8}e\left(1-\frac{113}{10}e^2\right)K_3(4n-3\dot{\theta})$$
$$-\frac{16129}{256}e^3K_3(5n-3\dot{\theta})+\frac{3}{8}e\left(1-\frac{11}{2}e^2\right)K_3(-\dot{\theta})+\frac{3}{8}e\left(1+\frac{15}{16}e^2\right)K_3(n-\dot{\theta})-\frac{27}{8}e\left(1+\frac{1}{3}e^2\right)K_3(2n-\dot{\theta})$$
$$-\frac{8427}{256}ne^3K_3(3n-\dot{\theta})\Bigg\}\;+\;O(e^5)\;+\;O(i^2) \tag{47}$$

To derive this equation, the following expressions were used:

$$
\begin{aligned}
F_{330}(i) &= 15 + O(i^2) \ , \\
F_{311}(i) &= -\frac{3}{2} + O(i^2) \ , \\
G_{30,-1}(e) &= -e + \frac{5}{4}e^3 + O(e^5) \ , \\
G_{300}(e) &= 1 - 6e^2 + O(e^4) \ , \\
G_{301}(e) &= 5e\left(1 - \frac{22}{5}e^2\right) \ , \\
G_{302}(e) &= \frac{127}{8}e^2\left(1 - \frac{3065}{762}e^2\right) + O(e^6) \ , \\
G_{31,-1}(e) &= e\,(1-e^2)^{-5/2} \ , \\
G_{310}(e) &= 1 + 2e^2 + O(e^4) \ , \\
G_{311}(e) &= 3e\left(1 + \frac{11}{12}e^2\right) + O(e^5) \ , \\
G_{312}(e) &= \frac{53}{8}e^2\left(1 + \frac{39}{106}e^2\right) + O(e^6) \ .
\end{aligned} \tag{48}
$$

In summary, a system of coupled differential equations is obtained for a and e from equations (31) and (32), and a second-order Runge-Kutta method is employed to integrate that system. An adaptive time-stepping scheme is applied to deal with the sharp variations of $K_l = k_l \sin\epsilon_l$, which happen when the semi-major axis of a moon approaches a value at which the argument of the K_l function goes through zero (further details are discussed in Section S 6). The libration magnitude is defined by the triaxiality (assumed constant) and by the semi-major axis and eccentricity whose evolution makes the libration magnitude change with time due to variations in a, e, and n. The magnitude can be calculated as[43]:

$$\mathcal{A}_j = \omega_0^2 \frac{G_{20(j+2z-2)}(e) - G_{20(-j+2z-2)}(e)}{\chi^2 - n^2}, \tag{49}$$

where

$$\omega_0^2 = \frac{3}{2}\frac{B-A}{C}\ \frac{GM^*}{a^3}, \tag{50}$$

and

$$\chi = \omega_0\sqrt{2G_{20(2z-2)}(e)}, \tag{51}$$

while A, B, and C are the moments of inertia along the principal axes of the body. Based on the formulation derived here, the solutions are robust for eccentricities as high as ~ 0.5.

Finally, to compute the inclination evolution, we proceed as in our derivation of da/dt and de/dt. For this purpose, we consider the quadrupole expression of Boué and Efroimsky (2019)[56] (their equation 164). The main inclination term is of the following form and only relevant to the planet:

$$\frac{di}{dt} = n \sin i \frac{M'}{M}\left(\frac{R}{a}\right)^5 \times \mathcal{I}(K_l, \dot{\theta}, n, i, e), \tag{52}$$

where $\mathcal{I}$ is given by

$$\begin{aligned}
\mathcal{I} = \Bigg[& \frac{243}{64}(1+\rho)e^4 K_2(-2n-\dot{\theta}) + \frac{27}{16}e^2\left[1+\rho+\left(\frac{11}{4}+\frac{9}{4}\rho\right)e^2\right]K_2(-n-\dot{\theta}) \\
& + \frac{3}{4}\left[1+\rho+\left(\frac{7}{2}+3\rho\right)e^2+\left(\frac{63}{8}+6\rho\right)e^4\right]K_2(-\dot{\theta}) + \frac{3}{16}e^2\left[1-\rho+\frac{1}{4}(1+\rho)e^2\right]K_2(n-2\dot{\theta}) \\
& + \frac{3}{2}e^2\left[1+\rho+\left(\frac{49}{16}+\frac{41}{16}\rho\right)e^2\right]K_2(n-\dot{\theta}) + \frac{3}{4}\left[1-\rho-\left(\frac{9}{2}-5\rho\right)e^2+\left(\frac{23}{4}-\frac{63}{8}\rho\right)e^4\right]K_2(2n-2\dot{\theta}) \\
& - \frac{3}{4}\left[1+\rho-\left(\frac{9}{2}+5\rho\right)e^2+\left(\frac{11}{16}+\frac{45}{16}\rho\right)e^4\right]K_2(2n-\dot{\theta}) + \frac{147}{16}e^2\left[1-\rho-\left(\frac{109}{28}-\frac{123}{28}\rho\right)e^2\right]K_2(3n-2\dot{\theta}) \\
& - \frac{147}{16}e^2\left[1+\rho-\left(\frac{109}{28}+\frac{123}{28}\rho\right)e^2\right]K_2(3n-\dot{\theta}) + \frac{867}{16}(1-\rho)e^4K_2(4n-2\dot{\theta}) - \frac{867}{16}(1+\rho)e^4K_2(4n-\dot{\theta})\Bigg] \\
& + O(i^3) + O(e^6),
\end{aligned} \tag{53}$$

with

$$\rho = \frac{MM'na^2}{(M+M')C\dot{\theta}}, \tag{54}$$

where C is the polar moment of inertia of the planet. Note that this equation does not depend on the dissipative properties of the satellite but only on those of the planet. Meanwhile, the rate of change of the inclination strongly depends on the semi-major axis of the satellite orbit. It is therefore expected that, as the satellite recedes from the planet (as we integrate backwards in time), di/dt decreases considerably. Note that since the inclinations remain small throughout the entire orbital history of the moons, the validity of the equations for de/dt and da/dt in Section 13 is guaranteed in spite of the truncation in (53).

14 Orbital evolution theory – tidal coefficients

This section summarises all the tidal coefficients that are required in the development of the orbital theory as formulated in the Methods section of the main text (cf. Eqs. 9, 11, 14, and 16).

Supplementary Table 3: φ_j^{2i}

$\boxed{\varphi_j^{2i}}$

$j \backslash 2i$	0	2	4	6
-1	0	0	0	$\frac{1}{1536}$
1	0	$-\frac{3}{8}$	$\frac{3}{32}$	$-\frac{13}{512}$
2	-3	15	$-\frac{189}{8}$	$\frac{155}{12}$
3	0	$-\frac{441}{8}$	$\frac{7749}{32}$	$-\frac{197775}{512}$
4	0	0	$-\frac{867}{2}$	1955
5	0	0	0	$-\frac{3570125}{1536}$

$\boxed{\varphi_j^{2i}}$

${}_j\backslash 2i$	8	10	12	14	16	18
-7	0	0	0	0	0	$\frac{232630513987207}{469654673817600}$
-6	0	0	0	0	$\frac{4782969}{20070400}$	$\frac{1594323}{20070400}$
-5	0	0	0	$\frac{1220703125}{11098128384}$	$\frac{13427734375}{177570054144}$	$\frac{1619873046875}{14611478740992}$
-4	0	0	$\frac{32}{675}$	$\frac{32}{675}$	$\frac{92}{1575}$	$\frac{7808}{127575}$
-3	0	$\frac{59049}{3276800}$	$\frac{59049}{2621440}$	$\frac{38558997}{1468006400}$	$\frac{18482337}{671088640}$	$\frac{72655602021}{2630667468800}$
-2	$\frac{1}{192}$	$\frac{7}{960}$	$\frac{949}{115200}$	$\frac{10193}{1209600}$	$\frac{127453}{15482880}$	$\frac{781813}{99532800}$
-1	$\frac{11}{12288}$	$\frac{619}{655360}$	$\frac{64537}{70778880}$	$\frac{33683687}{39636172800}$	$\frac{165074183}{211392921600}$	$\frac{195618433037}{273965226393600}$
1	$-\frac{113}{12288}$	$-\frac{2639}{327680}$	$-\frac{129709}{19660800}$	$-\frac{73185503}{13212057600}$	$-\frac{21004537637}{4439251353600}$	$-\frac{5242619992367}{1278504389836800}$
2	$-\frac{2881}{768}$	$\frac{3481}{6400}$	$-\frac{12791}{92160}$	$-\frac{288163}{5644800}$	$-\frac{1190849}{24084480}$	$-\frac{535500317}{12541132800}$
3	$\frac{1193715}{4096}$	$-\frac{41889501}{327680}$	$\frac{237091671}{6553600}$	$-\frac{1586248587}{209715200}$	$\frac{863843049}{939524096}$	$-\frac{220413818169}{751619276800}$
4	$-\frac{83551}{24}$	$\frac{131319}{40}$	$-\frac{2459537}{1280}$	$\frac{232033433}{302400}$	$-\frac{77502109}{345600}$	$\frac{1505096129}{30481920}$
5	$\frac{137418125}{12288}$	$-\frac{2936126875}{131072}$	$\frac{356500341875}{14155776}$	$-\frac{29029068521875}{1585446912}$	$\frac{79231092391625}{8455716864}$	$-\frac{5599532275549375}{1565515579392}$
6	$-\frac{2556801}{256}$	$\frac{66328119}{1280}$	$-\frac{5938832817}{51200}$	$\frac{13527027819}{89600}$	$-\frac{1497798429597}{11468800}$	$\frac{931614290433}{11468800}$
7	0	$-\frac{364996466863}{9830400}$	$\frac{981779068235}{4718592}$	$-\frac{2921128205246293}{5662310400}$	$\frac{2760195487312025}{3623878656}$	$-\frac{9940709866552998323}{13045963161600}$
8	0	0	$-\frac{5383010161}{43200}$	$\frac{56914314263}{75600}$	$-\frac{578658802849}{282240}$	$\frac{77318558814617}{22861440}$
9	0	0	0	$-\frac{3982050900860283}{10276044800}$	$\frac{82748209967119359}{32883343360}$	$-\frac{11230592195266666389}{1503238553600}$
10	0	0	0	0	$-\frac{2010318936125}{1769472}$	$\frac{880939918004375}{111476736}$
11	0	0	0	0	0	$-\frac{7313703704315548899059}{23013079017062400}$

Supplementary Table 4: $\hat{\varphi}_j^{2i}$

$\boxed{\hat{\varphi}_j^{2i}}$

$j \backslash 2i$	0	2	4	6
1	0	$-\frac{9}{4}$	$-\frac{81}{16}$	$-\frac{2295}{256}$
2	0	0	$-\frac{81}{8}$	$-\frac{63}{4}$
3	0	0	0	$-\frac{8427}{256}$

$\boxed{\hat{\varphi}_j^{2i}}$

$j \backslash 2i$	8	10	12	14	16	18
1	$-\frac{28403}{2048}$	$-\frac{3240741}{163840}$	$-\frac{87480539}{3276800}$	$-\frac{76230921863}{2202009600}$	$-\frac{143189681823}{3288334336}$	$-\frac{3798168072196597}{71028021657600}$
2	$-\frac{1661}{64}$	$-\frac{12027}{320}$	$-\frac{525521}{10240}$	$-\frac{13519469}{201600}$	$-\frac{729537581}{8601600}$	$-\frac{56670971611}{541900800}$
3	$-\frac{62487}{2048}$	$-\frac{18059643}{327680}$	$-\frac{96458913}{1310720}$	$-\frac{10219795947}{104857600}$	$-\frac{1455222699297}{11744051200}$	$-\frac{28832512267869}{187904819200}$
4	$-\frac{5929}{64}$	$-\frac{9933}{320}$	$-\frac{708871}{6400}$	$-\frac{1736021}{14400}$	$-\frac{27865091}{172032}$	$-\frac{2578148063}{12902400}$
5	0	$-\frac{15717645}{65536}$	$\frac{14736585}{262144}$	$-\frac{67620980465}{264241152}$	$-\frac{212874343975}{1409286144}$	$-\frac{13593131130225}{52613349376}$
6	0	0	$-\frac{30089667}{51200}$	$\frac{20778687}{44800}$	$-\frac{592612065}{802816}$	$-\frac{124700799}{20070400}$
7	0	0	0	$-\frac{1306918425967}{943718400}$	$\frac{9297259269991}{5033164800}$	$-\frac{6999935835286093}{2899102924800}$
8	0	0	0	0	$-\frac{31801945561}{10035200}$	$\frac{1606626956771}{270950400}$
9	0	0	0	0	0	$-\frac{37292291277118641}{5261334937600}$

Supplementary Table 5: $\gamma_0^{j,s}$

$\boxed{\gamma_0^{j,s}}$

$j \backslash s$	2	4	6	8	10	12	14	16	18
1	-3	3	$-\frac{5}{4}$	$\frac{7}{24}$	$-\frac{7}{160}$	$\frac{11}{2400}$	$-\frac{143}{403200}$	$\frac{143}{6773760}$	$-\frac{2431}{2438553600}$
2	0	$-\frac{3}{2}$	1	$-\frac{7}{24}$	$\frac{1}{20}$	$-\frac{11}{1920}$	$\frac{143}{302400}$	$-\frac{143}{4838400}$	$\frac{221}{152409600}$
3	0	0	$-\frac{1}{4}$	$\frac{1}{8}$	$-\frac{9}{320}$	$\frac{11}{2880}$	$-\frac{143}{403200}$	$\frac{13}{537600}$	$-\frac{221}{174182400}$
4	0	0	0	$-\frac{1}{48}$	$\frac{1}{120}$	$-\frac{11}{7200}$	$\frac{13}{75600}$	$-\frac{13}{967680}$	$\frac{17}{21772800}$
5	0	0	0	0	$-\frac{1}{960}$	$\frac{1}{2880}$	$-\frac{13}{241920}$	$\frac{1}{193536}$	$-\frac{17}{48771072}$
6	0	0	0	0	0	$-\frac{1}{28800}$	$\frac{1}{100800}$	$-\frac{1}{752640}$	$\frac{17}{152409600}$
7	0	0	0	0	0	0	$-\frac{1}{1209600}$	$\frac{1}{4838400}$	$-\frac{17}{696729600}$
8	0	0	0	0	0	0	0	$-\frac{1}{67737600}$	$\frac{1}{304819200}$
9	0	0	0	0	0	0	0	0	$-\frac{1}{4877107200}$

$\boxed{\gamma_1^{j,s}}$

$j \backslash s$	1	3	5	7	9	11	13	15	17
1	30	-42	$\frac{45}{2}$	$-\frac{77}{12}$	$\frac{91}{80}$	$-\frac{11}{80}$	$\frac{2431}{201600}$	$-\frac{2717}{3386880}$	$\frac{2431}{58060800}$
2	0	21	-18	$\frac{77}{12}$	$-\frac{13}{10}$	$\frac{11}{64}$	$-\frac{2431}{151200}$	$\frac{2717}{2419200}$	$-\frac{221}{3628800}$
3	0	0	$\frac{9}{2}$	$-\frac{11}{4}$	$\frac{117}{160}$	$-\frac{11}{96}$	$\frac{2431}{201600}$	$-\frac{247}{268800}$	$\frac{221}{4147200}$
4	0	0	0	$\frac{11}{24}$	$-\frac{13}{60}$	$\frac{11}{240}$	$-\frac{221}{37800}$	$\frac{247}{483840}$	$-\frac{17}{518400}$
5	0	0	0	0	$\frac{13}{480}$	$-\frac{1}{96}$	$\frac{221}{120960}$	$-\frac{19}{96768}$	$\frac{17}{1161216}$
6	0	0	0	0	0	$\frac{1}{960}$	$-\frac{17}{50400}$	$\frac{19}{376320}$	$-\frac{17}{3628800}$
7	0	0	0	0	0	0	$\frac{17}{604800}$	$-\frac{19}{2419200}$	$\frac{17}{16588800}$
8	0	0	0	0	0	0	0	$\frac{19}{33868800}$	$-\frac{1}{7257600}$
9	0	0	0	0	0	0	0	0	$\frac{1}{116121600}$

$\boxed{\gamma_2^{j,s}}$

$j \backslash s$	2	4	6	8	10	12	14	16
1	$\frac{825}{4}$	$-\frac{2753}{16}$	$\frac{6313}{96}$	$-\frac{9303}{640}$	$\frac{20153}{9600}$	$-\frac{68959}{322560}$	$\frac{2192333}{135475200}$	$-\frac{9231079}{9754214400}$
2	$-\frac{249}{2}$	$\frac{305}{2}$	$-\frac{421}{6}$	$\frac{139}{8}$	$-\frac{5207}{1920}$	$\frac{176803}{604800}$	$-\frac{55913}{2419200}$	$\frac{426439}{304819200}$
3	0	$-\frac{709}{16}$	$\frac{1063}{32}$	$-\frac{2685}{256}$	$\frac{21953}{11520}$	$-\frac{52613}{230400}$	$\frac{14001}{716800}$	$-\frac{125099}{99532800}$
4	0	0	$-\frac{301}{48}$	$\frac{817}{240}$	$-\frac{2941}{3600}$	$\frac{101}{864}$	$-\frac{54847}{4838400}$	$\frac{4987}{6220800}$
5	0	0	0	$-\frac{1817}{3840}$	$\frac{2323}{11520}$	$-\frac{37753}{967680}$	$\frac{17803}{3870720}$	$-\frac{72977}{195084288}$
6	0	0	0	0	$-\frac{637}{28800}$	$\frac{313}{40320}$	$-\frac{789}{627200}$	$\frac{38419}{304819200}$
7	0	0	0	0	0	$-\frac{3397}{4838400}$	$\frac{811}{3870720}$	$-\frac{81401}{2786918400}$
8	0	0	0	0	0	0	$-\frac{1091}{67737600}$	$\frac{2549}{609638400}$
9	0	0	0	0	0	0	0	$-\frac{5449}{19508428800}$

$\boxed{\gamma_3^{j,s}}$

$j \backslash s$	1	3	5	7	9	11	13	15
1	$-\frac{1647}{4}$	$\frac{5561}{8}$	$-\frac{38129}{96}$	$\frac{11165}{96}$	$-\frac{40039}{1920}$	$\frac{2042161}{806400}$	$-\frac{4303871}{19353600}$	$\frac{6010433}{406425600}$
2	357	$-\frac{2993}{4}$	$\frac{23023}{48}$	$-\frac{36377}{240}$	$\frac{11029}{384}$	$-\frac{4400891}{1209600}$	$\frac{639353}{1935360}$	$-\frac{655343}{29030400}$
3	0	$\frac{2137}{8}$	$-\frac{8463}{32}$	$\frac{32879}{320}$	$-\frac{50911}{2304}$	$\frac{2464253}{806400}$	$-\frac{1911013}{6451200}$	$\frac{11453}{537600}$
4	0	0	$\frac{5551}{96}$	$-\frac{3619}{96}$	$\frac{7553}{720}$	$-\frac{515197}{302400}$	$\frac{595907}{3225600}$	$-\frac{419393}{29030400}$
5	0	0	0	$\frac{1881}{320}$	$-\frac{6605}{2304}$	$\frac{300767}{483840}$	$-\frac{104549}{1290240}$	$\frac{2095}{290304}$
6	0	0	0	0	$\frac{1991}{5760}$	$-\frac{54389}{403200}$	$\frac{77323}{3225600}$	$-\frac{19639}{7526400}$
7	0	0	0	0	0	$\frac{31991}{2419200}$	$-\frac{83323}{19353600}$	$\frac{75289}{116121600}$
8	0	0	0	0	0	0	$\frac{6871}{19353600}$	$-\frac{40321}{406425600}$
9	0	0	0	0	0	0	0	$\frac{13}{1843200}$

$\boxed{\gamma_4^{j,s}}$

$j \backslash s$	2	4	6	8	10	12	14
1	$-\frac{47555}{32}$	$\frac{190709}{128}$	$-\frac{400233}{640}$	$\frac{1121033}{7680}$	$-\frac{23458073}{1075200}$	$\frac{35199901}{15482880}$	$-\frac{852863297}{4877107200}$
2	$\frac{8687}{4}$	$-\frac{34773}{16}$	$\frac{4644}{5}$	$-\frac{425111}{1920}$	$\frac{1512829}{44800}$	$-\frac{1387199}{387072}$	$\frac{85408297}{304819200}$
3	$-\frac{32127}{32}$	$\frac{185441}{128}$	$-\frac{934671}{1280}$	$\frac{8842181}{46080}$	$-\frac{100865411}{3225600}$	$\frac{9994067}{2867200}$	$-\frac{98657507}{348364800}$
4	0	$-\frac{23833}{64}$	$\frac{12277}{40}$	$-\frac{196591}{1920}$	$\frac{1944769}{100800}$	$-\frac{9191771}{3870720}$	$\frac{9035869}{43545600}$
5	0	0	$-\frac{68941}{1280}$	$\frac{31835}{1024}$	$-\frac{998839}{129024}$	$\frac{17575681}{15482880}$	$-\frac{10930351}{97542144}$
6	0	0	0	$-\frac{23699}{5760}$	$\frac{737969}{403200}$	$-\frac{5213}{14336}$	$\frac{13298189}{304819200}$
7	0	0	0	0	$-\frac{208333}{1075200}$	$\frac{5434133}{77414400}$	$-\frac{16170799}{1393459200}$
8	0	0	0	0	0	$-\frac{239213}{38707200}$	$\frac{1152077}{609638400}$
9	0	0	0	0	0	0	$-\frac{1387327}{9754214400}$

$\boxed{\gamma_5^{j,s}}$

$j \backslash s$	1	3	5	7	9	11	13
1	$\frac{22769}{16}$	$-\frac{1296283}{384}$	$\frac{4380193}{1920}$	$-\frac{42520013}{57600}$	$\frac{113941067}{806400}$	$-\frac{463361041}{25804800}$	$\frac{1135527679}{696729600}$
2	$-\frac{13539}{4}$	$\frac{2484625}{384}$	$-\frac{1952053}{480}$	$\frac{58912711}{46080}$	$-\frac{292763719}{1209600}$	$\frac{2374678163}{77414400}$	$-\frac{53957761}{19353600}$
3	$\frac{71825}{32}$	$-\frac{697647}{128}$	$\frac{9779869}{2560}$	$-\frac{14726891}{11520}$	$\frac{813614173}{3225600}$	$-\frac{850321511}{25804800}$	$\frac{854790599}{278691840}$
4	0	$\frac{81433}{48}$	$-\frac{3590417}{1920}$	$\frac{89371417}{115200}$	$-\frac{210499391}{1209600}$	$\frac{958855703}{38707200}$	$-\frac{854451569}{348364800}$
5	0	0	$\frac{191637}{512}$	$-\frac{303739}{1152}$	$\frac{149339629}{1935360}$	$-\frac{200654617}{15482880}$	$\frac{400813631}{278691840}$
6	0	0	0	$\frac{8889011}{230400}$	$-\frac{8043643}{403200}$	$\frac{116210893}{25804800}$	$-\frac{105142393}{174182400}$
7	0	0	0	0	$\frac{11083823}{4838400}$	$-\frac{10353229}{11059200}$	$\frac{159751717}{928972800}$
8	0	0	0	0	0	$\frac{2277181}{25804800}$	$-\frac{20783387}{696729600}$
9	0	0	0	0	0	0	$\frac{1327271}{557383680}$

$\boxed{\gamma_6^{j,s}}$

$j \backslash s$	2	4	6	8	10	12
1	$\frac{6360697}{1536}$	$-\frac{83914747}{15360}$	$\frac{205972691}{76800}$	$-\frac{238333495}{344064}$	$\frac{34401989173}{309657600}$	$-\frac{67943553227}{5573836800}$
2	$-\frac{4527427}{384}$	$\frac{11995117}{960}$	$-\frac{85032277}{15360}$	$\frac{218343289}{161280}$	$-\frac{1086174427}{5160960}$	$\frac{7897450723}{348364800}$
3	$\frac{6894791}{512}$	$-\frac{149105731}{10240}$	$\frac{67081587}{10240}$	$-\frac{2785868387}{1720320}$	$\frac{2911274687}{11468800}$	$-\frac{25580115979}{928972800}$
4	$-\frac{1024813}{192}$	$\frac{818159}{96}$	$-\frac{22057967}{4800}$	$\frac{1273775}{1008}$	$-\frac{4112465311}{19353600}$	$\frac{421956389}{17418240}$
5	0	$-\frac{20343329}{10240}$	$\frac{54424859}{30720}$	$-\frac{644732521}{1032192}$	$\frac{7580219749}{61931520}$	$-\frac{8635714091}{557383680}$
6	0	0	$-\frac{7421471}{25600}$	$\frac{1913875}{10752}$	$-\frac{133004803}{2867200}$	$\frac{816994861}{116121600}$
7	0	0	0	$-\frac{115244509}{5160960}$	$\frac{1077524291}{103219200}$	$-\frac{960692647}{445906944}$
8	0	0	0	0	$-\frac{5122889}{4838400}$	$\frac{1242901}{3110400}$
9	0	0	0	0	0	$-\frac{18025373}{530841600}$

$\boxed{\gamma_7^{j,s}}$

$j \backslash s$	1	3	5	7	9	11
1	$-\frac{1663559}{768}$	$\frac{121709581}{15360}$	$-\frac{312427823}{46080}$	$\frac{19673089399}{7741440}$	$-\frac{291425548999}{541900800}$	$\frac{2867948486117}{39016857600}$
2	$\frac{4244105}{384}$	$-\frac{195851269}{7680}$	$\frac{811588697}{46080}$	$-\frac{12636131167}{2150400}$	$\frac{1402888481}{1209600}$	$-\frac{986035976887}{6502809600}$
3	$-\frac{9859807}{512}$	$\frac{24914363}{640}$	$-\frac{4694903647}{184320}$	$\frac{11825097051}{1433600}$	$-\frac{23555895221}{14745600}$	$\frac{1149280143791}{5573836800}$
4	$\frac{4053463}{384}$	$-\frac{3400213}{120}$	$\frac{1948423099}{92160}$	$-\frac{317943461}{43008}$	$\frac{11099163623}{7372800}$	$-\frac{280439920391}{1393459200}$
5	0	$\frac{121754083}{15360}$	$-\frac{1736132939}{184320}$	$\frac{31935948797}{7741440}$	$-\frac{19885290673}{20643840}$	$\frac{1102592661521}{7803371520}$
6	0	0	$\frac{8062469}{4608}$	$-\frac{1689833129}{1290240}$	$\frac{4530651799}{11289600}$	$-\frac{1362209431217}{19508428800}$
7	0	0	0	$\frac{7010016683}{38707200}$	$-\frac{15241243613}{154828800}$	$\frac{14310329239}{619315200}$
8	0	0	0	0	$\frac{23423982107}{2167603200}$	$-\frac{89822032001}{19508428800}$
9	0	0	0	0	0	$\frac{2039795207}{4877107200}$

$\boxed{\gamma_8^{j,s}}$

$j \backslash s$	2	4	6	8	10
1	$-\frac{36667771}{6144}$	$\frac{137576377}{12288}$	$-\frac{58268412071}{8601600}$	$\frac{3483804392591}{1734082560}$	$-\frac{3962944769797}{11147673600}$
2	$\frac{7932001}{256}$	$-\frac{3629434021}{92160}$	$\frac{62558288021}{3225600}$	$-\frac{393958246799}{77414400}$	$\frac{1159836156341}{1393459200}$
3	$-\frac{1378786789}{20480}$	$\frac{5365102241}{73728}$	$-\frac{847780261361}{25804800}$	$\frac{3370548827407}{412876800}$	$-\frac{5974574495}{4644864}$
4	$\frac{124022959}{1920}$	$-\frac{425217367}{5760}$	$\frac{13920972659}{403200}$	$-\frac{34003821749}{3870720}$	$\frac{122575184351}{87091200}$
5	$-\frac{1391241377}{61440}$	$\frac{4788563821}{122880}$	$-\frac{114133290857}{5160960}$	$\frac{1565177035693}{247726080}$	$-\frac{609862623793}{557383680}$
6	0	$-\frac{154509701}{18432}$	$\frac{3653368319}{460800}$	$-\frac{105576999331}{36126720}$	$\frac{275386936571}{464486400}$
7	0	0	$-\frac{31536438929}{25804800}$	$\frac{975977916433}{1238630400}$	$-\frac{4758029916799}{22295347200}$
8	0	0	0	$-\frac{25549718947}{270950400}$	$\frac{4573097093}{99532800}$
9	0	0	0	0	$-\frac{99964117517}{22295347200}$

$\boxed{\gamma_9^{j,s}}$

$j \backslash s$	1	3	5	7	9
1	$\frac{72574433}{40960}$	$-\frac{33250133}{3072}$	$\frac{321566834083}{25804800}$	$-\frac{48892934193757}{8670412800}$	$\frac{424304933869777}{312134860800}$
2	$-\frac{139238303}{7680}$	$\frac{2812070945}{49152}$	$-\frac{1815292535809}{38707200}$	$\frac{21601089607747}{1238630400}$	$-\frac{144839901437071}{39016857600}$
3	$\frac{326578731}{5120}$	$-\frac{3318429817}{23040}$	$\frac{1712182537183}{17203200}$	$-\frac{13787028701293}{412876800}$	$\frac{295876625683021}{44590694400}$
4	$-\frac{45278785}{512}$	$\frac{8612926109}{46080}$	$-\frac{4880466678209}{38707200}$	$\frac{17258868186769}{412876800}$	$-\frac{22984018946099}{2786918400}$
5	$\frac{851962171}{20480}$	$-\frac{44593891643}{368640}$	$\frac{293291537465}{3096576}$	$-\frac{8497199910629}{247726080}$	$\frac{89611617850873}{12485394432}$
6	0	$\frac{713014643}{23040}$	$-\frac{41944969211}{1075200}$	$\frac{51535195929577}{2890137600}$	$-\frac{167924593843033}{39016857600}$
7	0	0	$\frac{1052720951633}{154828800}$	$-\frac{6613213406581}{1238630400}$	$\frac{151464161578421}{89181388800}$
8	0	0	0	$\frac{76155429263}{108380160}$	$-\frac{31037807709701}{78033715200}$
9	0	0	0	0	$\frac{26184666395077}{624269721600}$

$\boxed{\gamma_{10}^{j,s}}$

$j \backslash s$	2	4	6	8
1	$\frac{4188185133}{819200}$	$-\frac{668034376553}{45875200}$	$\frac{298635437603}{26214400}$	$-\frac{5008680379354717}{1248539443200}$
2	$-\frac{69622578569}{1474560}$	$\frac{288361412803}{3686400}$	$-\frac{3733878109439}{82575360}$	$\frac{14728473880769}{1114767360}$
3	$\frac{105043267843}{589824}$	$-\frac{90447675495017}{412876800}$	$\frac{176246672641693}{1651507200}$	$-\frac{2489696844203003}{89181388800}$
4	$-\frac{72784945777}{230400}$	$\frac{560166907039}{1612800}$	$-\frac{49295772110719}{309657600}$	$\frac{13961643516553}{348364800}$
5	$\frac{776330530877}{2949120}$	$-\frac{1732963120055}{5505024}$	$\frac{30099792470603}{198180864}$	$-\frac{705923122737949}{17836277760}$
6	$-\frac{613186054801}{7372800}$	$\frac{436748965809}{2867200}$	$-\frac{37201323168383}{412876800}$	$\frac{1036259700960391}{39016857600}$
7	0	$-\frac{4206593801911}{137625600}$	$\frac{7158257783303}{235929600}$	$-\frac{4137506209801739}{356725555200}$
8	0	0	$-\frac{229049541811}{51609600}$	$\frac{58107407588357}{19508428800}$
9	0	0	0	$-\frac{645135681793}{1887436800}$

$\boxed{\gamma_{11}^{j,s}}$

$j \backslash s$	1	3	5	7
1	$-\frac{4390861889}{4915200}$	$\frac{1961183621879}{206438400}$	$-\frac{38437694104309}{2477260800}$	$\frac{5499256218016573}{624269721600}$
2	$\frac{12960937279}{737280}$	$-\frac{25335942630283}{309657600}$	$\frac{1196416018969}{14155776}$	$-\frac{1266083597711297}{34681651200}$
3	$-\frac{20979287141}{184320}$	$\frac{22404670502027}{68812800}$	$-\frac{141336992746169}{550502400}$	$\frac{38716231419983}{412876800}$
4	$\frac{561041955133}{1843200}$	$-\frac{6585350448109}{9676800}$	$\frac{2333996611139251}{4954521600}$	$-\frac{1416438955564847}{8918138880}$
5	$-\frac{518643543809}{1474560}$	$\frac{2994059366393}{3870720}$	$-\frac{17684742866503}{33030144}$	$\frac{3766355622175117}{20808990720}$
6	$\frac{16753583267}{115200}$	$-\frac{1461464779987}{3225600}$	$\frac{76285236828841}{206438400}$	$-\frac{2867374053933953}{20808990720}$
7	0	$\frac{33195983160521}{309657600}$	$-\frac{234766934917157}{1651507200}$	$\frac{1501695875492263}{22295347200}$
8	0	0	$\frac{966755431567}{41287680}$	$-\frac{249061450017451}{13005619200}$
9	0	0	0	$\frac{1505225192085113}{624269721600}$

$\boxed{\gamma_{12}^{j,s}}$

$j \backslash s$	2	4	6
1	$-\frac{112405393703}{39321600}$	$\frac{256194365128103}{19818086400}$	$-\frac{2434459781946581}{178362777600}$
2	$\frac{14313033811823}{309657600}$	$-\frac{12498570084137}{117964800}$	$\frac{1677509997505583}{22295347200}$
3	$-\frac{239571154081783}{825753600}$	$\frac{2904792531811861}{6606028800}$	$-\frac{120767420385113}{495452160}$
4	$\frac{16651792420267}{19353600}$	$-\frac{3664938831889}{3538944}$	$\frac{3986190927755}{7962624}$
5	$-\frac{91659779628347}{70778880}$	$\frac{1912786165948037}{1321205760}$	$-\frac{5996938416572659}{8918138880}$
6	$\frac{32945086429187}{34406400}$	$-\frac{28119643773793}{23592960}$	$\frac{1463376996779051}{2477260800}$
7	$-\frac{684201699957701}{2477260800}$	$\frac{10590857503323379}{19818086400}$	$-\frac{23381239709702027}{71345111040}$
8	0	$-\frac{62410695774613}{619315200}$	$\frac{166206910739587}{1592524800}$
9	0	0	$-\frac{577143489956477}{39636172800}$

$\boxed{\gamma_{13}^{j,s}}$

$j \backslash s$	1	3	5
1	$\frac{4480458061}{14745600}$	$-\frac{113509427927533}{19818086400}$	$\frac{4932648254178133}{356725555200}$
2	$-\frac{692621429069}{61931520}$	$\frac{1586490110623811}{19818086400}$	$-\frac{811950375727963}{7431782400}$
3	$\frac{104673184486151}{825753600}$	$-\frac{3256104685646191}{6606028800}$	$\frac{4461263791004999}{9512681472}$
4	$-\frac{91340140787233}{154828800}$	$\frac{156492482258165}{99090432}$	$-\frac{14394426401891911}{11890851840}$
5	$\frac{314766782631703}{247726080}$	$-\frac{2809659549121933}{990904320}$	$\frac{28104217865113080 1}{142690222080}$
6	$-\frac{1355991878713}{1075200}$	$\frac{39617412502949}{13762560}$	$-\frac{336875717415931}{165150720}$
7	$\frac{72172041424697}{154828800}$	$-\frac{15307727148091081}{9909043200}$	$\frac{23309603694431853 1}{178362777600}$
8	0	$\frac{105529641662017}{309657600}$	$-\frac{376559490960019}{796262400}$
9	0	0	$\frac{26397815834028073}{356725555200}$

$\boxed{\gamma_{15}^{j,s}}$

$j \backslash s$	1	3
1	$-\frac{3469384763227}{46242201600}$	$\frac{1187663466854671}{475634073600}$
2	$\frac{19888331524783}{3963617280}$	$-\frac{127712690841809}{2264924160}$
3	$-\frac{2547496947290741}{26424115200}$	$\frac{31541032831484593}{59454259200}$
4	$\frac{4883476194008213}{6606028800}$	$-\frac{18839933887964653}{7431782400}$
5	$-\frac{469284844441745}{176160768}$	$\frac{648190780936041043}{95126814720}$
6	$\frac{6936784270529417}{1445068800}$	$-\frac{79914423777412117}{7431782400}$
7	$-\frac{109591789469563}{26214400}$	$\frac{783868077139349141}{79272345600}$
8	$\frac{17967831915895}{12845056}$	$-\frac{18230346413898349}{3715891200}$
9	0	$\frac{30182462841350683}{29727129600}$

$\boxed{\gamma_{14}^{j,s}}$

$j \backslash s$	2	4
1	$\frac{206796563366483}{184968806400}$	$-\frac{82215574092860581}{9988315545600}$
2	$-\frac{618579830111987}{19818086400}$	$\frac{64337807855429791}{624269721600}$
3	$\frac{8402777041707077}{26424115200}$	$-\frac{447073478617395173}{713451110400}$
4	$-\frac{7430296569379097}{4954521600}$	$\frac{17606260552429}{8257536}$
5	$\frac{6461512425366487}{1761607680}$	$-\frac{4349564850250920329}{998831554560}$
6	$-\frac{222276140779005643}{46242201600}$	$\frac{3412415816069604403}{624269721600}$
7	$\frac{253818565838765371}{79272345600}$	$-\frac{1685837673188956681}{407686348800}$
8	$-\frac{7380514090083647}{8670412800}$	$\frac{540458699263271861}{312134860800}$
9	0	$-\frac{1232692494304457819}{3995326218240}$

$\boxed{\gamma_{16}^{j,s}}$

$j \backslash s$	2
1	$\frac{131482629287941}{407686348800}$
2	$\frac{7661258420564069}{499415777280}$
3	$-\frac{22226193309071407}{89181388800}$
4	$\frac{5778045333852317}{3185049600}$
5	$-\frac{1363999477757941669}{199766310912}$
6	$\frac{35510799156457152389}{2497078886400}$
7	$-\frac{94340848292247889769}{5707608883200}$
8	$\frac{12526197981986130907}{1248539443200}$
9	$-\frac{19789563585947876009}{7990652436480}$

Supplementary Table 6: λ_j^{2i-1}

$\boxed{\lambda_j^{2i-1}}$				
$j \backslash 2i-1$	1	3	5	7
-2	0	0	0	$\frac{1}{192}$
-1	0	0	$\frac{1}{1024}$	$\frac{17}{24576}$
1	$\frac{3}{16}$	$-\frac{3}{64}$	$-\frac{35}{1024}$	$-\frac{175}{24576}$
2	$\frac{3}{4}$	$-\frac{63}{16}$	$\frac{27}{4}$	$-\frac{3299}{768}$
3	$-\frac{147}{16}$	$\frac{3759}{64}$	$-\frac{150933}{1024}$	$\frac{1525953}{8192}$
4	0	$-\frac{867}{8}$	$\frac{10421}{16}$	$-\frac{310463}{192}$
5	0	0	$-\frac{714025}{1024}$	$\frac{105299675}{24576}$
6	0	0	0	$-\frac{852267}{256}$

$\boxed{\lambda_j^{2i-1}}$

${}_j\diagdown^{2i-1}$	9	11	13	15	17
-7	0	0	0	0	$\frac{33232930569601}{104367705292800}$
-6	0	0	0	$\frac{1594323}{10035200}$	$-\frac{6908733}{80281600}$
-5	0	0	$\frac{244140625}{3170893824}$	$-\frac{4638671875}{355140108288}$	$\frac{861572265625}{29222957481984}$
-4	0	$\frac{8}{225}$	$\frac{4}{675}$	$\frac{4}{315}$	$\frac{61}{8505}$
-3	$\frac{19683}{1310720}$	$\frac{177147}{26214400}$	$\frac{17970579}{2936012800}$	$\frac{193818501}{46976204800}$	$\frac{15029958483}{5261334937600}$
-2	$\frac{13}{3840}$	$\frac{563}{230400}$	$\frac{3943}{2419200}$	$\frac{2951}{2764800}$	$\frac{1904023}{2786918400}$
-1	$\frac{577}{1310720}$	$\frac{12769}{47185920}$	$\frac{12959141}{79272345600}$	$\frac{40473781}{422785843200}$	$\frac{9536091053}{182643484262400}$
1	$-\frac{5201}{655360}$	$-\frac{237091}{39321600}$	$-\frac{130286017}{26424115200}$	$-\frac{7343600351}{1775700541440}$	$-\frac{9052063323217}{2557008779673600}$
2	$\frac{1289}{1024}$	$-\frac{25999}{102400}$	$\frac{9569}{921600}$	$-\frac{250247}{15052800}$	$-\frac{818693}{68812800}$
3	$-\frac{85340127}{655360}$	$\frac{725981637}{13107200}$	$-\frac{6616127097}{419430400}$	$\frac{148062766923}{46976204800}$	$-\frac{151996417911}{300647710720}$
4	$\frac{1395551}{640}$	$-\frac{430553}{240}$	$\frac{4725763337}{4838400}$	$-\frac{7265523173}{19353600}$	$\frac{10430507833}{97542144}$
5	$-\frac{2949543325}{262144}$	$\frac{158224764775}{9437184}$	$-\frac{50749964351125}{3170893824}$	$\frac{25510094869225}{2415919104}$	$-\frac{37167304047148325}{7305739370496}$
6	$\frac{109744167}{5120}$	$-\frac{6191465853}{102400}$	$\frac{71414520309}{716800}$	$-\frac{124297728921}{1146880}$	$\frac{3840730800633}{45875200}$
7	$-\frac{52142352409}{3932160}$	$\frac{21286018449073}{235929600}$	$-\frac{3103858544107391}{11324620800}$	$\frac{899635438879070 11}{181193932800}$	$-\frac{15814983098946990889}{26091926323200}$
8	0	$-\frac{5383010161}{115200}$	$\frac{1629711040201}{4838400}$	$-\frac{49681058130967}{45158400}$	$\frac{5306383534261451}{2438553600}$
9	0	0	$-\frac{442450100095587}{2936012800}$	$\frac{378432207128810421}{328833433600}$	$-\frac{12113553017690673723}{3006477107200}$
10	0	0	0	$-\frac{402063787225}{884736}$	$\frac{1637474036163575}{445906944}$
11	0	0	0	0	$-\frac{6648821549377771726369}{5114017559347200}$

Supplementary Table 7: $\hat{\lambda}_j^{2i-1}$

$\boxed{\hat{\lambda}_j^{2i-1}}$

$j \backslash 2i-1$	1	3	5	7
1	$-\frac{9}{8}$	$-\frac{45}{32}$	$-\frac{999}{512}$	$-\frac{10043}{4096}$
2	0	$-\frac{81}{16}$	$-\frac{45}{16}$	$-\frac{653}{128}$
3	0	0	$-\frac{8427}{512}$	$\frac{4929}{4096}$
4	0	0	0	$-\frac{5929}{128}$

$\boxed{\hat{\lambda}_j^{2i-1}}$

$j \backslash 2i-1$	9	11	13	15	17
1	$-\frac{968501}{327680}$	$-\frac{22665719}{6553600}$	$-\frac{3488799931}{880803840}$	$-\frac{2201362888069}{493250150400}$	$-\frac{705270944819797}{142056043315200}$
2	$-\frac{1861}{320}$	$-\frac{140657}{20480}$	$-\frac{50772389}{6451200}$	$-\frac{458120711}{51609600}$	$-\frac{1338763001}{135475200}$
3	$-\frac{8061723}{655360}$	$-\frac{24220341}{2621440}$	$-\frac{2503082907}{209715200}$	$-\frac{310605553233}{23488102400}$	$-\frac{5548949079117}{375809638400}$
4	$\frac{154}{5}$	$-\frac{510211}{12800}$	$-\frac{112849}{23040}$	$-\frac{534407009}{25804800}$	$-\frac{244133119}{12902400}$
5	$-\frac{15717645}{131072}$	$\frac{77607165}{524288}$	$-\frac{82475458145}{528482304}$	$\frac{443312655515}{8455716864}$	$-\frac{16937466865475}{315680096256}$
6	0	$-\frac{30089667}{102400}$	$\frac{75371433}{143360}$	$-\frac{24124153401}{40140800}$	$\frac{7345300413}{20070400}$
7	0	0	$-\frac{1306918425967}{1887436800}$	$\frac{9760494525089}{6039797760}$	$-\frac{12355157174800909}{5798205849600}$
8	0	0	0	$-\frac{31801945561}{20070400}$	$\frac{1232639743459}{270950400}$
9	0	0	0	0	$-\frac{37292291277118641}{10522669875200}$

Supplementary Table 8: $\eta_i^{j,s}$

$\boxed{\eta_{-1}^{j,s}}$

$j \backslash s$	2	4	6	8	10	12	14	16	18
1	$-\frac{3}{2}$	$\frac{3}{2}$	$-\frac{5}{8}$	$\frac{7}{48}$	$-\frac{7}{320}$	$\frac{11}{4800}$	$-\frac{143}{806400}$	$\frac{143}{13547520}$	$-\frac{2431}{4877107200}$
2	0	$-\frac{3}{4}$	$\frac{1}{2}$	$-\frac{7}{48}$	$\frac{1}{40}$	$-\frac{11}{3840}$	$\frac{143}{604800}$	$-\frac{143}{9676800}$	$\frac{221}{304819200}$
3	0	0	$-\frac{1}{8}$	$\frac{1}{16}$	$-\frac{9}{640}$	$\frac{11}{5760}$	$-\frac{143}{806400}$	$\frac{13}{1075200}$	$-\frac{221}{348364800}$
4	0	0	0	$-\frac{1}{96}$	$\frac{1}{240}$	$-\frac{11}{14400}$	$\frac{13}{151200}$	$-\frac{13}{1935360}$	$\frac{17}{43545600}$
5	0	0	0	0	$-\frac{1}{1920}$	$\frac{1}{5760}$	$-\frac{13}{483840}$	$\frac{1}{387072}$	$-\frac{17}{97542144}$
6	0	0	0	0	0	$-\frac{1}{57600}$	$\frac{1}{201600}$	$-\frac{1}{1505280}$	$\frac{17}{304819200}$
7	0	0	0	0	0	0	$-\frac{1}{2419200}$	$\frac{1}{9676800}$	$-\frac{17}{1393459200}$
8	0	0	0	0	0	0	0	$-\frac{1}{135475200}$	$\frac{1}{609638400}$
9	0	0	0	0	0	0	0	0	$-\frac{1}{9754214400}$

$\boxed{\eta_{0}^{j,s}}$

$j \backslash s$	1	3	5	7	9	11	13	15	17
1	6	-12	$\frac{15}{2}$	$-\frac{7}{3}$	$\frac{7}{16}$	$-\frac{11}{200}$	$\frac{143}{28800}$	$-\frac{143}{423360}$	$\frac{2431}{135475200}$
2	0	6	-6	$\frac{7}{3}$	$-\frac{1}{2}$	$\frac{11}{160}$	$-\frac{143}{21600}$	$\frac{143}{302400}$	$-\frac{221}{8467200}$
3	0	0	$\frac{3}{2}$	-1	$\frac{9}{32}$	$-\frac{11}{240}$	$\frac{143}{28800}$	$-\frac{13}{33600}$	$\frac{221}{9676800}$
4	0	0	0	$\frac{1}{6}$	$-\frac{1}{12}$	$\frac{11}{600}$	$-\frac{13}{5400}$	$\frac{13}{60480}$	$-\frac{17}{1209600}$
5	0	0	0	0	$\frac{1}{96}$	$-\frac{1}{240}$	$\frac{13}{17280}$	$-\frac{1}{12096}$	$\frac{17}{2709504}$
6	0	0	0	0	0	$\frac{1}{2400}$	$-\frac{1}{7200}$	$\frac{1}{47040}$	$-\frac{17}{8467200}$
7	0	0	0	0	0	0	$\frac{1}{86400}$	$-\frac{1}{302400}$	$\frac{17}{38707200}$
8	0	0	0	0	0	0	0	$\frac{1}{4233600}$	$-\frac{1}{16934400}$
9	0	0	0	0	0	0	0	0	$\frac{1}{270950400}$

$\boxed{\eta_1^{j,s}}$

$j \backslash s$	2	4	6	8	10	12	14	16
1	$\frac{345}{8}$	$-\frac{1401}{32}$	$\frac{3661}{192}$	$-\frac{17717}{3840}$	$\frac{911}{1280}$	$-\frac{49159}{645120}$	$\frac{60203}{10035200}$	$-\frac{784927}{2167603200}$
2	$-\frac{63}{2}$	42	$-\frac{1015}{48}$	$\frac{169}{30}$	$-\frac{149}{160}$	$\frac{3971}{37800}$	$-\frac{83369}{9676800}$	$\frac{13}{24192}$
3	0	$-\frac{429}{32}$	$\frac{675}{64}$	$-\frac{8977}{2560}$	$\frac{5123}{7680}$	$-\frac{89353}{1075200}$	$\frac{94757}{12902400}$	$-\frac{15041}{30965760}$
4	0	0	$-\frac{101}{48}$	$\frac{283}{240}$	$-\frac{281}{960}$	$\frac{1307}{30240}$	$-\frac{5213}{1209600}$	$\frac{1511}{4838400}$
5	0	0	0	$-\frac{87}{512}$	$\frac{569}{7680}$	$-\frac{28417}{1935360}$	$\frac{13711}{7741440}$	$-\frac{911}{6193152}$
6	0	0	0	0	$-\frac{1}{120}$	$\frac{1}{336}$	$-\frac{11089}{22579200}$	$\frac{53}{1058400}$
7	0	0	0	0	0	$-\frac{379}{1382400}$	$\frac{3211}{38707200}$	$-\frac{1453}{123863040}$
8	0	0	0	0	0	0	$-\frac{73}{11289600}$	$\frac{23}{13547520}$
9	0	0	0	0	0	0	0	$-\frac{71}{619315200}$

$\boxed{\eta_2^{j,s}}$

$j \backslash s$	1	3	5	7	9	11	13	15
1	$-\frac{327}{4}$	$\frac{1233}{8}$	$-\frac{9565}{96}$	$\frac{5159}{160}$	$-\frac{12007}{1920}$	$\frac{651761}{806400}$	$-\frac{68783}{921600}$	$\frac{1261403}{243855360}$
2	$\frac{357}{4}$	$-\frac{789}{4}$	$\frac{401}{3}$	$-\frac{3587}{80}$	$\frac{34483}{3840}$	$-\frac{1444399}{1209600}$	$\frac{2431}{21504}$	$-\frac{99619}{12441600}$
3	0	$\frac{641}{8}$	$-\frac{2611}{32}$	$\frac{10467}{320}$	$-\frac{83851}{11520}$	$\frac{839597}{806400}$	$-\frac{224003}{2150400}$	$\frac{111917}{14515200}$
4	0	0	$\frac{925}{48}$	$-\frac{6143}{480}$	$\frac{10469}{2880}$	$-\frac{182537}{302400}$	$\frac{53989}{806400}$	$-\frac{18643}{3483648}$
5	0	0	0	$\frac{403}{192}$	$-\frac{11953}{11520}$	$\frac{110479}{483840}$	$-\frac{39017}{1290240}$	$\frac{149}{54432}$
6	0	0	0	0	$\frac{1493}{11520}$	$-\frac{20609}{403200}$	$\frac{4939}{537600}$	$-\frac{41137}{40642560}$
7	0	0	0	0	0	$\frac{1777}{345600}$	$-\frac{3631}{2150400}$	$\frac{89399}{348364800}$
8	0	0	0	0	0	0	$\frac{229}{1612800}$	$-\frac{48731}{1219276800}$
9	0	0	0	0	0	0	0	$\frac{67}{23224320}$

$\boxed{\eta_3^{j,s}}$

$j \backslash s$	2	4	6	8	10	12	14
1	$-\frac{21255}{64}$	$\frac{271475}{768}$	$-\frac{123499}{768}$	$\frac{621161}{15360}$	$-\frac{5939929}{921600}$	$\frac{21960257}{30965760}$	$-\frac{6879301}{120422400}$
2	$\frac{4719}{8}$	$-\frac{116567}{192}$	$\frac{128911}{480}$	$-\frac{255827}{3840}$	$\frac{25593509}{2419200}$	$-\frac{45154813}{38707200}$	$\frac{38392679}{406425600}$
3	$-\frac{19275}{64}$	$\frac{115821}{256}$	$-\frac{597223}{2560}$	$\frac{641693}{10240}$	$-\frac{67444943}{6451200}$	$\frac{61623623}{51609600}$	$-\frac{7693621}{77414400}$
4	0	$-\frac{23833}{192}$	$\frac{20147}{192}$	$-\frac{136771}{3840}$	$\frac{4123699}{604800}$	$-\frac{275077}{322560}$	$\frac{4398301}{58060800}$
5	0	0	$-\frac{9849}{512}$	$\frac{115783}{10240}$	$-\frac{11048333}{3870720}$	$\frac{485967}{1146880}$	$-\frac{13765531}{325140480}$
6	0	0	0	$-\frac{395}{256}$	$\frac{80189}{115200}$	$-\frac{360887}{2580480}$	$\frac{459229}{27095040}$
7	0	0	0	0	$-\frac{208343}{2764800}$	$\frac{4275161}{154828800}$	$-\frac{4280917}{928972800}$
8	0	0	0	0	0	$-\frac{1367}{552960}$	$\frac{206791}{270950400}$
9	0	0	0	0	0	0	$-\frac{126127}{2167603200}$

$\boxed{\eta_4^{j,s}}$

$j \backslash s$	1	3	5	7	9	11	13
1	$\frac{24193}{64}$	$-\frac{20095}{24}$	$\frac{2232473}{3840}$	$-\frac{5702117}{28800}$	$\frac{258053953}{6451200}$	$-\frac{14783483}{2764800}$	$\frac{707721157}{1393459200}$
2	$-\frac{15681}{16}$	$\frac{364907}{192}$	$-\frac{290039}{240}$	$\frac{8927209}{23040}$	$-\frac{364144573}{4838400}$	$\frac{401973}{40960}$	$-\frac{53307059}{58060800}$
3	$\frac{43095}{64}$	$-\frac{55743}{32}$	$\frac{400743}{320}$	$-\frac{545157}{1280}$	$\frac{61156327}{716800}$	$-\frac{36538619}{3225600}$	$\frac{498263623}{464486400}$
4	0	$\frac{27145}{48}$	$-\frac{414357}{640}$	$\frac{3950587}{14400}$	$-\frac{18886547}{302400}$	$\frac{87118681}{9676800}$	$-\frac{314307277}{348364800}$
5	0	0	$\frac{513319}{3840}$	$-\frac{1113803}{11520}$	$\frac{22286941}{774144}$	$-\frac{677069}{138240}$	$\frac{30624113}{55738368}$
6	0	0	0	$\frac{555563}{38400}$	$-\frac{1367699}{179200}$	$\frac{22551787}{12902400}$	$-\frac{13756051}{58060800}$
7	0	0	0	0	$\frac{2463053}{2764800}$	$-\frac{2386541}{6451200}$	$\frac{10650713}{154828800}$
8	0	0	0	0	0	$\frac{341573}{9676800}$	$-\frac{8424559}{696729600}$
9	0	0	0	0	0	0	$\frac{18853}{19353600}$

$\boxed{\eta_5^{j,s}}$

$j \backslash s$	2	4	6	8	10	12
1	$\frac{3704953}{3072}$	$-\frac{15221377}{10240}$	$\frac{112613299}{153600}$	$-\frac{1118827917}{5734400}$	$\frac{20121975317}{619315200}$	$-\frac{13766831089}{3715891200}$
2	$-\frac{2892187}{768}$	$\frac{1263513}{320}$	$-\frac{53719409}{30720}$	$\frac{695722717}{1612800}$	$-\frac{10541705029}{154828800}$	$\frac{868015153}{116121600}$
3	$\frac{4548103}{1024}$	$-\frac{101354707}{20480}$	$\frac{138786857}{61440}$	$-\frac{29109939893}{51609600}$	$\frac{18430053463}{206438400}$	$-\frac{18186003391}{1857945600}$
4	$-\frac{683209}{384}$	$\frac{11504597}{3840}$	$-\frac{10622857}{6400}$	$\frac{20787503}{44800}$	$-\frac{3055769779}{38707200}$	$\frac{2110699721}{232243200}$
5	0	$-\frac{8718503}{12288}$	$\frac{8058607}{12288}$	$-\frac{813411079}{3440640}$	$\frac{5826124357}{123863040}$	$-\frac{2237882701}{371589120}$
6	0	0	$-\frac{16698217}{153600}$	$\frac{110558537}{1612800}$	$-\frac{939128363}{51609600}$	$\frac{324869249}{116121600}$
7	0	0	0	$-\frac{64024591}{7372800}$	$\frac{2567559977}{619315200}$	$-\frac{6458660261}{7431782400}$
8	0	0	0	0	$-\frac{1170947}{2764800}$	$\frac{15106919}{92897280}$
9	0	0	0	0	0	$-\frac{14748077}{1061683200}$

$\boxed{\eta_6^{j,s}}$

$j \backslash s$	1	3	5	7	9	11
1	$-\frac{872943}{1024}$	$\frac{4813543}{1920}$	$-\frac{921770971}{460800}$	$\frac{7178895463}{9676800}$	$-\frac{230130795289}{1445068800}$	$\frac{108799751533}{4877107200}$
2	$\frac{6210857}{1536}$	$-\frac{13555561}{1536}$	$\frac{1097036731}{184320}$	$-\frac{362561267}{184320}$	$\frac{40085609077}{103219200}$	$-\frac{997573407349}{19508428800}$
3	$-\frac{6835241}{1024}$	$\frac{141981907}{10240}$	$-\frac{23491027}{2560}$	$\frac{771402715}{258048}$	$-\frac{17153333687}{29491200}$	$\frac{46732982197}{619315200}$
4	$\frac{1351153}{384}$	$-\frac{9745837}{960}$	$\frac{225435367}{28800}$	$-\frac{8993789107}{3225600}$	$\frac{6354465407}{11059200}$	$-\frac{11996360791}{154828800}$
5	0	$\frac{17393429}{6144}$	$-\frac{324807233}{92160}$	$\frac{175446745}{110592}$	$-\frac{46713835471}{123863040}$	$\frac{145741780141}{2601123840}$
6	0	0	$\frac{67187379}{102400}$	$-\frac{3277329481}{6451200}$	$\frac{115045714631}{722534400}$	$-\frac{2441359969}{86704128}$
7	0	0	0	$\frac{68153083}{967680}$	$-\frac{2704350493}{68812800}$	$\frac{14973217337}{1592524800}$
8	0	0	0	0	$\frac{260266787}{60211200}$	$-\frac{7340699509}{3901685760}$
9	0	0	0	0	0	$\frac{1483487713}{8670412800}$

$\boxed{\eta_7^{j,s}}$

$j \backslash s$	2	4	6	8	10
1	$-\frac{149727647}{61440}$	$\frac{155864751}{40960}$	$-\frac{4426663009}{2064384}$	$\frac{10797972126287}{17340825600}$	$-\frac{17243822330131}{156067430400}$
2	$\frac{93952097}{7680}$	$-\frac{896925851}{61440}$	$\frac{44924873743}{6451200}$	$-\frac{39763735267}{22118400}$	$\frac{5700875160973}{19508428800}$
3	$-\frac{1048933601}{40960}$	$\frac{2268428349}{81920}$	$-\frac{214946221871}{17203200}$	$\frac{512367188359}{165150720}$	$-\frac{129742491151}{265420800}$
4	$\frac{6081475}{256}$	$-\frac{432634279}{15360}$	$\frac{2165962973}{161280}$	$-\frac{16726054291}{4838400}$	$\frac{55551320611}{99532800}$
5	$-\frac{66249643}{8192}$	$\frac{3629650189}{245760}$	$-\frac{17874184561}{2064384}$	$\frac{178698259919}{70778880}$	$-\frac{432464713873}{975421440}$
6	0	$-\frac{193137247}{61440}$	$\frac{1333226933}{430080}$	$-\frac{424071056197}{361267200}$	$\frac{63117639931}{260112384}$
7	0	0	$-\frac{3504047651}{7372800}$	$\frac{783679385501}{2477260800}$	$-\frac{558242239781}{6370099200}$
8	0	0	0	$-\frac{1277485193}{33868800}$	$\frac{919564435}{48771072}$
9	0	0	0	0	$-\frac{63613501087}{34681651200}$

$\boxed{\eta_8^{j,s}}$

$j \backslash s$	1	3	5	7	9
1	$\frac{65652473}{61440}$	$-\frac{563582879}{122880}$	$\frac{92955405499}{20643840}$	$-\frac{5483932464937}{2890137600}$	$\frac{1285208299777}{2890137600}$
2	$-\frac{269639453}{30720}$	$\frac{739024483}{30720}$	$-\frac{204074346391}{11059200}$	$\frac{273003532891}{41287680}$	$-\frac{2389160130767}{1734082560}$
3	$\frac{275400323}{10240}$	$-\frac{43435464343}{737280}$	$\frac{460345468843}{11468800}$	$-\frac{5511201000007}{412876800}$	$\frac{58779091690057}{22295347200}$
4	$-\frac{43362121}{1280}$	$\frac{3416637469}{46080}$	$-\frac{78771223009}{1548288}$	$\frac{5273431096139}{309657600}$	$-\frac{52329578737}{15482880}$
5	$\frac{121708789}{8192}$	$-\frac{34357420961}{737280}$	$\frac{2345355924239}{61931520}$	$-\frac{3473845411853}{247726080}$	$\frac{2581617644773}{867041280}$
6	0	$\frac{4278085159}{368640}$	$-\frac{26483840827}{1720320}$	$\frac{10491735514513}{1445068800}$	$-\frac{139668210217891}{78033715200}$
7	0	0	$\frac{116968933337}{44236800}$	$-\frac{890500845139}{412876800}$	$\frac{6978589997179}{9909043200}$
8	0	0	0	$\frac{25385138803}{90316800}$	$-\frac{52652632731}{321126400}$
9	0	0	0	0	$\frac{10711909210169}{624269721600}$

$\boxed{\eta_9^{j,s}}$

$j \backslash s$	2	4	6	8
1	$\frac{44039579957}{14745600}$	$-\frac{15824165056211}{2477260800}$	$\frac{14328069012029}{3303014400}$	$-\frac{26332156657147}{18496880640}$
2	$-\frac{70067602561}{2949120}$	$\frac{5369825407643}{154828800}$	$-\frac{5158776395993}{275251200}$	$\frac{6514444951201}{1238630400}$
3	$\frac{158625899173}{1966080}$	$-\frac{11227169865391}{117964800}$	$\frac{29933237272409}{660602880}$	$-\frac{77153221103897}{6606028800}$
4	$-\frac{121953672479}{921600}$	$\frac{354916665553}{2419200}$	$-\frac{5975801542697}{88473600}$	$\frac{15834223266853}{928972800}$
5	$\frac{611761614557}{5898240}$	$-\frac{338595836519}{2621440}$	$\frac{126344102042327}{1981808640}$	$-\frac{200404252881719}{11890851840}$
6	$-\frac{153296598947}{4915200}$	$\frac{3137330952221}{51609600}$	$-\frac{30768980959823}{825753600}$	$\frac{97464415569691}{8670412800}$
7	0	$-\frac{1402198607219}{117964800}$	$\frac{40766822971729}{3303014400}$	$-\frac{1156044273778537}{237817036800}$
8	0	0	$-\frac{20359967739}{11468800}$	$\frac{2005898347471}{1625702400}$
9	0	0	0	$-\frac{11084606975429}{79272345600}$

$\boxed{\eta_{10}^{j,s}}$

$j \backslash s$	1	3	5	7
1	$-\frac{5936440751}{7372800}$	$\frac{281978655779}{51609600}$	$-\frac{23197484399917}{3303014400}$	$\frac{2190705315745913}{624269721600}$
2	$\frac{33884150431}{2949120}$	$-\frac{13195184307097}{309657600}$	$\frac{3083498074211}{78643200}$	$-\frac{329558861040259}{20808990720}$
3	$-\frac{369336211}{6144}$	$\frac{10748243908261}{68812800}$	$-\frac{55407789534559}{471859200}$	$\frac{1239018762271579}{29727129600}$
4	$\frac{255337520419}{1843200}$	$-\frac{5908578342719}{19353600}$	$\frac{520188991137763}{2477260800}$	$-\frac{3143898589948211}{44590694400}$
5	$-\frac{423037867387}{2949120}$	$\frac{5082108800729}{15482880}$	$-\frac{153243709285603}{660602880}$	$\frac{3305021363349331}{41617981440}$
6	$\frac{16753575491}{307200}$	$-\frac{3155846928817}{17203200}$	$\frac{36726833683589}{235929600}$	$-\frac{6190102661048177}{104044953600}$
7	0	$\frac{36884410649 53}{88473600}$	$-\frac{577733424743393}{9909043200}$	$\frac{1019127205812299}{35672555520}$
8	0	0	$\frac{2900265243481}{309657600}$	$-\frac{6483559163023}{812851200}$
9	0	0	0	$\frac{27367721939759}{27745320960}$

$\boxed{\eta_{11}^{j,s}}$

$j \backslash s$	2	4	6
1	$-\frac{433172126543}{183500800}$	$\frac{292869682869259}{39636172800}$	$-\frac{755533686525503}{118908518400}$
2	$\frac{2660036179859}{88473600}$	$-\frac{40257079179961}{707788800}$	$\frac{539499339154079}{14863564800}$
3	$-\frac{263905748342627}{1651507200}$	$\frac{974127678603403}{4404019200}$	$-\frac{3464935877861461}{29727129600}$
4	$\frac{2030759822381}{4838400}$	$-\frac{608627628721811}{1238630400}$	$\frac{173811058773157}{743178240}$
5	$-\frac{570491186057201}{990904320}$	$\frac{1034737867040471}{1585446912}$	$-\frac{454273880894017}{1486356480}$
6	$\frac{81637985496899}{206438400}$	$-\frac{848417792268337}{1651507200}$	$\frac{554332437901141}{2123366400}$
7	$-\frac{76022436811607}{707788800}$	$\frac{1755155869080827}{7927234560}$	$-\frac{33519955430307049}{237817036800}$
8	0	$-\frac{24964285882541}{619315200}$	$\frac{81273844410421}{1857945600}$
9	0	0	$-\frac{202375045386037}{33973862400}$

$\boxed{\eta_{12}^{j,s}}$

$j \backslash s$	1	3	5
1	$\frac{388547729327}{990904320}$	$-\frac{12586819797803}{2831155200}$	$\frac{225374398759721}{28538044416}$
2	$-\frac{2430854986367}{247726080}$	$\frac{258343452813277}{4954521600}$	$-\frac{10743635536519061}{178362777600}$
3	$\frac{20036945966999}{235929600}$	$-\frac{232251792132631}{825753600}$	$\frac{58405280353216723}{237817036800}$
4	$-\frac{25175706455981}{77414400}$	$\frac{2015484051149861}{2477260800}$	$-\frac{107413449480948707}{178362777600}$
5	$\frac{299886137513597}{495452160}$	$-\frac{2668022569167251}{1981808640}$	$\frac{133343876882760763}{142690222080}$
6	$-\frac{13845777226823}{25804800}$	$\frac{1407300088225909}{1101004800}$	$-\frac{680562796851687}{734003200}$
7	$\frac{8019113491633}{44236800}$	$-\frac{12850249538216431}{19818086400}$	$\frac{67956070081136099}{118908518400}$
8	0	$\frac{4221184611389}{30965760}$	$-\frac{164903228272031}{825753600}$
9	0	0	$\frac{2399800894049011}{79272345600}$

$\boxed{\eta_{13}^{j,s}}$

$j \backslash s$	2	4
1	$\frac{1409122906677049}{1109812838400}$	$-\frac{24433255937099561}{3995326218240}$
2	$-\frac{38504062021513}{1468006400}$	$\frac{84194246367743411}{1248539443200}$
3	$\frac{11370780177215621}{52848230400}$	$-\frac{175295396102510419}{475634073600}$
4	$-\frac{8564805643401541}{9909043200}$	$\frac{51222963017142551}{44590694400}$
5	$\frac{59279616563426639}{31708938240}$	$-\frac{4356874183498906357}{1997663109120}$
6	$-\frac{68523571904642713}{30828134400}$	$\frac{1071080624306333789}{416179814400}$
7	$\frac{216876196102131707}{158544691200}$	$-\frac{2107300595320261267}{1141521776640}$
8	$-\frac{11808824968785709}{34681651200}$	$\frac{14396140786293431}{19508428800}$
9	0	$-\frac{560314875104889503}{4439251353600}$

$\boxed{\eta_{15}^{j,s}}$

$j \backslash s$	2
1	$-\frac{259980449939039}{532710162432}$
2	$\frac{9144448769839927}{554906419200}$
3	$-\frac{14095713084776741}{67947724800}$
4	$\frac{221992170898005827}{178362777600}$
5	$-\frac{287624123641309919}{71345111040}$
6	$\frac{275608308121757381}{36993761280}$
7	$-\frac{12809199119827883699}{1630745395200}$
8	$\frac{274436840334357187}{62426972160}$
9	$-\frac{1285036760811529423}{1268357529600}$

$\boxed{\eta_{14}^{j,s}}$

$j \backslash s$	1	3
1	$-\frac{146462446424423}{1109812838400}$	$\frac{25697310483841771}{9988315545600}$
2	$\frac{91971870042607}{15854469120}$	$-\frac{229671327225984871}{4994157772800}$
3	$-\frac{4323676913942387}{52848230400}$	$\frac{345241012673170697}{951268147200}$
4	$\frac{657581961441479}{1321205760}$	$-\frac{27030185835638917}{17836277760}$
5	$-\frac{2645716616611591}{1761607680}$	$\frac{2925800269902574361}{799065243648}$
6	$\frac{604782405112007}{256901120}$	$-\frac{882074774612809879}{166471925760}$
7	$-\frac{6054295311544603}{3303014400}$	$\frac{6468895390788443227}{1426902220800}$
8	$\frac{3593565775679}{6422528}$	$-\frac{165101957434340557}{78033715200}$
9	0	$\frac{34572633913775987}{83235962880}$

$\boxed{\eta_{16}^{j,s}}$

$j \backslash s$	1
1	$\frac{1033059867325999}{31962609745920}$
2	$-\frac{2371151354170769}{951268147200}$
3	$\frac{11984741009891131}{211392921600}$
4	$-\frac{190640670438324823}{356725555200}$
5	$\frac{5669553338007335851}{2283043553280}$
6	$-\frac{285899985423950791}{46242201600}$
7	$\frac{11973169590973537147}{1426902220800}$
8	$-\frac{1823347244087926049}{312134860800}$
9	$\frac{258517349914243253}{158544691200}$

Supplementary References

1. Jacobson, R. & Lainey, V. Martian satellite orbits and ephemerides. *Planet. Space Sci.* **102**, 35–44 (2014).
2. Konopliv, A. S., Park, R. S. & Folkner, W. M. An improved JPL Mars gravity field and orientation from Mars orbiter and lander tracking data. *Icarus* **274**, 253–260 (2016).
3. Khan, A. *et al.* A geophysical perspective on the bulk composition of Mars. *J. Geophys. Res. Planets* **123**, 575–611 (2018).
4. Peale, S. Origin and evolution of the natural satellites. *Annu. Rev. Astron. Astrophys.* **37**, 533–602 (1999).
5. Seidelmann, P. *et al.* Report of the iau/iag working group on cartographic coordinates and rotational elements of the planets and satellites: 2000. *Celest. Mech. Dyn. Astron.* **82**, 83–111 (2002).
6. Willner, K. *et al.* Phobos control point network, rotation, and shape. *Earth Planet. Sci. Lett.* **294**, 541–546 (2010).
7. Pätzold, M. *et al.* Phobos mass determination from the very close flyby of Mars Express in 2010. *Icarus* **229**, 92–98 (2014).
8. Yuan, D.-N., Sjogren, W. L., Konopliv, A. S. & Kucinskas, A. B. Gravity field of mars: A 75th degree and order model. *J. Geophys. Res. Planets* **106**, 23377–23401 (2001).
9. Rivoldini, A., Van Hoolst, T., Verhoeven, O., Mocquet, A. & Dehant, V. Geodesy constraints on the interior structure and composition of Mars. *Icarus* **213**, 451–472 (2011).
10. Rosenblatt, P. The origin of the Martian moons revisited. *Astron. Astrophys. Rev.* **19**, 44 (2011).
11. Rubincam, D. P., Chao, B. F. & Thomas, P. C. The gravitational field of Deimos. *Icarus* **114**, 63–67 (1995).
12. Rambaux, N. The libration magnitude of Deimos. *Private Communications* **2**, 2 (2).
13. Kopeikin, S., Efroimsky, M. & Kaplan, G. *Relativistic celestial mechanics of the solar system* (John Wiley & Sons, 2011).

14. Bagheri, A., Khan, A., Al-Attar, D., Crawford, O. & Giardini, D. Tidal response of Mars constrained from laboratory-based viscoelastic dissipation models and geophysical data. *J. Geophys. Res. planets* (2019).

15. Sundberg, M. & Cooper, R. A composite viscoelastic model for incorporating grain boundary sliding and transient diffusion creep; correlating creep and attenuation responses for materials with a fine grain size. *Philos. Mag.* **90**, 2817–2840 (2010).

16. Jackson, I. & Faul, U. H. Grainsize-sensitive viscoelastic relaxation in olivine: Towards a robust laboratory-based model for seismological application. *Phys. Earth Planet. Inter.* **183**, 151–163 (2010).

17. Connolly, J. The geodynamic equation of state: what and how. *Geochem. Geophys. Geosyst.* **10** (2009).

18. Stixrude, L. & Lithgow-Bertelloni, C. Thermodynamics of mantle minerals - I. Physical properties. *Geophys. J. Int.* **162**, 610–632 (2005a).

19. Stixrude, L. & Lithgow-Bertelloni, C. Thermodynamics of mantle minerals - II. Phase equilibria. *Geophys. J. Int.* **184**, 1180–1213 (2011).

20. Taylor, G. J. The bulk composition of Mars. *Chem Erde* **73**, 401–420 (2013).

21. Rivoldini, A., Van Hoolst, T., Verhoeven, O., Mocquet, A. & Dehant, V. Geodesy constraints on the interior structure and composition of Mars. *Icarus* **213**, 451–472 (2011).

22. Bruck Syal, M., Rovny, J., Owen, J. M. & Miller, P. L. Excavating Stickney crater at Phobos. *Geophys. Res. Lett* **43**, 10–595 (2016).

23. Asphaug, E., Ostro, S. J., Hudson, R., Scheeres, D. J. & Benz, W. Disruption of kilometre-sized asteroids by energetic collisions. *Nature* **393**, 437 (1998).

24. Asphaug, E., Ryan, E. V. & Zuber, M. T. Asteroid interiors. *Asteroids III* **1**, 463–484 (2002).

25. Rovny, J., Owen, J. M., Howley, K. & Wasem, J. Modeling Impact Cratering on Phobos. In *LPSC*, vol. 44, 1076 (2013).

26. Le Maistre, S., Rivoldini, A. & Rosenblatt, P. Signature of Phobos' interior structure in its gravity field and libration. *Icarus* **321**, 272–290 (2019).

27. Black, B. & Mittal, T. The demise of Phobos and development of a Martian ring system. *Nat. Geosci.* **8**, 913 (2015).

28. Hurford, T. *et al.* Tidal disruption of Phobos as the cause of surface fractures. *J. Geophys. Res. planets* **121**, 1054–1065 (2016).

29. Soter, S. & Harris, A. The equilibrium figures of Phobos and other small bodies. *Icarus* **30**, 192–199 (1977).

30. Simioni, E., Pajola, M., Massironi, M. & Cremonese, G. Phobos grooves and impact craters: A stereographic analysis. *Icarus* **256**, 90–100 (2015).

31. Dimitrovski, A. *On the tidal response and interior structure of Phobos*. Master's thesis, ETH Zurich (2020).

32. Goldreich, P. & Sari, R. Tidal evolution of rubble piles. *Astrophys J* **691**, 54 (2009).

33. Nimmo, F. & Matsuyama, I. Tidal dissipation in rubble-pile asteroids. *Icarus* **321**, 715–721 (2019).

34. McKinnon, W. *et al.* The solar nebula origin of (486958) arrokoth, a primordial contact binary in the kuiper belt. *Science* **367** (2020).

35. Jutzi, M. The shape and structure of small asteroids as a result of sub-catastrophic collisions. *Planet. Space Sci.* **177**, 104695 (2019).

36. Jutzi, M. & Benz, W. Formation of bi-lobed shapes by sub-catastrophic collisions-a late origin of comet 67p's structure. *Astron. Astrophys.* **597**, A62 (2017).

37. Szeto, A. M. Orbital evolution and origin of the Martian satellites. *Icarus* **55**, 133–168 (1983).

38. Singer, S. F. Origin of the Martian satellites Phobos and Deimos. In *Exp. Phobos and Deimos*, vol. 1377, 36 (2007).

39. Hesselbrock, A. J. & Minton, D. A. An ongoing satellite–ring cycle of Mars and the origins of Phobos and Deimos. *Nat. Geosci.* **10**, 266 (2017).

40. Efroimsky, M. Bodily tides near spin–orbit resonances. *Celest. Mech. Dyn. Astron.* **112**, 283–330 (2012).

41. Efroimsky, M. Tidal dissipation compared to seismic dissipation: In small bodies, Earths, and super-Earths. *Astrophys. J.* **746**, 150 (2012). `1105.3936`.

42. Efroimsky, M. Tidal evolution of asteroidal binaries. ruled by viscosity. ignorant of rigidity. *Astron. J.* **150**, 98 (2015).

43. Efroimsky, M. Dissipation in a tidally perturbed body librating in longitude. *Icarus* **306**, 328–354 (2018).

44. Canup, R. & Salmon, J. Origin of Phobos and Deimos by the impact of a Vesta-to-Ceres sized body with Mars. *Sci. Adv.* **4**, eaar6887 (2018).

45. Craddock, R. A. Are Phobos and Deimos the result of a giant impact? *Icarus* **211**, 1150–1161 (2011).

46. Citron, R. I., Genda, H. & Ida, S. Formation of Phobos and Deimos via a giant impact. *Icarus* **252**, 334–338 (2015).

47. Hyodo, R., Genda, H., Charnoz, S. & Rosenblatt, P. On the impact origin of Phobos and Deimos. I. Thermodynamic and physical aspects. *Astron. J.* **845**, 125 (2017).

48. Lognonné, P. *et al.* Constraints on the shallow elastic and anelastic structure of Mars from InSight seismic data. *Nat. Geosci.* **13**, 213–220 (2020).

49. Giardini, D. *et al.* The seismicity of Mars. *Nat. Geosci.* **13**, 205–212 (2020).

50. Morschhauser, A., Grott, M. & Breuer, D. Crustal recycling, mantle dehydration, and the thermal evolution of Mars. *Icarus* **212**, 541–558 (2011).

51. Thiriet, M., Michaut, C., Breuer, D. & Plesa, A.-C. Hemispheric dichotomy in lithosphere thickness on Mars caused by differences in crustal structure and composition. *J. Geophys. Res. planets* **123**, 823–848 (2018).

52. Samuel, H., Lognonné, P., Panning, M. & Lainey, V. The rheology and thermal history of Mars revealed by the orbital evolution of Phobos. *Nature* **569**, 523 (2019).

53. Efroimsky, M. & Lainey, V. Physics of bodily tides in terrestrial planets and the appropriate scales of dynamical evolution. *J. Geophys. Res. Planets* **112**, E12003 (2007). `0709.1995`.

54. Bills, B. G., Neumann, G. A., Smith, D. E. & Zuber, M. T. Improved estimate of tidal dissipation within Mars from MOLA observations of the shadow of Phobos. *J. Geophys. Res. Planets* **110**, 7004 (2005).

55. Frouard, J. & Efroimsky, M. Tides in a body librating about a spin–orbit resonance: generalisation of the Darwin–Kaula theory. *Celest. Mech. Dyn. Astron.* **129**, 177–214 (2017).

56. Boué, G. & Efroimsky, M. Tidal evolution of the Keplerian elements. *Celest. Mech. Dyn. Astron.* **131**, 30 (2019).

57. Efroimsky, M. & Makarov, V. V. Tidal friction and tidal lagging. applicability limitations of a popular formula for the tidal torque. *Astron. J.* **764**, 26 (2013). `1209.1615`.

58. Efroimsky, M. Long-term evolution of orbits about a precessing oblate planet: 1. the case of uniform precession. *Celest. Mech. Dyn. Astron.* **91**, 75–108 (2005).

59. Goldreich, P. Inclination of satellite orbits about an oblate precessing planet. *Astron. J.* **70**, 5 (1965).

60. Efroimsky, M. Long-term evolution of orbits about a precessing oblate planet. 2. the case of variable precession. *Celest. Mech. Dyn. Astron.* **96**, 259–288 (2006).

61. Gurfil, P., Lainey, V. & Efroimsky, M. Long-term evolution of orbits about a precessing oblate planet: 3. a semianalytical and a purely numerical approach. *Celest. Mech. Dyn. Astron.* **99**, 261–292 (2007).

Acknowledgements This work was supported by a grant from the Swiss National Science Foundation (SNSF project 172508 “Mapping the internal structure of Mars”). This is InSight contribution number 96.

Competing Interests The authors declare that they have no competing financial interests.

Correspondence Correspondence and requests for code should be addressed to A.B.(amirhossein.bagheri@erdw.ethz.ch)